MARS
The International Journal of Mars Science and Exploration

MARS INFORMATICS
Open Access Journals

Science

A detailed geologic characterization of Eberswalde crater, Mars

Melissa S. Rice[1], James F. Bell III[2], Sanjeev Gupta[3], Nicholas H. Warner[4], Kate Goddard[3] and Ryan B. Anderson[5]

[1]Division of Geological and Planetary Sciences, California Institute of Technology, MC 150-21, Pasadena, CA 91125, USA, mrice@caltech.edu; [2]School of Earth and Space Exploration, Arizona State University, Tempe, Arizona, USA; [3]Dept. of Earth Science and Engineering, Imperial College London, London, UK; [4]Jet Propulsion Laboratory, California Institute of Technology, 4800 Oak Grove Dr., Pasadena, CA 91109, USA; [5]U.S. Geological Survey Astrogeology Team, Flagstaff, AZ 86001, USA

Citation: MARS 8, 15-57, 2013; doi:10.1555/mars.2013.0002
Submitted: September 20,2011; Accepted: September 13,2012; Published: May 10, 2013
Editor: Jeffrey Plescia, Johns Hopkins University Applied Physics Laboratory
Reviewed: Alan Howard, University of Virginia; Rebecca Williams, Planetary Science Institute

Abstract

Background: Eberswalde crater, selected as one of four finalist landing sites for the Mars Science Laboratory mission, is best known for the spectacularly preserved, inverted, fan-shaped deposit along its western margin. This feature has been interpreted as a lacustrine delta, although the timing and duration of an Eberswalde crater lake is poorly understood. The aim of this study is to place more broadly observed fluvio-lacustrine activity throughout the crater's floor within the larger context of Eberswalde's geologic history, and to infer the sequence of deposition and erosion of the observed stratigraphic and geomorphic units.

Method: We have identified and mapped stratigraphic and geomorphic units within all of Eberswalde crater using orbital imagery from the HiRISE, MOC and CTX cameras, and we have calculated crater statistics to infer the relative ages of crater floor materials. Using topographic datasets derived from HiRISE, CTX and MOLA, we determine the unit associations, successions, and geometries and develop a model for the depositional and erosional history within the crater.

Conclusion: We have produced maps of ten stratigraphic and seven geomorphic units identified within Eberswalde crater. Our observations of the stratigraphy, geomorphology, topography and crater densities imply a complex relationship between deposition and exhumation within Eberswalde crater, and we infer the following sequence of major events: (1) Eberswalde crater forms in the Noachian (> 3.6 Ga); (2) Holden crater forms southwest of Eberswalde crater in the late Noachian to Early Hesperian, and its associated ejecta blanket covers the floor of Eberswalde crater and heavily modifies the southern rim; (3) Extensive faulting from regional stresses creates the first-order topography within the crater, and vein-like features form in some units from fracturing, fluid circulation, and cementation; (4) Valley features are carved in the crater walls as water flows into the crater, creating an Eberswalde lake in which delta formation occurs. The distribution of features interpreted as inverted channels and lacustrine deposits implies that the lake extended into the easternmost portion of the crater and at least six fluvio-deltaic systems formed; (5) Extensive exhumation and degredation of the crater floor materials occurs, perhaps simultaneously with the deposition of an airfall mantling unit; (6) Very little besides aeolian sediment transport activity occurs in the Amazonian.

Introduction

Ancient layered outcrops on Mars that could represent lacustrine sediments have been high priority targets of observation in recent decades (*e.g.,* Malin and Edgett 2000; McEwen et al. 2007a; Malin et al. 2007; Murchie et al. 2007). Studies of these outcrops can both help to constrain the activity of liquid water on Mars during the planet's early history (the Noachian Period, before about 3.6 Ga) and to identify regions of potential astrobiologic interest for future landed missions. However, the distribution of water on Mars in space and time remains largely unresolved, in part because

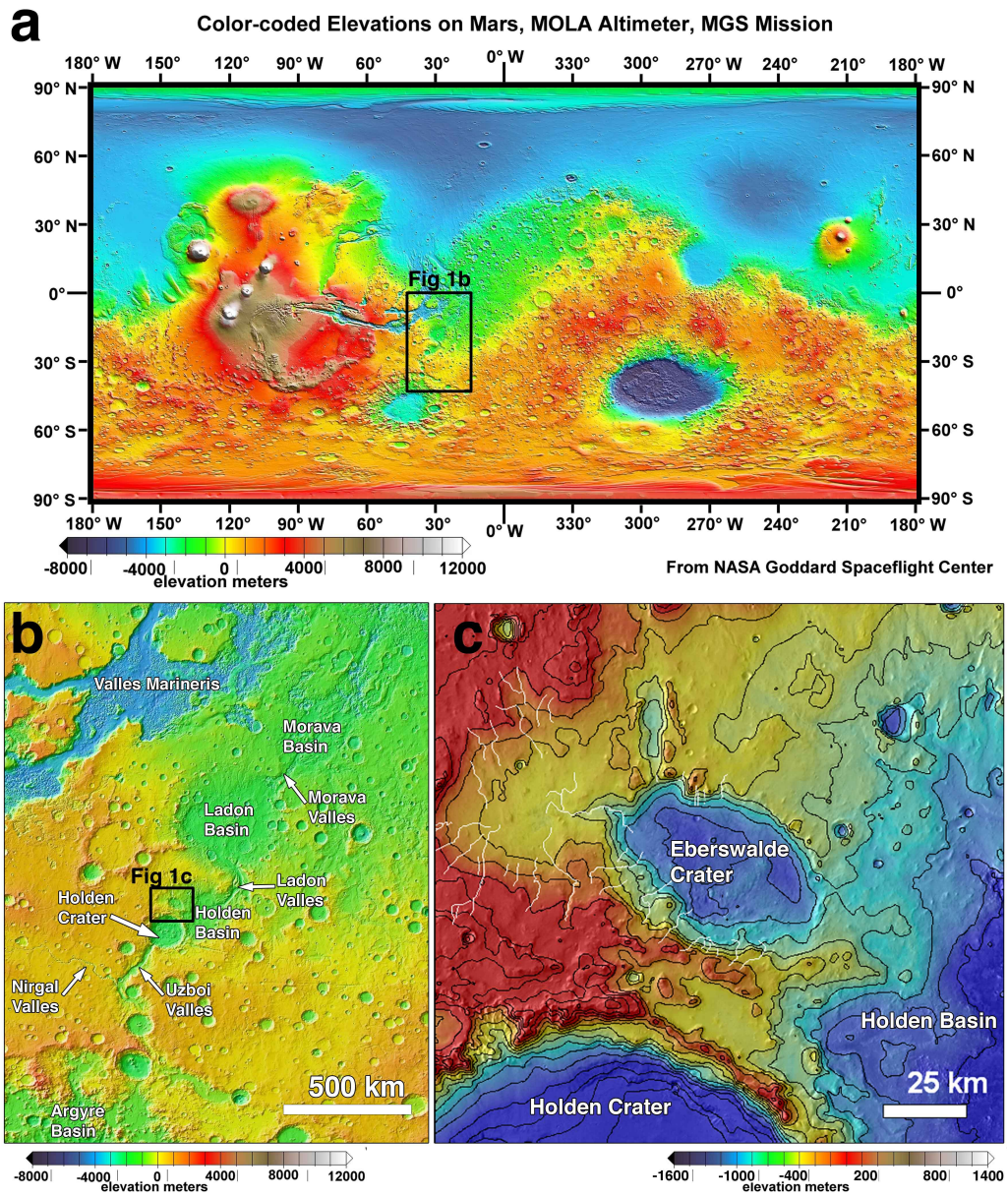

Figure 1. (a) Global topographic map of Mars based on MOLA data (Smith et al., 2001); (b) MOLA map of the Uzboi-Ladon-Morava system, with the location of Eberswalde crater indicated by the black box; (c) MOLA map of Eberswalde crater and immediate surroundings with 200 m contour lines drawn in black. Locations of major drainage channels are indicated by white lines. Note that the color scale of (c) is different from that of (a) and (b). (figure1.jpg)

of the scarcity of identified landforms that are clearly diagnostic of specific aqueous processes (Malin and Edgett 2000). Perhaps the most spectacularly preserved example of such a rare landform on Mars is the inverted fan-shaped deposit in Eberswalde crater that has been interpreted as the remnant of an ancient delta (*e.g.,* Malin and Edgett 2003). As described in the discovery paper by Malin and Edgett (2003), the location, form and structure of this landform "uniquely reflect materials deposited within an aqueous sedimentary environment."

Geologic setting

Eberswalde crater is centered at 24S 33W within the Erythraeum region of Mars (Figure 1a). It is located immediately north-northeast of Holden crater along the Uzboi-Ladon-Morava system (Figure 1b), a proposed fluvial network of valleys and impact craters connecting Argyre Basin to Ares Vallis (*e.g.,* Grant and Parker 2002). Holden crater's continuous ejecta blanket extends across the degraded southern rim of Eberswalde crater indicating its younger relative age. Although earlier reports suggested a Noachian age for the Holden impact event (Moore et al. 2003), new constraints from crater statistics suggest formation during the Early to Late Hesperian period (Irwin and Grant 2011). Both Holden crater and Eberswalde crater rest within the Holden basin, which is one of several large,

Mid-Noachian-age, multi-ringed impact basins that pre-dates valley network formation in the Uzboi-Ladon-Morava system. Fluvial incision of the interior rim of Holden basin by branching valley networks and infilling of the basin by layered sediment has been constrained to the Late Noachian period, possibly extending into the Hesperian (Grant and Parker 2002; Irwin and Grant 2011). These relative associations place the formation of Eberswalde crater to some time in the Late Noachian to Early Hesperian.

Fluvio-lacustrine activity

Valley networks incise the intracrater plains north of Holden crater and appear to have transported sediment into the western portion of Eberswalde crater, building the layered, fan-shaped landform that has been interpreted as a lacustrine delta (Malin and Edgett 2003; Moore et al. 2003; Bhattacharya et al. 2005; Wood 2006; Lewis and Aharonson 2006; Pondrelli et al. 2008; Pondrelli et al. 2011) or as an alluvial fan (Jerolmack et al. 2004). These valley networks post-date Holden ejecta, indicating that fluvial activity into Eberswalde and delta development occurred at some point after the Early-Late Hesperian (Irwin and Grant 2011).

The Eberswalde fan, which extends 13 km by 11 km and covers 115 km^2 of the western basin floor, consists of at least three lobes of layered rock and cross-cutting, sinuous ridges (Malin and Edgett 2003). While Jerolmack et al. (2004) examined a scenario in which the fan was built subaerially (*i.e.*, as an alluvial fan), Bhattacharya et al. (2005) note that alluvial fans should be dominated by sheet floods and debris flows, not the highly sinuous channelized flows observed at Eberswalde. Bhattacharya et al. (2005) also argued that the transition from laterally continuous and smooth basal layers to bifurcating channel networks in the upper layered strata suggests a complex evolution consistent with a deltaic origin.

Estimates of the time required to form the fan vary widely, ranging from ~100 years (in the alluvial fan scenario; Jerolmack et al. 2004) to ~10^5 years (in a deltaic environment; Bhattacharya et al. 2005). While Wood (2006) argued that the sinuosity indexes, meander-bend migration, and ridge-and-swale point-bar topography infer stable deposition in a long-lived lake, Lewis and Aharonson (2006) concluded, based on a quantitative analysis of the stratigraphy, that the delta more likely formed during a small number of shorter lacustrine episodes.

The source of the water that transported fan-building sediment into Eberswalde crater is also debated. Several branching fluvial systems enter Eberswalde crater from the terrain that borders the crater's western, northern, and southern rims, contributing sediment to several fans within the crater (Rice et al. 2011). No channels have been identified that enter from the east, although the terrain east of Eberswalde occurs within the Holden basin and has been disrupted by a chaos formation event (Irwin and Grant 2011). To the immediate south and southwest of Eberswalde crater, the channels clearly superimpose the continuous ejecta blanket of Holden crater indicating that fluvial incision post-dates the Holden impact. To the northwest and north, superposition relationships with Holden ejecta are less clear, although models of ejecta thickness indicate meters to tens of meters of ejecta at these locations (Garvin and Frawley 1998). From these relative associations and from the morphology of the channel systems, it has been suggested that runoff may have been related either to localized processes that are tied directly to the formation of Holden crater, or to longer term precipitation that was controlled by regional or global climate conditions (Moore et al. 2003).

There are three main mechanisms by which Holden impact induced runoff may have occurred: (1) release of ground water through localized, sustained impact-induced hydrothermal activity (Ivanov and Piarazzo 2011); (2) through disruption of an existing liquid water aquifer leading to instantaneous fluvial activity (Wang et al. 2005; Harrison et al. 2010); or (3) melting of ground ice or surface snow by hot ejecta (Mangold 2011). Of the three hypotheses, the ejecta melting hypothesis fits best with the morphologic observation that most of the Eberswalde channels are derived only from within the mapped extent of Holden ejecta. However, Irwin (2011) suggests that impact induced runoff by ground ice melting would have led to overfilling of the crater, above the level of the preserved delta, as evaporation could not keep up with the initial pulse of runoff.

Irwin (2011) postulates that ephemeral and intermittent runoff production via precipitation over longer timescales is a more likely scenario in the broader context of the occurrence of valley networks, alluvial fans, and the putative deltas throughout this region. Irwin (2011) hypothesizes that the Eberswalde delta would have required conditions resembling an arid terrestrial desert over timescales of >10^3 to 10^4 years, in order for evaporation to keep up with runoff. By this model, precipitation occurred during a longer-term global to regional climate change event. Alternatively, a lake may have formed within Holden crater immediately following the impact. The formation of small lake effect storms across this lake may explain localized precipitation and runoff in the area around Holden and Eberswalde craters (Kite et al. 2011). The presence of an ancient lake within Holden crater has been postulated based on the stratigraphic observations of finely-layered sediments that superimpose impact breccia floor materials of Holden crater (Grant et al. 2008).

Other fans and fan-form features have been recently identified in high-resolution imaging elsewhere on Mars; some have also been interpreted as potential deltas or deltaic landforms. For example, Weitz et al. (2006) interpreted a terraced fan deposit within one of the troughs of Coprates Catena as a delta deposited into a shallow, potentially Hesperian lake that formed in the trough. Di Achille et al. (2007) have interpreted a number of fan-shaped deposits at nearly constant topographic elevation within Shalbatana Vallis as late Hesperian deltas, deltaic deposits, and shorelines. However, Kraal et al. (2008) have questioned the evidence for persistent, long-duration flow associated with many of these features, instead favoring a model involving single, short-duration outflow events depositing sediments

over previous (non-deltaic) fan-shaped deposits. These recent studies have helped to justify new observations of the Eberswalde fan deposit using higher resolution data sets.

A reinterpretation of the discharge into Eberswalde crater was made possible by new high-resolution (~25 cm/pix) images from the Mars Reconnaissance Orbiter (MRO) High Resolution Imaging Science Experiment (HiRISE) instrument (McEwen et al. 2007a). Boulders on the surface of the fan were interpreted by Schieber (2007) and Howard et al. (2007) as having been transported by the flow that deposited the fan. Kraal and Postma (2008) also interpreted the fan as having formed in a debris flow based on their analysis of the bend forms. However, Pondrelli et al. (2008) supported the deltaic interpretation based on the complex stratal organization visible in HiRISE images. Furthermore, Rice et al. (2011) identified a total of six fan-shaped plateaus in the crater which they interpreted as fluvio-deltaic systems because, as seen in the high-resolution images, channel bifurcation occurs basinward of the crater rim implying that fluvially-transported sediments were deposited along a shoreline and into a standing body of water.

Because of the long-lived lake interpretation, Eberswalde crater was selected as a high-priority candidate landing site for the Mars Science Laboratory (MSL) mission, scheduled to launch in November 2011 and land in the summer of 2012 (Grant et al. 2011). The primary objective of the MSL mission is to search for past and present habitable environments on Mars (Grotzinger 2009). The selection of candidate landing sites was based in part on their potential for having preserved biomarkers (Grant et al. 2011); sediment deposition in a low-energy environment, such as a quiescent lake, typically has very high preservation potential (Summons et al. 2011). The identification of phyllosilicate minerals at the fan terminus and in the crater basin, which may have formed *in-situ* or have been eroded from the source basin to the west (Milliken and Bish 2010), enhanced Eberswalde's appeal as a landing site. However, Gale Crater was selected as the final landing site over Eberswalde Crater in July 2011.

Objectives of this work

In this work, our aim is not to settle the long-standing debates about the duration of a lake in Eberswalde crater or the source of the water. Rather, we address a different question that has not been examined in the current literature: what are the depositional histories of *all* units within the crater? We do this by examining a variety of imaging and topographic datasets. Pondrelli et al. (2008) mapped units within the Eberswalde crater basin, but not at sufficient resolution to develop specific hypotheses for all materials; Pondrelli et al. (2011) provided an analysis of the putative delta, but did not extend their analysis to the rest of Eberswalde crater. Schieber (2008) identified potential high-priority science targets in the center of the crater based on HiRISE imagery, and Rice et al. (2011) identified candidate fluvio-deltaic systems and mapped the distribution of putative faults, but neither study comprehensively mapped the full extents of crater floor units.

Here we present stratigraphic and morphologic unit maps of features within Eberswalde crater that directly bear on the fluvial and aqueous history of the basin, including the putative deltaic deposits. In the next section, we describe the orbital datasets used in the study and our mapping methodology. We then provide descriptions, depositional hypotheses, and interpretations of each inferred stratigraphic and morphologic unit; descriptions of the associations, successions and geometries of these units; and finally crater statistics and inferred relative ages of crater floor materials. In the discussion we present our inferred depositional and erosional history model within Eberswalde crater, with our conclusions summarized in the final section. While one goal of this work is to characterize a high-priority landing site for future missions, the detailed mapping and interpretation of sedimentary units within Eberswalde crater are critical to understanding the geologic history of Mars in general.

Data and Methods

Imaging datasets: MOC, CTX and HiRISE

Our detailed investigation of Eberswalde crater was made possible through the extensive imaging coverage of the crater by instruments on the Mars Global Surveyor (MGS) and MRO spacecraft. For the primary base map for this study, we used radiometrically-calibrated data from the MRO Context Camera (CTX) (Malin et al. 2007; Bell et al., 2011) to generate a 6 m/pixel mosaic of Eberswalde crater. CTX images cover the entire crater and surrounding drainage basin (a list of images is provided in the Appendix). We calibrated and projected these CTX observations using the USGS Integrated Software for Imagers and Spectometers (ISIS) software package (*e.g.*, Eliason et al. 2001).

We also use CTX images to estimate the albedo of surface units (Eliason et al. 2001). Dividing the radiometrically-corrected CTX images by the cosine of the solar incidence angle at the time of each observation gives an estimate of the Lambert (isotropically scattering surface) albedo over the CTX bandpass (611±189 nm; Bell et al. 2011), which is essentially the ratio of the reflectance of a surface to that of a perfectly diffuse surface under the same viewing conditions. These Lambert-corrected images enable direct comparison between images taken in different viewing geometries; however, uncertainties still exist due to seasonal lighting variations, local incidence angle, interannual differences in aeolian surface dust covering, and variable atmospheric dust opacity. Combining these uncertainties with the estimated accuracy of the CTX radiometric calibration (Bell et al. 2011), we estimate that the uncertainties on the CTX-derived Lambert albedo values reported here are around ±20%.

Because Eberswalde crater was selected as one of the four finalist MSL landing sites (Grant et al. 2010), it has been targeted repeatedly by the MRO HiRISE instrument (McEwen et al. 2007a).

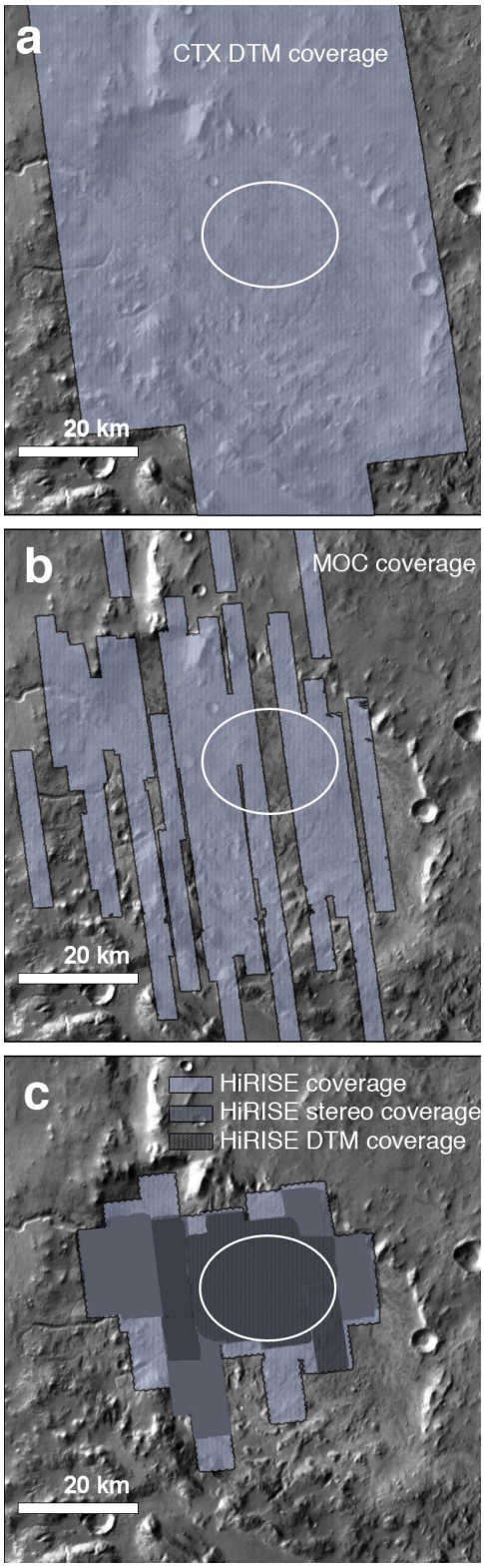

Figure 2. Footprint maps showing the imaging coverage of Eberswalde crater used in this study: (a) CTX DTMs; (b) MOC NA images; (c) HiRISE images, stereo anaglyphs, and DTMs. The location of the proposed landing ellipse is outlined in white. All footprints are shown over a THEMIS daytime IR basemap (Christensen et al. 2006). (figure2.jpg)

The ~0.27 m/pixel HiRISE data cover the majority of the north and center of the crater floor, including the entire area identified as the potential MSL landing ellipse (Figure 2c; a full list of images is given in the Appendix). HiRISE has three color filters: blue-green (BG; λ_{eff}=502±157 nm), red (RED; λ_{eff}=686±267 nm), and near-infrared (IR; λ_{eff}=878±143 nm) (McEwen et al. 2007a; Delamere et al. 2010); these filters enable the creation of false color images over a limited portion of the field of view (BG and IR data can only be acquired for a central strip covering 20% of each HiRISE RED image). We acquired map-projected HiRISE RED and false color observations from the Planetary Data System (PDS), which we use as the primary dataset for our mapping.

In locations without HiRISE coverage, we have used MGS Mars Orbiter Camera (MOC) images (Malin and Edgett 2001; Malin et al. 2010) to study small-scale features at ~1.5 m/pixel resolution. MOC coverage of Eberswalde crater is shown in Figure 2b, and product IDs are listed in the Appendix. We radiometrically-calibrated and projected all MOC observations with ISIS using similar methods as for CTX.

Topography: MOLA, CTX DTMs and HiRISE DTMs

We used a topographic map based on MGS Mars Orbiter Laser Altimeter (MOLA) data (Zuber et al. 1992; Smith et al. 2001) to provide regional-scale topographic context for Eberswalde crater at ~1 m vertical resolution and a spatial grid resolution of 1/64° in latitude × 1/32° in longitude (~ 0.86 × 0.43 km^2 at Eberswalde crater) (Figure 1). We augmented this topography with three digital terrain models (DTMs) within the crater derived from the CTX stereo pair images listed in the Appendix (Edwards and Broxton, 2006; Broxton and Edwards, 2008). For topographic investigations of specific, smaller-scale features, we used DTMs derived from HiRISE stereo pairs (Kirk et al. 2008). HiRISE DTMs for candidate MSL landing sites have been made publically available as soon as possible following their production (McEwen et al. 2010), including four DTMs within Eberswalde crater as of October 2010 (from stereo pair images listed in the Appendix). The spatial coverages of the CTX and HiRISE DTMs used in this study are shown in Figure 2.

Identification and mapping of units

In this study we have identified and mapped the distribution of stratigraphic units based on CTX, HiRISE and MOC images. We define a stratigraphic unit as a sheetlike, wedgelike, or tabular body of rock that underlies the surface (or unconsolidated material on the surface) and exhibits consistent features that can be identified in orbital images. Each stratigraphic unit has a limited surface exposure, the horizontal extent of which can be mapped, and the vertical extent of which usually has to be inferred but in some cases can be constrained by topography. We identify stratigraphic units through the principles of photographic interpretation and planetary mapping originally defined for lunar geology

(*e.g.*, Shoemaker and Hackman, 1962; Wilhelms, 1974; 1990). These include the following geologic attributes: albedo, color, texture (the aggregate appearance of meter-scale features), pattern (the aggregate appearance of 10-100 m-scale features), relief (topography as determined by shading and DTM data), and retention of small (< 50 m) craters. Fortunately, because the inferred surface dust cover (Ruff and Christensen 2002) is uniformly low throughout the Eberswalde crater region (Rogers et al. 2009), our mapping is only minimally hindered by the obscuring effects of surface dust that plague photogeologic studies of many other regions on Mars.

Our mapping of stratigraphic units and determination of relations between them is based on identification of specific contacts. All the terrain enclosed by a contact is interpreted to belong to one unit, and the geometric distributions of the contacts is inferred to reflect depositional patterns and age relationships of the units (*e.g.*, Wilhelms, 1990). Also, we use the geometry of a contact itself to aid interpretation of the unit it bounds; for example, a cohesive rock unit will typically form sharp contacts along scarps and cliff faces, whereas unconsolidated material will often grade imperceptibly with subjacent units. We note that in the latter case, the transition between units can be ambiguous, and some simplifications and uncertainties are necessarily involved in mapping the distribution of units. Thus, dividing lines between our interpreted stratigraphic units is often a matter of judgment.

We take care to distinguish stratigraphic units from geomorphic units, which we define as landforms with consistent surface morphologies that can be identified in orbital images. We identify geomorphic units on the basis of their planimetric configurations (the two-dimensional shapes of features), albedo, color, and context (the relation of features to one another). Unlike stratigraphic units, geomorphic units do not necessarily occupy unique locations within the inferred stratigraphic column. In some cases, the composition of geomorphic units appears to be distinct from that of stratigraphic units (*e.g.*, the vein-like features); in other cases, geomorphic units appear to be comprised of multiple stratigraphic units (*e.g.*, the fan-form plateaus).

Impact crater statistics

Impact crater counts on planetary surfaces are obtained for two primary reasons: (1) to estimate a relative and/or absolute model age of a geologic unit (stratigraphic or geomorphic) from the cumulative size frequency distribution of mapped craters (Hartmann and Neukum 2001; Ivanov, 2001); and (2) to relate the preservation state of impact craters from the slope of the cumulative size frequency curve to specific geologic processes that are involved in crater resurfacing and/or retention (Hartmann 2005; Neukum et al. 2010). While Grant and Wilson (2011) have provided crater statistics for the large Eberswalde fan, the surface area of this feature is arguably too small to derive an accurate formation age from crater counts. However, impact crater statistics can provide a wealth of information regarding the geologic history of surfaces on Mars even when the aerial extent of a mapped unit is not sufficient to obtain an accurate model age. No impact crater statistics have yet been published from the floor of Eberswalde crater that extend to sub-kilometer-sized craters. Within this range, surface conditions on Mars that lead to erosion and burial of impact craters can be identified, and, in some cases, related to specific resurfacing processes and the material properties (cohesion) of a geologic unit.

For this analysis, we obtained impact crater statistics from the floor of Eberswalde crater to place these materials within a general temporal context for geologic events on Mars. Furthermore, we utilized the density of impact craters on specific geologic units as a proxy for understanding material cohesion and surface processes (burial) in the context of observed surface properties (*e.g.* morphology, thermophysical properties). Unique geologic units were not separated for counting because the areas of individual geologic units are too small (on the order of 100 km^2) to obtain accurate model ages at the available image resolution. Rather, the model ages (using the chronology functions of Hartmann and Neukum 2001) are derived from a blanket count, taken across what we have interpreted as the interior floor, within the rim of the crater. The model age that we provide here therefore represents only a bulk constraint on the average crater retention age of all units that we have identified on the floor of the crater.

We counted all craters on the floor of Eberswalde crater with diameters (D) > 100 m from a full res (6 m/pix) CTX mosaic using the Mars Editing and Assessment toolset (Simpson et al., 2008). This Visual Basic® application allows craters to be tagged and measured on an image backdrop, while saving relevant diameter and location data to an ESRI® shapefile. The freeware program Craterstats was used to plot the crater statistics and to fit isochrons (with uncertainties) to estimate absolute ages (Michael and Neukum 2008). Crater statistics are presented here in table form as crater densities for N(0.1), N(0.5), N(1), N(5) (where N represents the cumulative number of craters counted per 10^6 km^2) and on log10 cumulative frequency plots (Hartmann and Neukum 2001). A resurfacing correction was made following Michael and Neukum (2010).

Inferred stratigraphic units

We have identified ten stratigraphic units within Eberswalde crater, which we have mapped in Figure 3. Because the southern rim of the crater is severely degraded, we cannot objectively define where Eberswalde crater ends and the plains between Eberswalde and Holden craters begin; in this work, we have chosen to use the -1200 m contour line as the boundary of our mapping region. The detailed descriptions of our observations, hypotheses, and interpretations of each unit are given below, and a summary of all units is provided in Table 1.

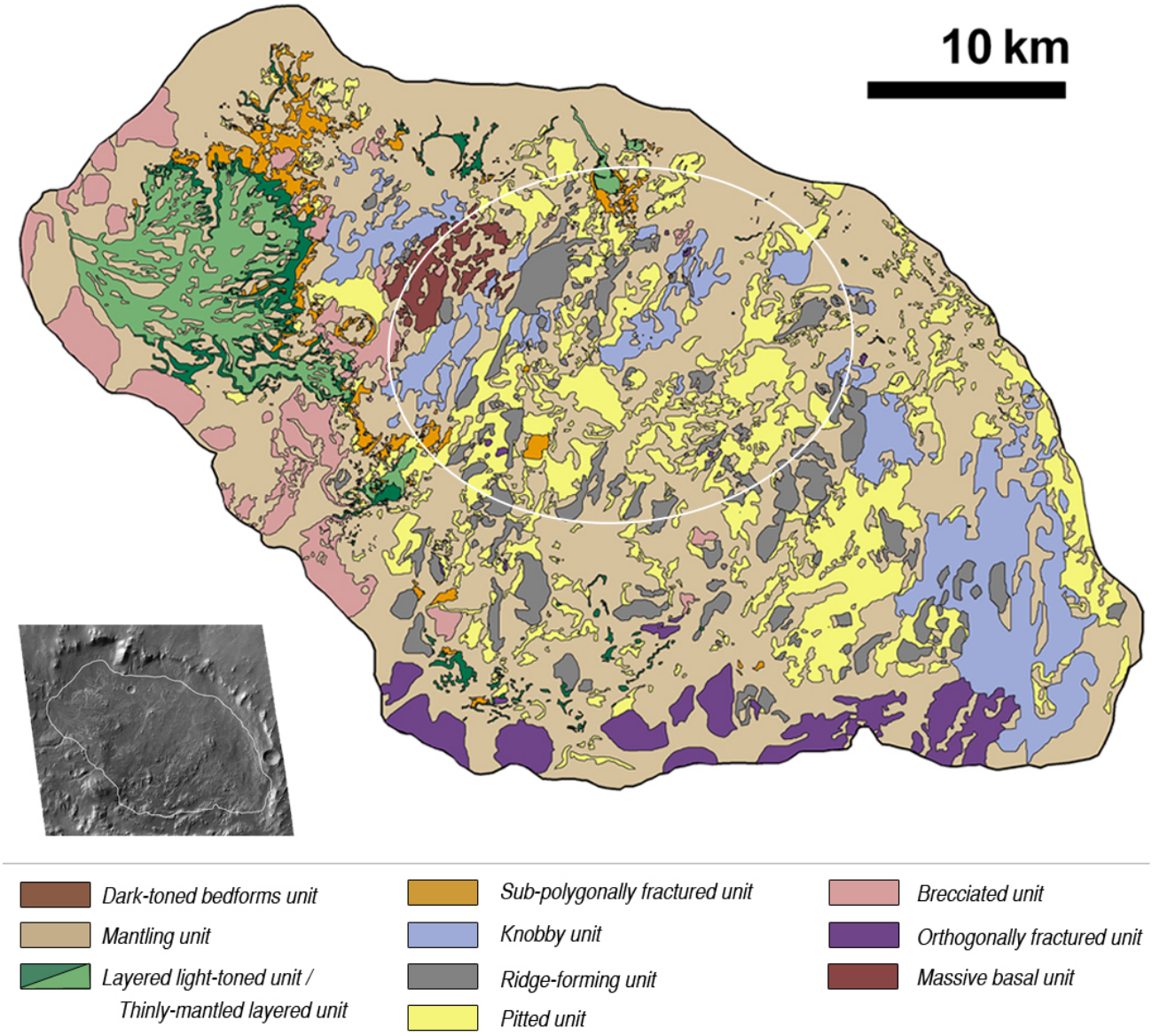

Figure 3. Map of inferred stratigraphic units inside Eberswalde crater. The boundary of the mapped region is defined by the -1200 m contour line. The white line indicates the location of the proposed MSL landing ellipse. See text for detailed descriptions of units. (figure3.jpg)

Massive, basal unit

Observations. The massive, basal unit is distinct from other crater floor materials in that it is light-toned, extensively fractured (although with no apparent systematic pattern to the fractures) and has no visible layering. While most occurrences of this unit (mapped in Figure 3) are flat-lying and variably covered by the mantling unit, the most prominent examples are where the unit forms mounds with steep ridges (Figure 4). No outcrops appear be forming and/or shedding boulders; we observe no blocks that may have fallen from the high ridges. In false-color HiRISE images, this unit exhibits distinct whitish to blueish hues that distinguish these outcrops from other units (Figure 4c).

Hypotheses and interpretations. These materials appear to have originated from the deeply-eroded, well-exposed basement of Eberswalde crater, and we interpret them as fractured, pre-crater-fill bedrock (which may be autochthonous material from the Eberswalde impact). The colors, erosional expressions, and fracture patterns associated with the massive, basal unit are distinct from all other units within the crater, and there is no evidence suggesting that these outcrops are sedimentary or crater-fill deposits. Furthermore, they are only exposed in the topographically lowest, most deeply exhumed portion of the crater. We propose that this location in the western crater, where the massive, basal unit is exposed, is a "window" through the crater-filling units into the basement material that underlies the whole of the crater.

Table 1. Summary of stratigraphic units

Stratigraphic Unit	Figures	Description	Contact Relationships	Interpretation*	Comparison to Previous Studies
Massive, basal unit	4	Massive; extensively fractured; distinct hues in HiRISE color	Obscured contact with the pitted unit; unable to discern the relationship	Fractured Eberswalde bedrock	[1,2] Lava flows and pyroclastic materials
Orthogonally-fractured unit	5	Massive; orthogonally-fractured	Obscured contact with the pitted unit; unable to discern the relationship	Megabreccia (allocthonous or parautocthonous)	[1,2] Lava flows and pyroclastic materials
Brecciated unit	6, 24, 25	Megaclasts encased in a light-toned, finer-grained matrix; in places cut by light-toned, vein-like lineations	Overlain by the layered, light-toned unit; Obscured contact with the discontinuous, light-toned unit	Megabreccia (allocthonous)	[1,2] Lava flows and pyroclastic materials; [3] Megabreccia
Pitted unit	7, 25, 26, 27	Light-toned; clusters of quasi-circular depressions	Cut by vein-like features; obscured contact with the brecciated, ridge-forming unit; overlain by the fractured and layered light-toned units	Erosional expression of the brecciated unit	[2] Lacustrine deposits
Ridge-forming unit	8	Massive; no systematic fractures; possible layering; boulder-shedding	Overlies the pitted unit	Sedimentary rock? Outcrops of other units obscured by airfall deposits?	[1,2] Lava flows and pyroclastic materials
Knobby unit	9	Isolated hillocks of light-toned rock, spaced >50 m apart	Contacts with other units obscured by the mantling unit	Eroded remnants of the sub polygonally fractured and/or layered light-toned units	none
Sub-polygonally fractured unit	10, 25, 26, 27	Sub-polygonally fractured; occurs as isolated mesas or extensive deposits; boulder-shedding	Overlies the discontinuous light-toned unit; underlies the fractured light-toned unit; onlaps the brecciated ridge-forming unit; overlies vein-like features	Lacustrine bottomset deposits	[2] Lacustrine deposits
Layered, light-toned unit	11-13, 23, 24	Layers < 10 m thick; sometimes sub-polygonally or orthogonally fractured; boulder-shedding; layers have variable resistances to erosion	Overlies the fractured and discontinuous light-toned units; onlaps the brecciated, ridge-forming unit (BR3)	Deltaic and/or alluvial sediments	[2-10] Deltaic sediments; [11] Alluvial fan sediments
Mantling unit	14	Smooth; retains small craters; cliff-forming; grades into linear bedforms	Overlies and obscures all units but the dark-toned bedforms unit	Aeolian deposits	[2] Aeolian deposits
Dark-toned beforms unit	15	Dark-toned; complex bedforms	Abuts the brecciated, ridge-forming unit	Modern aeolian deposits	none

Table 1 continued.

Stratigraphic Unit	Elevations (m)†	Thickness (m)	Albedo	Mineralogy
Massive, basal unit	-1585 to -1495	> 30	0.13 to 0.15	[13]Olivine
Orthogonally-fractured unit	-1405 to -1200	> 70	0.11 to 0.18	unknown
Brecciated unit	-1570 to -1200	> 60	0.11 to 0.17	[12,13]Fe/Mg phyllosilicates
Pitted unit	-1545 to -1200	> 130	0.11 to 0.16	unknown
Ridge-forming unit	-1540 to -1200	> 90	0.10 to 0.17	[12,13]Fe/Mg phyllosilicates
Knobby unit	-1580 to -1200	> 15	0.11 to 0.15	unknown
Sub-polygonally fractured unit	-1495 to -1300	< 9	0.12 to 0.15	[12,13]Fe/Mg phyllosilicates
Layered, light-toned unit	-1465 to -1320	< 50	0.13 to 0.25	[12,13]Fe/Mg phyllosilicates; [13]Unidentified hydrated minerals; [13]High-calcium pyroxene
Mantling unit	-1585 to -1200	< 5	0.09 to 0.13	[13]High-calcium pyroxene; [13]Olivine
Dark-toned beforms unit	-1500 to -1450	< 5	0.07 to 0.09	unknown

* See text for a description of alternate hypotheses

† Observations were restricted to below -1200 m

[1] Scott & Tanaka (1986); [2] Pondrelli et al. (2008); [3] Scheiber (2007) ; [4] Malin & Edget (2003); [5] Moore et al. (2003); [6] Bhattacharya et al. (2005); [7] Wood (2006); [8] Lewis & Aharaonson (2006); [9] Pondrelli et al. (2008); [10] Pondrelli et al. (2010); [11] Jerolmack et al. (2004); [12] Milliken & Bish (2010); [13] McKeown & Rice (2011)

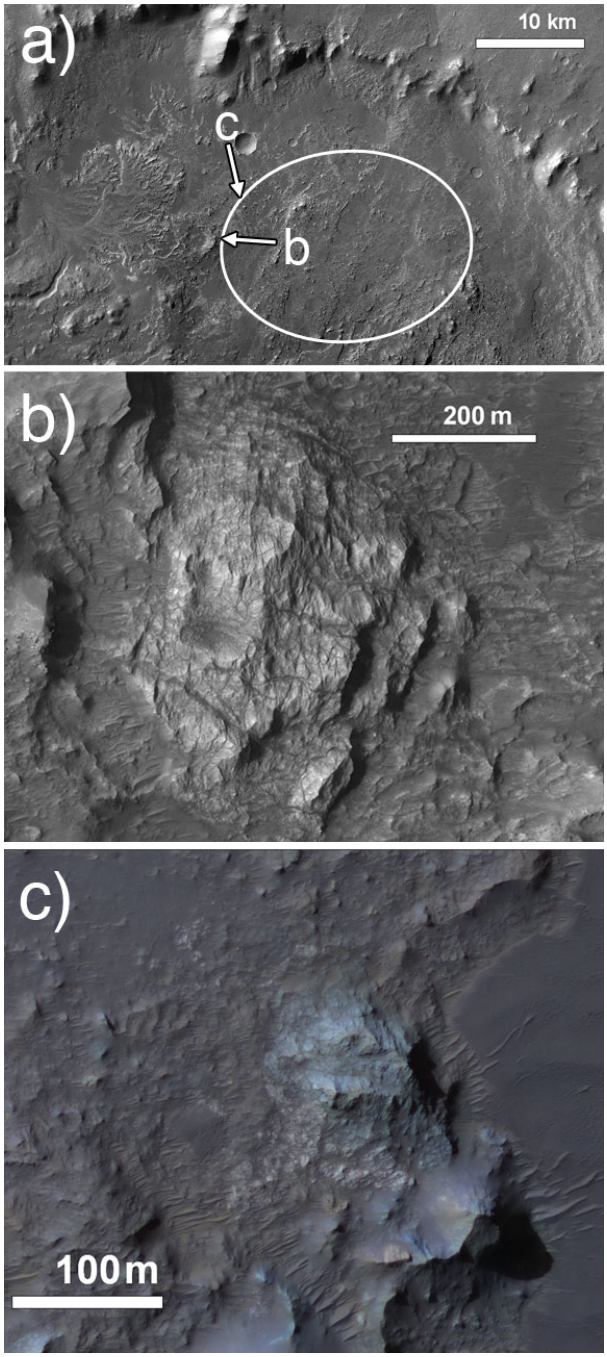

Figure 4. Examples of the massive, basal unit: (a) CTX mosaic of Eberswalde crater indicating the locations of 4b-c and the proposed MSL landing ellipse; (b) example of the massive, basal unit near the rim of an impact crater (from HiRISE observation ESP_020034_1560_RED); (c) Example of color variations within the massive, basal unit (from HiRISE observation PSP_010052_1560_COLOR). North is oriented at the top of the page in all images. (figure4.jpg)

Orthogonally-fractured unit

Observations. The orthogonally-fractured unit is homogeneous, systematically fractured, and massive. It occurs as outcrops several kilometers wide along the eroded southern crater rim, and also as smaller (0.5-1 km) isolated outcrops (Figure 5). The fracture spacing ranges from 5-50 m, and orientations are typically NNW-SSE and ENE-WSW. In some locations, the fractures appear to have eroded deeply (Figure 5b), creating clusters of four-sided columns. In others, the fractures are mantled (Figure 5c), and only the surfaces of the separate forms are visible.

Hypotheses and interpretations. Like the massive, basal unit, the orthogonally-fractured unit can also be interpreted as pre-crater-fill basement material. In this scenario, the orthogonally-fractured outcrops would have undergone a different set of stresses than the massive, basal unit in order to create the fracture sets exemplified in Figure 5, and are composed of different mineralogies that do not exhibit similar blueish hues (*e.g.*, Figure 4c) in false color images.

An alternate hypothesis is that the orthogonally-fractured outcrops are large (>100 m) ejecta blocks from the Holden impact event. The large Holden crater to the southwest is younger than Eberswalde crater (*e.g.*, Malin and Edgett 2003), and ejecta from the Holden impact event would likely have been deposited along the southern rim of Eberswalde crater and within the basin. The linear depression extending northward from the northwestern rim of Eberswalde crater (Figure 1c) may have formed from a Holden ejecta ray, implying that large blocks could have been ejected even further than the northern Eberswalde rim. It is plausible, therefore, that large outcrops of this unit were ejected from Holden and perhaps developed their orthogonal fracture patterns upon impact.

Brecciated unit

Observations. The brecciated unit is composed of angular, partially- to fully-formed megaclasts (meters to tens of meters in size) encased in a light-toned matrix (*e.g.* Figure 6d-f). In false color HiRISE images, the megaclasts are heterogeneous and distinct in hue (light blue to blue-green) from the matrix and other crater floor materials (*e.g.*, Figure 6f). Shadows cast by some megaclasts imply that they protrude from the matrix (Figure 6e inset); in some outcrops, however, shadows indicate pits in the matrix where megaclasts may have been removed.

Some outcrops of the brecciated unit contain long (up to 2 km) light-toned veins with variable widths (<1-20 m). In the western portion of the crater, the veins are sub-parallel at the kilometer scale (Figure 6b) but appear random at smaller scales (Figure 6c). Some wider veins (Figure 6c) are heterogeneous in color and texture, and appear to consist of angular clasts. Milliken and Bish (2010) detected phyllosilicate minerals within these outcrops using data from the MRO Compact Reconnaissance Imaging Spectrometer for Mars (CRISM); the spatial resolution of the instrument (~18 m/pix), however, did not allow them to determine whether the phyllosilicates were confined to the veins or to the darker, massive material or megaclasts.

Hypotheses and interpretations. Pondrelli et al. 2008 interpreted these crater floor materials as a series of eroded remnants of lava flows and pyroclastic materials, based on

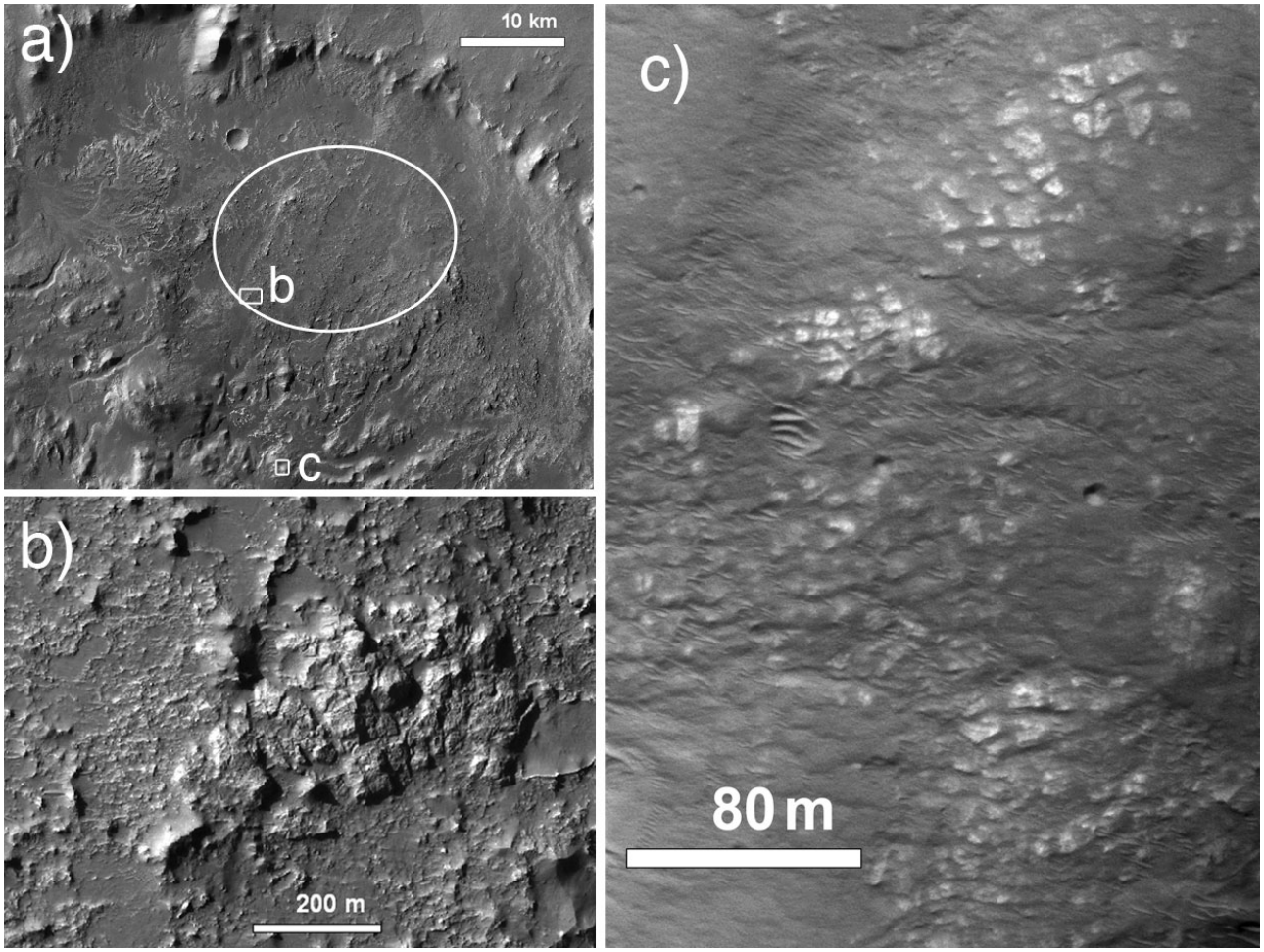

Figure 5. Examples of the orthogonally fractured unit: (a) CTX mosaic of Eberswalde crater indicating the locations of 5b-c and the proposed MSL landing ellipse; (b) example of an isolated, orthogonally fractured outcrop (from HiRISE observation PSP_010052_1560_RED); (c) example of the orthogonally fractured unit along the southern crater rim (from HiRISE observation ESP_018557_1560_RED). North is oriented at the top of the page in all images. (figure5.jpg)

the pre-MGS maps of Scott and Tanaka (1986). However, the lack of observable planform flow features, preserved lava surface textures, or volcanic constructs on or near Eberswalde crater make it difficult to confirm a volcanic hypothesis. In addition, given the observed size of the breccia blocks (meters to tens of meters), it is unlikely that these deposits are volcanic as they would have to have been derived from a proximal and explosive volcanic source that has not been detected. While a volcanoclastic interpretation cannot be completely ruled out for the brecciated unit, we consider the lack of primary volcanic morphologies within the crater as the best possible evidence against this hypothesis.

Our observations are more consistent with the interpretation by Schieber (2007) that these outcrops are megabreccia derived from impact events. In terrestrial impact craters, megabreccias have been described as poorly sorted deposits that are commonly lithified and consist of large (meter-scale) angular to subrounded clasts (*e.g.*, French 1998). Based on their morphology and distribution, impact megabreccia can be distinguished as parautocthonous (having formed nearly in-place) or allocthonous (consisting of rocks derived from elsewhere).

Ejecta from the Holden impact event would likely have been deposited along the southern rim of Eberswalde crater and within the basin as allocthonous megabreccia. Using empirical expressions for the radial decay of ejecta thickness by Garvin and Frawley (1998), we estimate that the entire floor of Eberswalde crater could have been covered by Holden ejecta (up to ~1.6 km thick in southern Eberswalde, and 100-200 m thick near the northern Eberswalde rim). The spatial distribution of the brecciated unit (Figure 3) is consistent with the hypothesis that these materials are related to the Holden impact event.

Because of the heterogeneous colors of megaclasts that we interpret as evidence for a heterogeneous lithology within this unit (*e.g.*, Figure 6f), we suggest that these materials are allocthonous megabreccia comprised of blocks ejected during the Holden impact. These blocks are held in place by a matrix material, which may be more erosion-resistant than the blocks themselves, as indicated by the pits remaining in

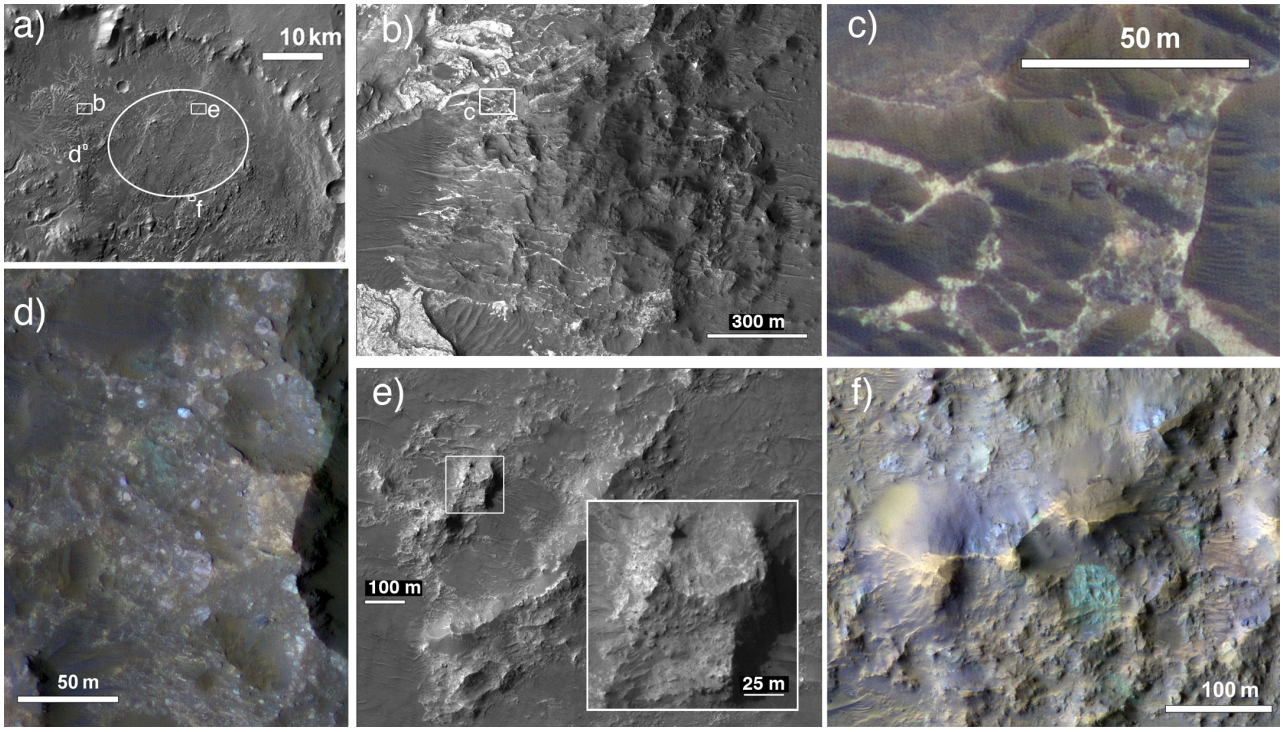

Figure 6. Examples of the brecciated unit: (a) CTX mosaic of Eberswalde crater indicating the locations of 6b-f and the proposed MSL landing ellipse; (b) example with sub-parallel, linear veins (from HiRISE observation ESP_012610_1560_RED); (c) close-up, color image of a vein in the brecciated unit (location shown in (b)); (d) color variations in megaclasts along a crater rim (from HiRISE observation PSP_04000 _1560_COLOR); (e) outcrop of the brecciated unit (from HiRISE observation PSP_019335_1560_RED), with the inset showing ~5-10 m megaclasts encased in a light-toned, fine-grained matrix (from HiRISE observation PSP_019190_1560_RED); (f) example of color variations of megaclasts in the eastern portion of the crater (from HiRISE observation ESP_011265_1560_COLOR). North is oriented at the top of the page in all images. (figure6.jpg)

some place where blocks appear to have been removed. Alternatively, the blocks may be "falling out" of a more erodible matrix, as is suggested by the blocks protruding from the matrix (Figure 6e-f); however, a lag of boulders is not observed at the base of large outcrops.

The vein-cut outcrops, however, may be parautocthonous megabreccia formed nearly in-place during the Eberswalde crater impact event. Their color, morphology, and dissection by light-toned veins (*e.g.*, Figure 6b) are consistent with parautocthonous megabreccia previously identified near the rim of Holden crater (Grant et al. 2008; Tornabene et al. 2009). The light-toned veins in megabreccia near Holden crater have been interpreted as breccia injection dikes formed by the circulation of hydrothermal fluids following the impact event (Tornabene et al. 2009), and we adopt a similar interpretation for the veins observed in the Eberswalde.

Pitted unit

Observations. The pitted unit covers much of the floor of Eberswalde crater (Figure 3). This unit is light-toned and is characterized by a pitted morphology, which transitions over several hundred meters from dense clusters of < 30 m wide pits to isolated light-toned quasi-circular depressions < 10 m wide (*e.g.*, Figure 7b). In places, the quasi-circular depressions are variably covered with and filled by the mantling unit (Figure 7c). The unit exhibits a range of topographic expressions: flat-laying, scarp-forming, ridge-forming, and undulating.

This unit appears to grade continuously into the brecciated unit, making it difficult to determine the boundary between these units; furthermore, the average CTX albedo of the pitted material (~0.14) is the same as the matrix material of the brecciated unit. Our mapping of these units (Figure 3) is thus rather equivocal. Ultimately, we distinguish this pitted unit from the brecciated unit by the absence of megaclasts entrained in the light-toned material. *Hypotheses and interpretations*. While Pondrelli et al. (2008) interpreted this unit as lacustrine sediments that were emplaced in the deepest part of a possible Eberswalde lake, we have observed no evidence for layering that would support that hypothesis. Also, the pitted morphology is inconsistent with the observed erosional morphology of other putative lacustrine sediments on Mars (*e.g.*, Grant et al. 2008; Warner et al. 2010). We therefore propose three alternate interpretations for this unit: (1) the depressions are the result of heterogenous erosion of an ancient surface saturated with small impact craters; (2) the pitted morphology formed as a result of de-volatilization and degradation of an ancient, basal impact melt surface; and (3) the light-toned material may be the erosionally resistant matrix of the brecciated unit and/or the vein-like features within the brecciated material, and the pitted morphology may result from the "holes" left

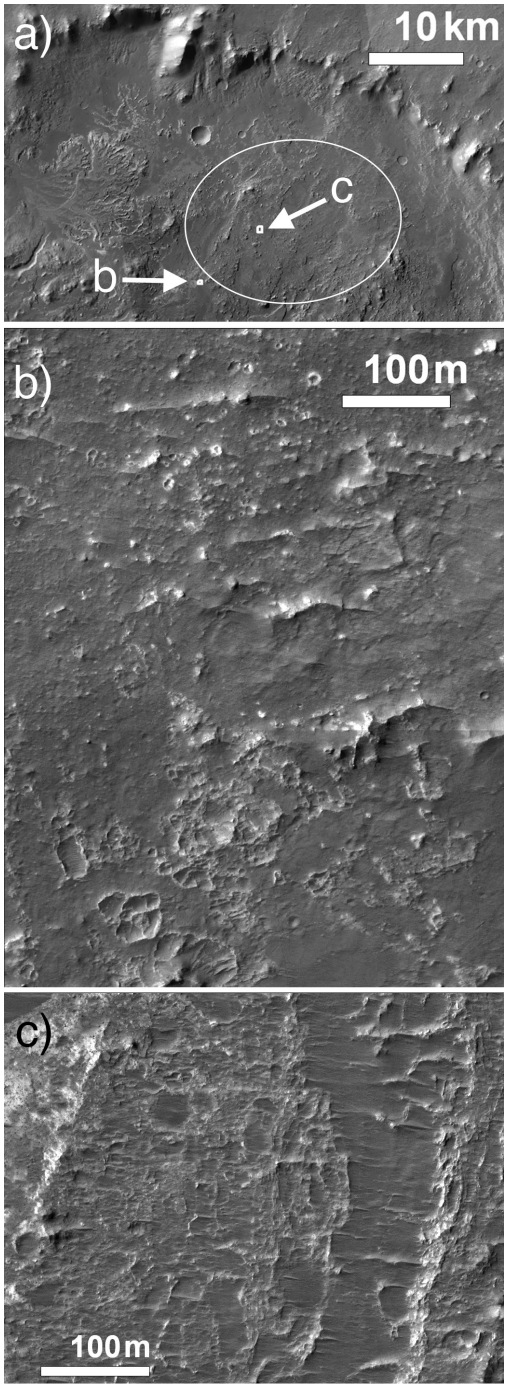

Figure 7. Examples of the pitted unit: (a) CTX mosaic of Eberswalde crater indicating the locations of 7b-c and the proposed MSL landing ellipse; (b) example of pitted, discontinuous light-toned material (bottom half of image) transitioning northward to isolated, light-toned, quasi-circular depressions (from HiRISE observation PSP_010474_1560_RED); (c) example of pitted material variably covered and filled by the darker-toned mantling unit (from HiRISE observation PSP_010052_1560_RED). North is oriented at the top of the page in all images. (figure7.jpg)

by megaclasts that have since been removed. There are similarities between the pitted, discontinuous light-toned unit and the brecciated unit, such as their albedos and the sizes of the pits/megaclasts, that support hypothesis (3). The apparent gradational relationship between the pitted and brecciated units is consistent with this hypothesis as well. In support of hypothesis (2), we note that for large, near-pristine impact craters on Mars, a pitted surface texture is often observed on the crater floor, within materials that immediately superpose the primary bedrock of the impact crater. A key example is the relatively pristine pitted terrain within the floor of the 50-km-wide, Hesperian to Early Amazonian-age Mojave crater (Williams and Malin 2008), which has pits covering the vast portions of the crater floor, terraces and rims (Boyce et al. 2011). This pitted material has been interpreted as impact melt that, upon cooling and solidification, underwent devolatilization (McEwen et al. 2007b; Tornabene et al. 2007; Williams and Malin 2008).

According to that model, the pits would be regions of collapse formed by surface deflation due to volume loss within the cooled melt. The surface texture of the pitted unit within Eberswalde crater may therefore represent a degraded example of such devolatalized terrain, with the possible addition of degraded, small impact craters. In this hypothesis, we would expect the pitted unit to predate and underlie the brecciated unit, which we interpret as allochtonous ejecta from the Holden impact; however, these types of contact relationships have not been clearly observed (see Unit Associations, Successions and Geometries below).

Pondrelli et al. (2011) termed this unit the "non-layered member" of the "Eberswalde Formation"; however, we do not associate this unit with the fan deposits based on observed contact relationships (see Unit Associations, Successions and Geometries for further discussion). Consistent with all interpretations, the pitted unit likely represents exposed remnants of ancient floor material that is unrelated to the younger, fluvio-lacustrine processes that formed the putative delta.

Ridge-forming unit

Observations. The ridge-forming unit (Figure 8) has the most extreme local relief of any material within Eberswalde crater, and it is characterized by sharp peaks, scarps and ridges. This unit includes outcrops that appear homogeneous in albedo and color, are not extensively fractured, and that contain horizontal lineations that may indicate layering. Possiblye layering is also indicated by the shadows cast from more erosionally-resistant material that forms cliffs or overhangs (*e.g.*, Figure 8c). It is often unclear whether the homogeneous appearance is due to a single composition of the outcrop or a uniform covering of dust and/or the mantling unit. In many occurrences, this unit exhibits steep cliffs along linear scarps (*e.g.*, Figure 8d). Boulders observed at the base of these cliffs likely have been shed from these outcrops (*e.g.*, Figure 8f).

Hypotheses and interpretations. A hypothesis for the homogeneous appearance of the ridge-forming unit is that these outcrops are in fact other crater floor units (*e.g.,* the brecciated unit and/or orthogonally fractured unit) that have been draped by the mantling unit. The mantling may be

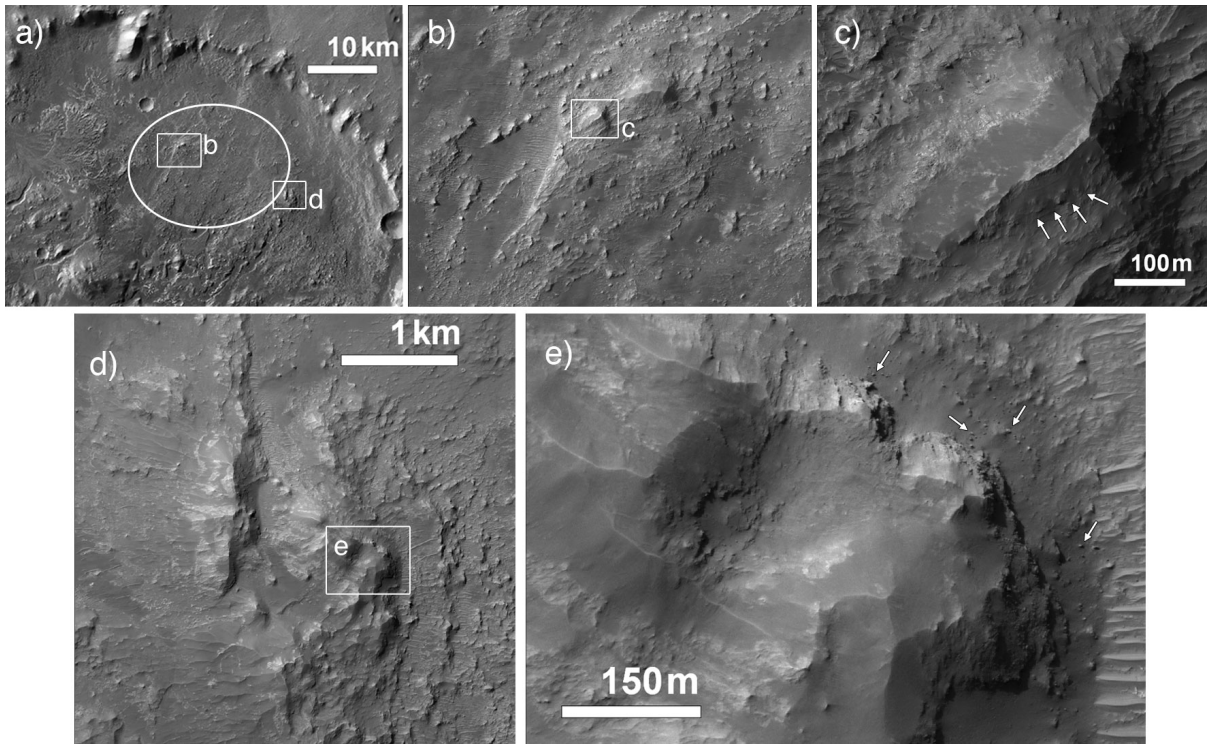

Figure 8. Examples of the ridge-forming unit: (a) CTX mosaic of Eberswalde crater indicating the locations of 8b,d and the proposed MSL landing ellipse; (b) example of the ridge-forming unit with extreme topography within the landing ellipse (from HiRISE observation PSP_010474_1560_RED); (c) close-up example showing possible layering, location shown in (b); (d) example of the ridge-forming unit along a topographic divide in the east of the crater (from HiRISE image ESP_016210_1560_RED); (e) close-up of a cliff shedding boulders, location shown in (d). North is oriented at the top of the page in all images. (figure8.jpg)

obscuring the light-toned veins, heterogeneous colors, or other defining characteristics of the underlying outcrop, and the layered appearance may result from fractures in the cemented mantling material. Light-toned material visible at the base of some outcrops is consistent with the hypothesis that these are outcrops of the pitted or brecciated units covered by mantling. Alternately, the ridge-forming unit may represent layered strata consisting of aeolian deposits, volcanic ash, or fluvial/lacustrine sediments.

Knobby unit

Observations. Much of the west-central portion of the Eberswalde crater floor is covered with isolated hillocks of light-toned rock which we have mapped as the "knobby" unit (Figure 3). The knobs are typically < 30 m wide, < 50 m high, and spaced > 50 m apart (Figure 9). While most consist of massive, light-toned, rock-forming peaks or ridges, some knobs are rounded and covered with meter-size boulders (*e.g.*, Figure 9c).

Hypotheses and interpretations. It is unclear whether the meter-size boulders observed in HiRISE images represent formerly *in-situ*, eroded clasts or materials that were deposited on the surface of the knobby unit after it was emplaced. If the boulders are not in place, one possible interpretation for the knobby unit is that it was derived from a laterally extensive ejecta deposit that was possibly associated with nearby impact crater formation. If the boulders are in place, however, the knobs likely represent a series of erosion-resistant mesas and hills that are remnants of a more extensive unit(s) that once covered the west-central portion of the Eberswalde basin floor, possibly including the sub-polygonally fractured unit and/or the layered light-toned unit (although no layering is observed in the knobs at the scale of HiRISE observations). Because the density of boulders is greatest on the knobs themselves (Figure 9c), we favor the interpretation that the boulders are erosional.

An alternate, albeit speculative, hypothesis is that the knobs may be erosional remnants of glacial or periglacial features like pingos or thermokarst-like hummocks that were formed in previously ice-rich terrain. For example, deflation of ice-rich terrain has been proposed as a possible explanation for "hummocky terrain" in Gusev Crater (Gregg et al. 2007); however, those hummocks typically have much closer spacing and consist of poorly consolidated debris, which is not consistent with our observations.

Sub-polygonally fractured unit

Observations. Light-toned materials composed of angular, sub-polygonal blocks outcrop in several major locations within Eberswalde crater (Figure 3). The polygons are ~1-6 m in diameter, and the shapes of adjacent polygons are complementary (*i.e.*, the fractured forms fit together like

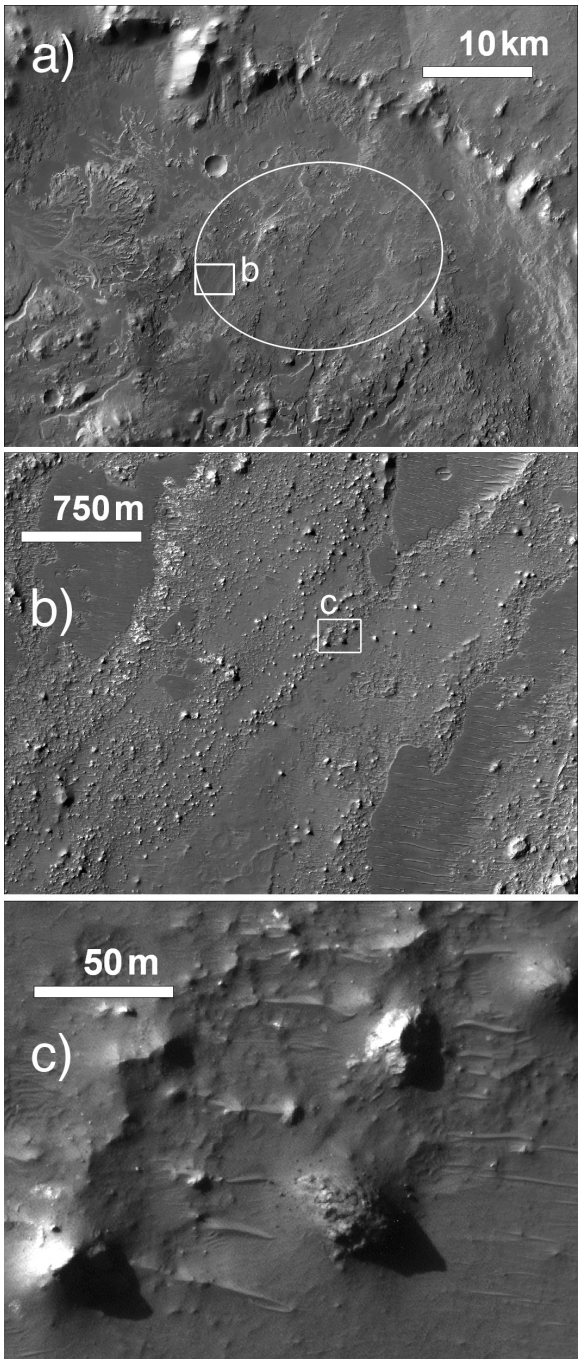

Figure 9. Examples of the knobby unit: (a) CTX mosaic of Eberswalde crater indicating the location of 9b and the proposed MSL landing ellipse; (b) a large extent of the knobby unit, covered by patches of the smooth mantling unit (from HiRISE observation PSP_010052_1560_RED). The white box indicates the location of 9c; (c) examples of knobs composed of massive, light-toned, ridge-forming material and a mound covered with meter-size boulders. North is oriented at the top of the page in all images. (figure9.jpg).

puzzle pieces and are not chaotically organized) (Figure 10). In places, the fractured light-toned unit clearly is weathering into meter-scale blocks (such as in Figure 10b) where this unit outcrops as isolated mesas.

Over the spatial distribution of this unit (Figure 3), we observe an apparent degradation of the continuous, fractured rock into a lag of boulders on the surface. Figure 10c shows an example of an intermediate stage of degradation, where the unit consists mainly of boulders, although complementary edges are still observed. Outcrops in the center of the crater, however, consist mainly of light-toned boulders (Figure 10f).

While other stratigraphic units also exhibit extensive fracturing (such as the layered light-toned unit), we restrict our characterization of the sub-polygonally fractured unit to flat-lying, spatially extensive exposures. This unit may conform to topography in some instances, such as along the bedforms near the fan-form feature in the north of the crater (Figure 10d); however, it is unclear whether the fractured material drapes preexisting bedforms, or whether the bedforms are within this unit (*e.g.*, as wind-carved transverse erosional ridges; Montgomery et al. 2011).

Hypotheses and interpretations. The complementary form of the fractures suggests that the light-toned material has been fractured in place, as opposed to having been deposited as a breccia (Pondrelli et al. 2008). The fracturing could represent desiccation cracks in dehydrated sulfate- or clay-rich strata. In support this hypothesis, CRISM data are consistent with the presence of phyllosilicate minerals (Milliken and Bish 2010). However, Schieber (2007) argued that desiccation cracks of clay-rich mudstones are typically much smaller than those observed in Eberswalde, and that the fracturing is more likely due to thermal contraction of sandstones encrusted by evaporite minerals. An alternate hypothesis is that the fracturing is due to tectonic stress; however, we have observed no preferred orientation to the fractures bounding polygons. Jerolmack et al. (2004) extrapolated that, if the fan-shaped feature in western Eberswalde were an alluvial fan and not a delta, the fan sediments would have extended 45 km from the western rim past the center of the Eberswalde basin. Because all exposures of the fractured light-toned unit occur within this distance from the western rim (Figure 3), it is possible that these outcrops are the remnants of such extensive fan deposits. Alternately, if the fan-shaped feature is indeed a delta, the fractured light-toned unit may represent an extended delta bottomset and associated lacustrine sediments. This hypothesis is consistent with the detection of phyllosilicate minerals (Milliken and Bish 2010) and the unit's association with other fan-shaped features in Eberswalde.

An additional hypothesis is that the light-toned material consists of tephra (volcanic airfall) deposited subaerially or subaqueously within the crater. However, this interpretation cannot be confirmed from morphology alone, but will likely require *in-situ* observations of composition and stratigraphy. Fallout tephra deposits systematically thin away from the source and drape local topography. While we have observed no systematic trend in unit thickness, this does not rule out tephra deposits from multiple volcanic source regions or

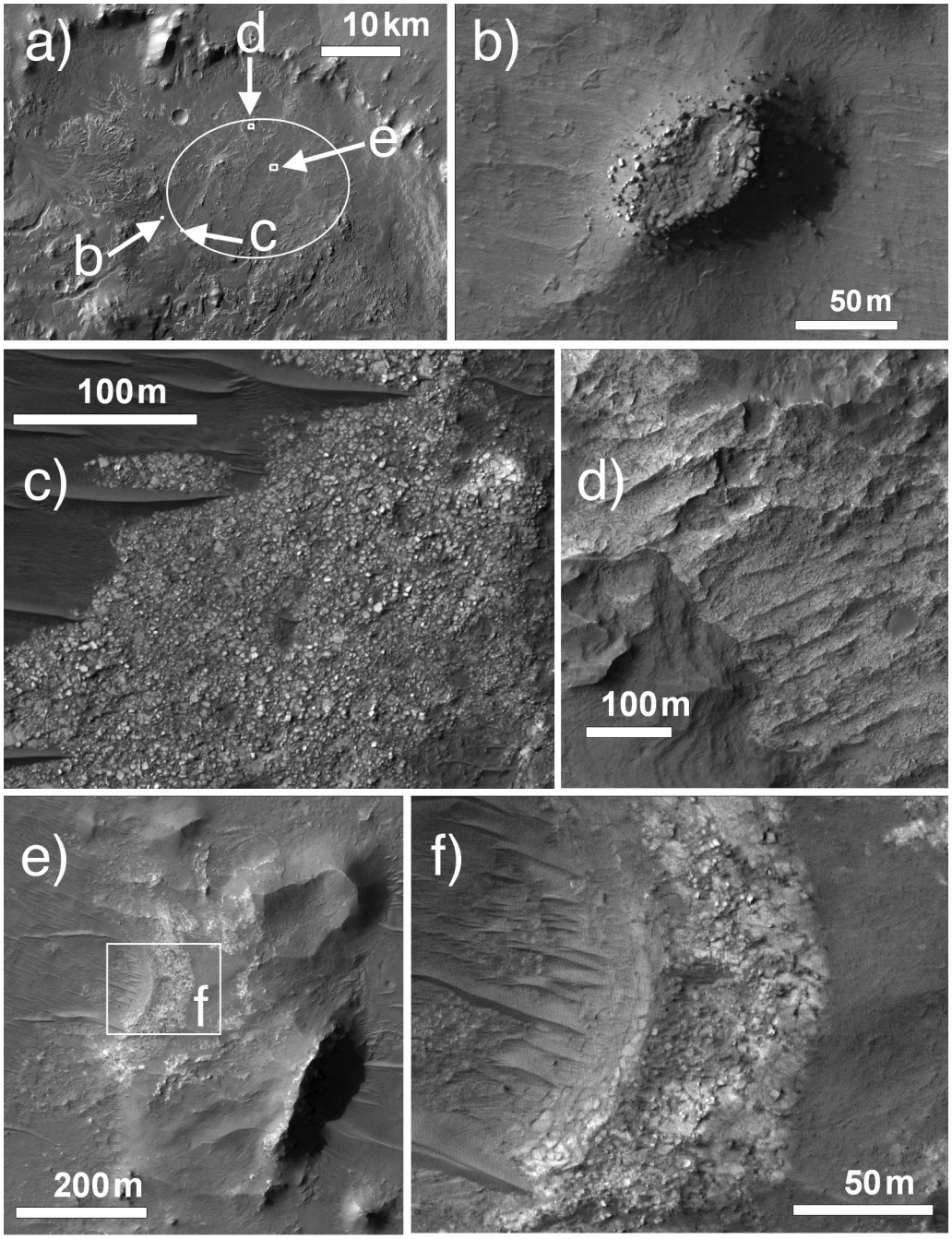

Figure 10. Examples of the sub-polygonally fractured unit: (a) CTX mosaic of Eberswalde crater indicating the locations of 10b-e and the proposed MSL landing ellipse; (b) an isolated mesa of the sub-polygonally fractured unit shedding boulders (from HiRISE observation PSP_010553_1560_RED); (c) an extensive outcrop at the edge of the landing ellipse (from HiRISE observation PSP_010052_1560_RED); (d) bedform features in the sub-polygonally fractured unit (from HiRISE observation PSP_010474_1560_RED); (e-f) fractured light-toned rock along the rim of a partially-preserved impact crater (from HiRISE observation ESP_019335_1560_RED). North is oriented at the top of the page in all images. (figure10.jpg)

from regionally/globally extensive airfall. However, we also have identified no occurrences of this unit draped at varying elevations, which is the strongest observation against a subaerial volcanic airfall hypothesis. As we elaborate in the Unit Associations, Successions and Geometries section, the fractured light-toned material is restricted to occurrences below a common elevation in the Eberswalde basin.

Layered light-toned unit

Observations. Light-toned rock that is clearly layered at the scales of HiRISE and MOC images crops out near the north, west, and southern rims of Eberswalde crater, and the most extensive outcrops are associated with the putative delta in the west of the crater (Figures 11-13). This layered light-toned unit has the highest CTX albedo (up to 0.25) of any

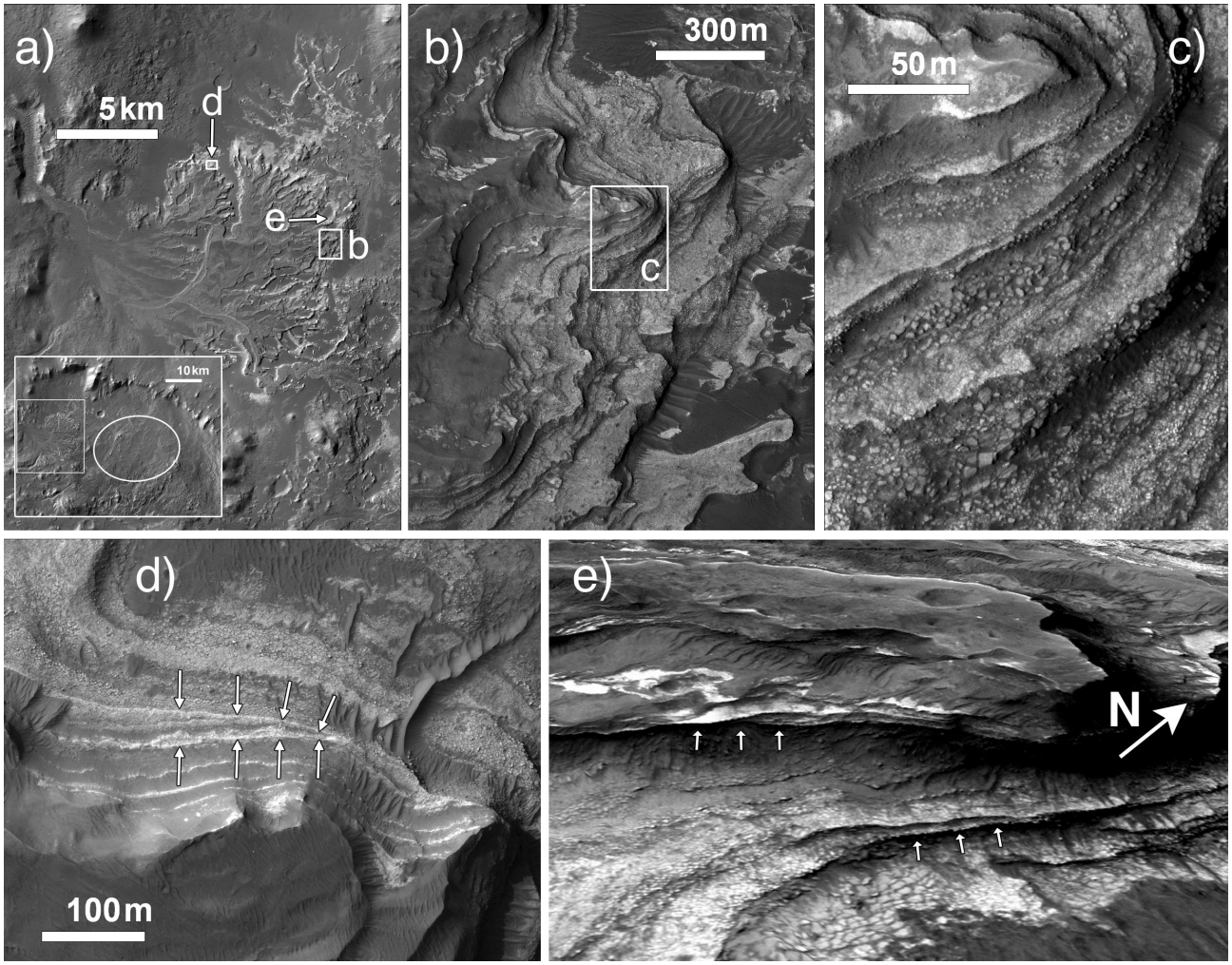

Figure 11. Examples of the layered light-toned unit exposed at the putative Eberswalde delta: (a) the locations of 11b-e at the terminus of the putative delta (from CTX observation P01_001336), with the inset indicating the locations of the putative delta and the proposed MSL landing ellipse within Eberswalde crater; (b) stair-step layers along the eastern front of the putative delta (from HiRISE observation PSP_004000_1560_RED), the white box indicates the location of 11c; (c) sub-polygonal fracturing in light-toned layers; (d) a possible downlap relationship in the north lobe (from HiRISE observation PSP_001534_1560_RED); (e) perspective view showing shadows cast by overhanging layers (from HiRISE observation PSP_004000_1560_RED draped over a DTM). North is oriented at the top of the page in all images unless otherwise noted. (figure11.jpg)

material within the crater. Because there are albedo variations between layers, it is possible that the unit consists of light and dark layers that represent lithologic or sedimentologic variations in the outcrop; however, we are often unable to discern whether the lower albedo is a true characteristic of the darker layers, or if these layers are more consistently covered by a mantling unit. Some layers at the edge of the putative delta are more erosionally resistant than others and form thin (< 50 cm) overhangs that cast shadows upon the layers below (Figure 11e). The layers have measured dips of 1-3° (Lewis and Aharonson 2006), and no clear clinoforms are observed at the front of the putative delta (*e.g.*, Figure 11e). We have observed only one possible downlap relationship in the northern lobe of the putative delta (Figure 11d), although some layers appear to pinch out.

The upper layers of the putative delta have no obvious fracturing, while the lower layers are extensively polygonally fractured (Figure 11c) and appear to be forming and shedding boulders that have fallen to the bottom of the cliff face. These lower layers are morphologically similar to some outcrops of the sub-polygonally fractured unit described in the previous section. In some layers along the edge of the delta, randomly oriented blocks appear to be resting on or within a finer-grained, darker-toned material. Although the top surface of the putative delta is thinly mantled, layering is discernable beneath this veneer in the planform features described extensively in previous studies, and which have been interpreted as channels, meander bends and chute cut-offs (Malin and Edgett 2003; Moore et al. 2003; Bhattacharya et al. 2005; Wood 2006; Lewis and Aharonson 2006; Pondrelli et al. 2008). The expression of layering on this surface differs from the layered light-toned unit visible at the putative delta front, as the albedo is significantly lower (0.13 as opposed to 0.25) and fracturing cannot be discerned (see Figure 14 of Pondrelli et al. 2008).

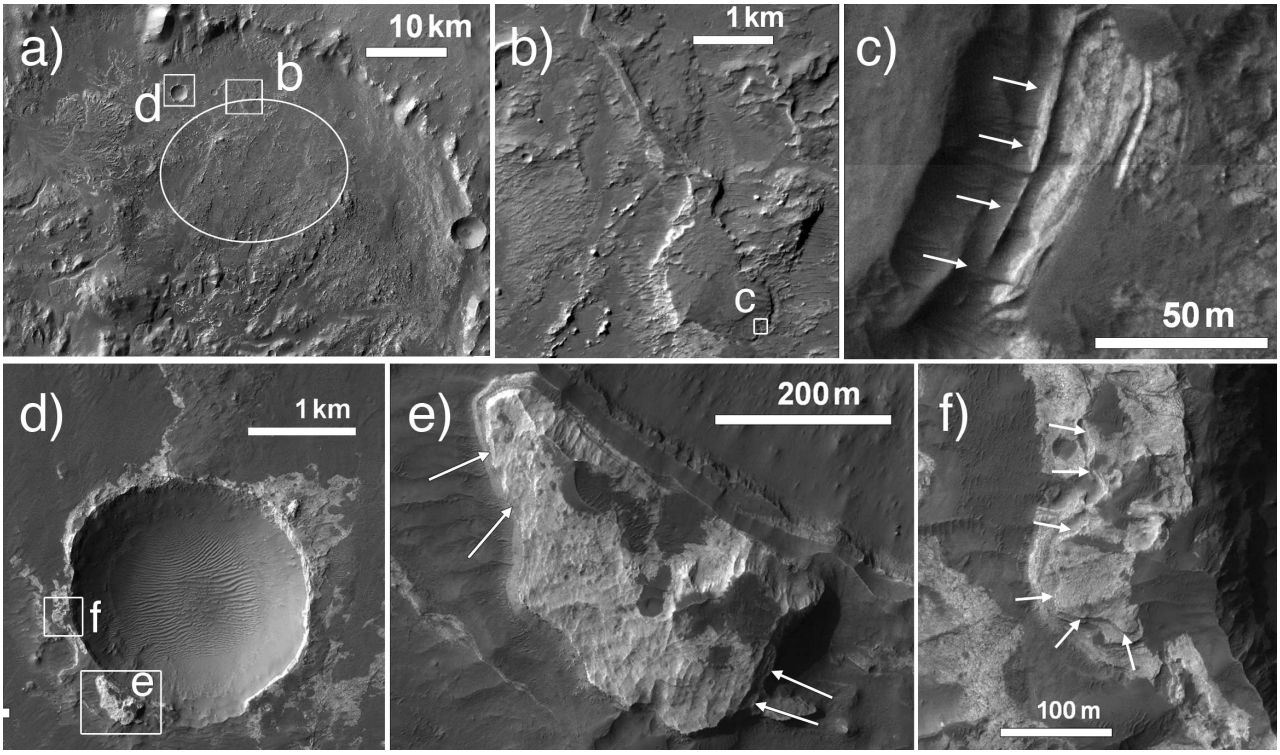

Figure 12. Examples of the layered light-toned unit in northern Eberswalde, with arrows indicating traceable layers: (a) CTX mosaic of Eberswalde crater indicating the location of 12b,d and the proposed MSL landing ellipse; (b) a lobate plateau of layered rocks in the north of Eberswalde crater (from HiRISE observation PSP_010764_1560_RED), the white box indicates the location of 12c; (c) layers exposed along the edge of a lobate plateau (from HiRISE observation PSP_010764_1560_RED); (d) context for layered rocks along the rim of a crater (from HiRISE observation PSP_010553_1560_RED), the white boxes indicate the locations of 12e-f; (e) a plateau of light-toned, layered rocks (from HiRISE observation PSP_010553_1560_RED); (f) layered rocks (partially mantled) (from HiRISE observation PSP_010553_1560_RED). North is oriented at the top of the page in all images. (figure12.jpg)

Because of these distinctions, we have mapped such surfaces as a subunit of the layered light-toned unit (indicated as the "thinly-mantled layered unit" in Figure 3). Similar layering expressions are visible on the surfaces of other fan-form planteaus and sinuous ridges (e.g., Figure 19d).

The distribution of layering in other locations is shown in Figure 3. In northern Eberswalde crater, the light-toned layered unit is visible along the edge of a fan-shaped feature and individual layers are traceable for < 100 m (Figures 12b-c). Layered rock also crops out along the rim of an impact crater (Figures 12d-f). In these locations, the light-toned layered unit is not as extensively fractured as in the putative delta. Where the uppermost surface is not covered by the mantling unit, the rock appears to have eroded into "scalloped" depressions (*e.g.*, Figure 12e), similar to those observed in on Tharsis Montes, at White Rock in Pollack Crater (Bridges et al. 2010) and within Gale Crater (Anderson and Bell 2010).

In southwest Eberswalde, the layered light-toned unit is associated with a more extensive exposure of other light-toned materials (Figure 13b) and exhibits a diverse range of morphologies (Figures 13c-f). The material is clearly fractured along the cliff face of a plateau of layered rock (Figure 13c), but ~2 km further south, where visible along the edges of sinuous landforms, the layers are not fractured and are covered more extensively by the mantling unit. The layered rock forms both cliff faces (*i.e.*, Figure 13e) and "stair-step" geometries (*i.e.*, Figure 13f). In southern Eberswalde (Figures 13g-i), the light-toned layers are sub-polygonally fractured and associated with 1-5 m boulders.

Hypotheses and interpretations. There is no clear evidence that the light-toned layered unit breaks into granule-sized particles (2-4 mm; Sharp, 1963), as we observe no light-toned dunes associated with the layered unit. Rather, we observe the layers to be fractured and shedding 1-10 m boulders. However, there is no extensive talus at the bottom of cliff faces. As Jerolmack et al. (2004) noted, a lack of talus may indicate that the unit erodes to sand-sized or finer grains (< 300 μm; Sharp, 1963) that are carried away by the wind. Given these observations, we interpret the light-toned, layered unit as being composed largely of weakly lithified, fine-grained material that, due to its fracturing, sheds boulders that are easily disintegrated. This hypothesis is consistent with the identification of Mg/Fe-phyllosilicates within the layers of the putative delta (Milliken and Bish 2010; McKeown and Rice 2011).

Based on the analyses of stratal geometries and discussions in Malin and Edgett (2003), Moore et al. (2003), Bhattacharya et al. (2005), Wood (2006), Lewis and Aharonson (2006) and Pondrelli et al. (2008), we interpret

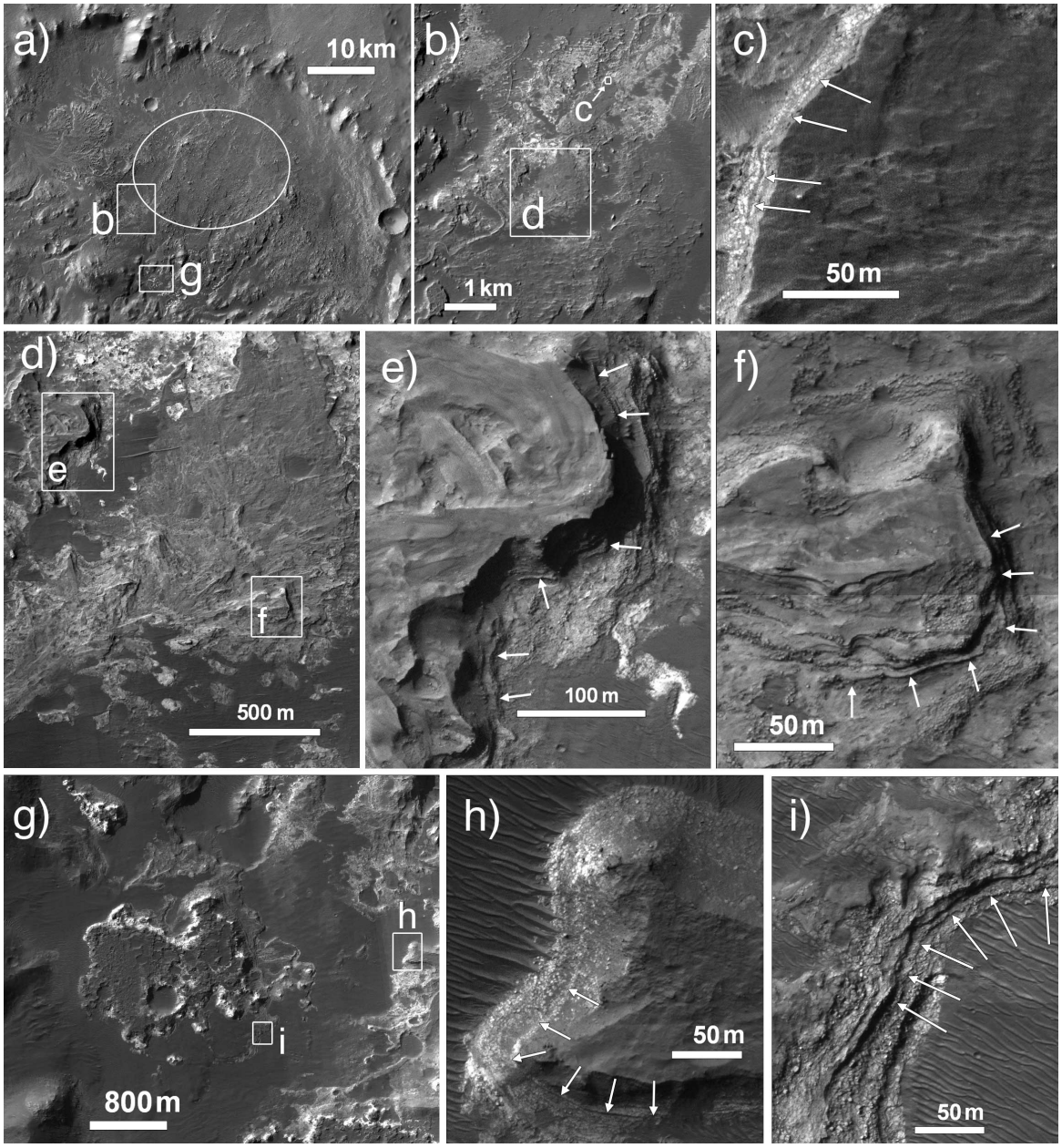

Figure 13. Examples of the layered light-toned unit in southern Eberswalde, with arrows indicating traceable layers: (a) CTX mosaic of Eberswalde crater indicating the location of 13b,g and the proposed MSL landing ellipse; (b) context for layered deposits in southwest Eberswalde crater, white boxes indicate the locations of 13c-d (from CTX observation P21_009274); (c) example of light-toned layers exposed in a cliff face (from HiRISE observation PSP_010553_1560_RED); (d) example of a fan-like plateau comprised of light-toned layers and context for 13e-f (from HiRISE observation ESP_018056_1560_RED); (e) example of layers exposed at the edge of a sinuous landform (from HiRISE observation ESP_018056_1560_RED) (f) example of light-toned layers exposed along a digitate landform (from HiRISE observation ESP_018056_1560_RED); (g) context for layered deposits in southwest Eberswalde crater, white boxes indicate the locations of 13h-i (from HiRISE observation ESP_018056_1560_RED); (h) example of light-toned layers exposed in along a digitate landform; (i) example of light-toned layers exposed beneath a tabular mesa. North is oriented at the top of the page in all images. (figure13.jpg)

the layered rock in western Eberswalde crater to be deltaic sediments. We interpret the layers in the northern (Figure 12), southwestern (Figures 13b-f), and southern (Figures 13g-i) portions of the Eberswalde basin as deltaic sediments as well due to their morphology, their association with possible fluvial features such as sinuous ridges and valleys, as well as their confinement to the margins of the crater (Rice et al. 2011).

The presence of layered light-toned material along the rim of a crater in northern Eberswalde (Figure 12d-f), however, is enigmatic. If this crater had been substantially eroded and later buried by deltaic sediments, it is unclear why the topographic crater would have been subsequently exposed. If

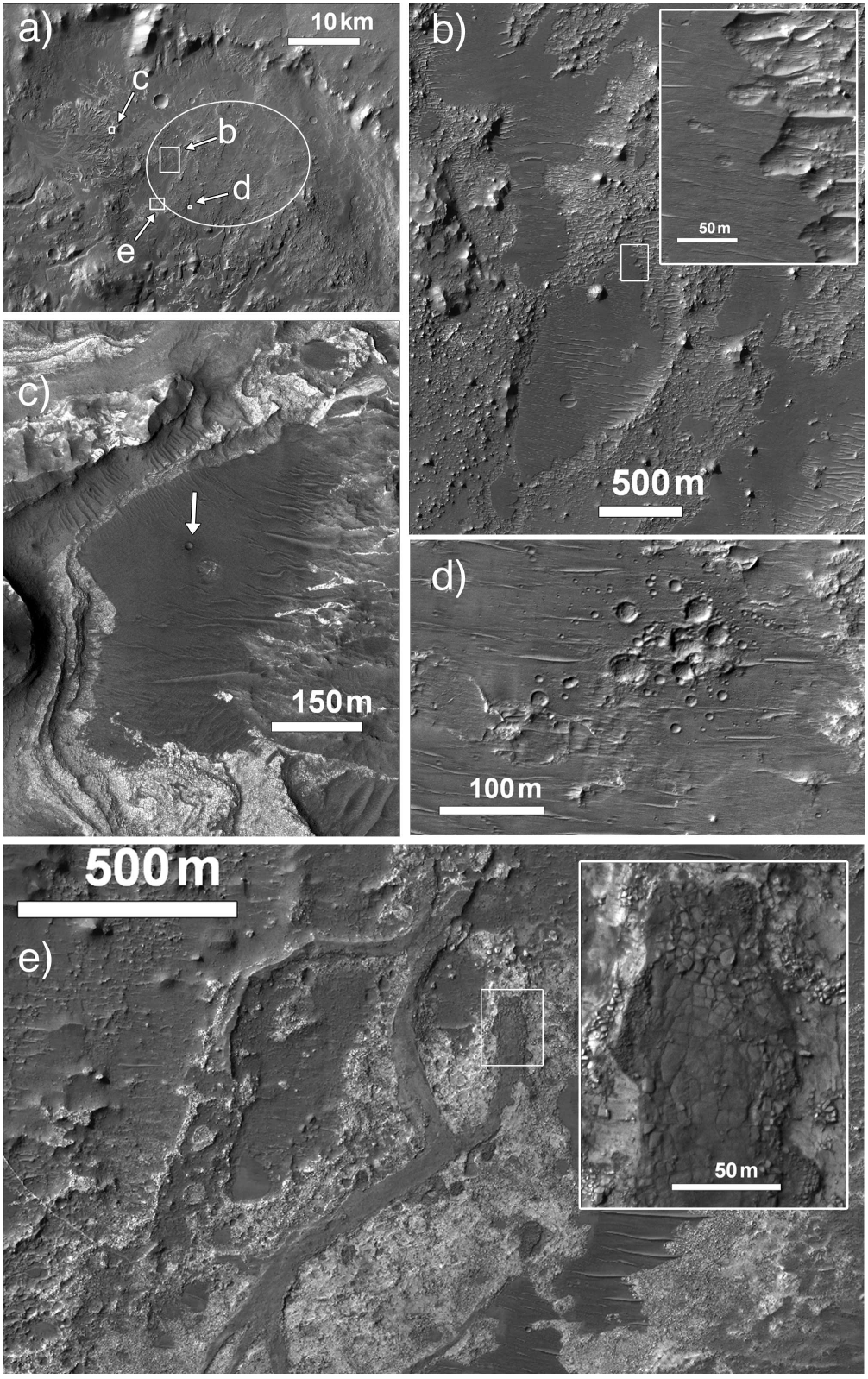

Figure 14. Examples of the mantling unit: (a) CTX mosaic of Eberswalde crater indicating the locations of 14b-e and the proposed MSL landing ellipse; (b) extensive occurrence of the mantling unit with the inset showing its cliff-forming nature (from HiRISE observation PSP_010052_1560_RED); (c) occurrence of the mantling unit where it onlaps underlying units; the arrow indicates a fresh impact crater exposing darker material in its ejecta (from HiRISE observation ESP_012610_1560_RED); (d) a cluster of fresh impact craters preserved in the mantling unit (from HiRISE observation PSP_010474_1560_RED); (e) the mantling unit covering a sinuous landform, the inset shows that the unit is thin enough to reveal the fractured nature of the material it covers (from HiRISE observation PSP_010052_1560_RED). North is oriented at the top of the page in all images. (figure14.jpg)

the crater is younger and represents an impact into deltaic layers, we would expect to see significant ejecta around the rim, which we do not observe. One possible explanation is that a fluvio-deltaic system was diverted around the raised rim of this crater, depositing layered material around its rim, and the rim material was subsequently eroded.

Additional hypotheses are that the layers are volcanic ash (deposited either subaqueously or subaerially), aeolian deposits, or potentially impact-generated base surge deposits (from large impacts which scatter enormous amounts of debris distally, as has been suggested for the layered rock in Meridian Planum by Knauth et al. 2005).

Mantling unit

Observations. The mantling unit consists of a dark (albedo 0.09-0.13), fine-grained, smooth material that covers the majority of the Eberswalde basin (Figure 3). Many small craters and clusters of craters are preserved in this unit (*e.g.*, Figure 14d), and in places the smooth mantling grades into aeolian bedforms with E-W trending crests typically ~100 m in length with ~40 m spacing (*e.g.*, Figures 14c-d). Near topographic obstacles, the bedforms are oriented perpendicular to cliff faces.

The mantling unit generally obscures the underlying topography, and it can terminate directly against another unit (*e.g.*, Figure 14c) or form cliffs along an erosional surface (*e.g.*, Figure 14b inset). No boulders are observed at the base of these cliffs, and no bedding planes have been observed along their edges. In places, the mantling is thin enough to reveal the form of the sub-polygonally fractured rock (Figure 13e) or sinuous landforms beneath (*e.g.*, Figure 11e). A fresh crater in the mantling unit near the terminus of the putative delta (Figure 13c) reveals that the underlying material has an even lower albedo than most surficial deposits.

Hypotheses and interpretations. Similar mantling deposits elsewhere on Mars have been interpreted as airfall dust deposits (*e.g.*, Christensen 1986; Bridges et al. 2010; Malin et al. 2010). Because of the preservation of small craters and its cliff-forming nature, we interpret the mantling unit as at least partially lithified. This implies that the bedforms are not recent; old, inactive, indurated bedforms have been widely observed across the planet (*e.g.*, Malin and Edgett 2001).

The absence of talus at the base of cliffs, however, implies that the indurated mantling material easily disintegrates into grain sizes small enough to be transported away by wind. The observation that the underlying material has a lower albedo than the surficial deposits suggests that the indurated mantling is covered by a thin layer of higher-albedo dust or has been altered at the surface, at least in places.

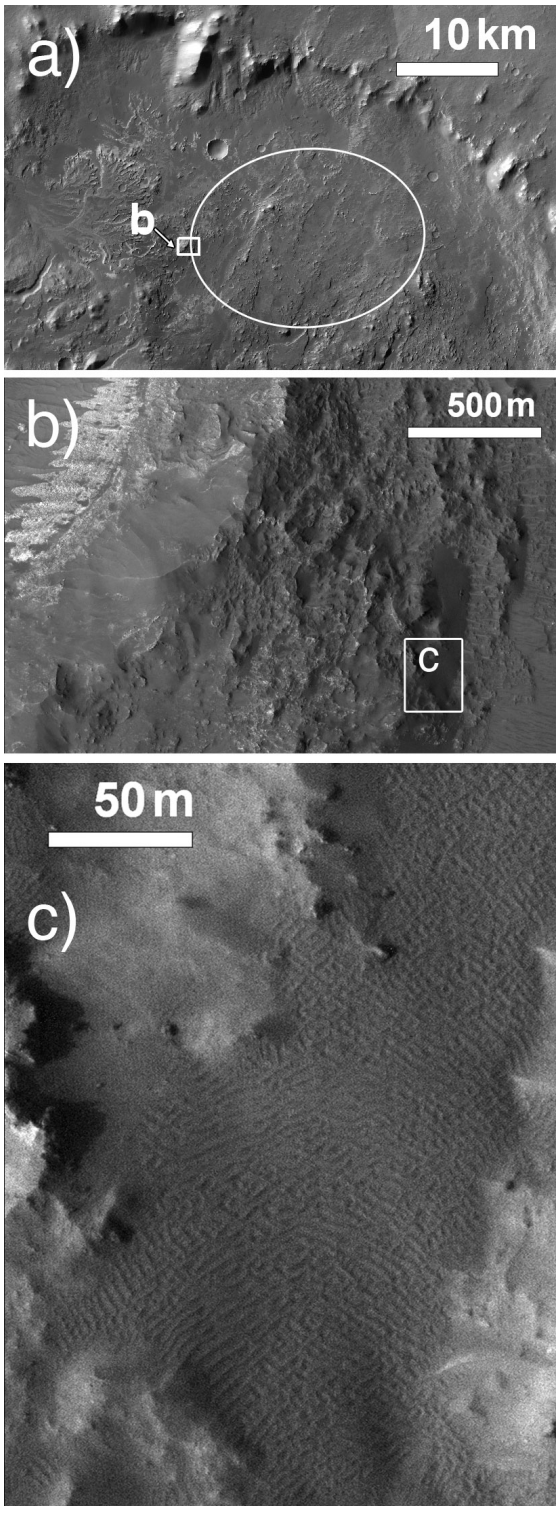

Figure 15. Examples of the dark-toned bedforms unit: (a) CTX mosaic of Eberswalde crater indicating the location of 15b and the proposed MSL landing ellipse; (b) context for the bedforms shown in 15c against the rim of an impact crater (from HiRISE observation ESP_012610_1560_RED); (c) dark-toned, complex bedforms preserving no small craters. North is oriented at the top of the page in all images. (figure15.jpg)

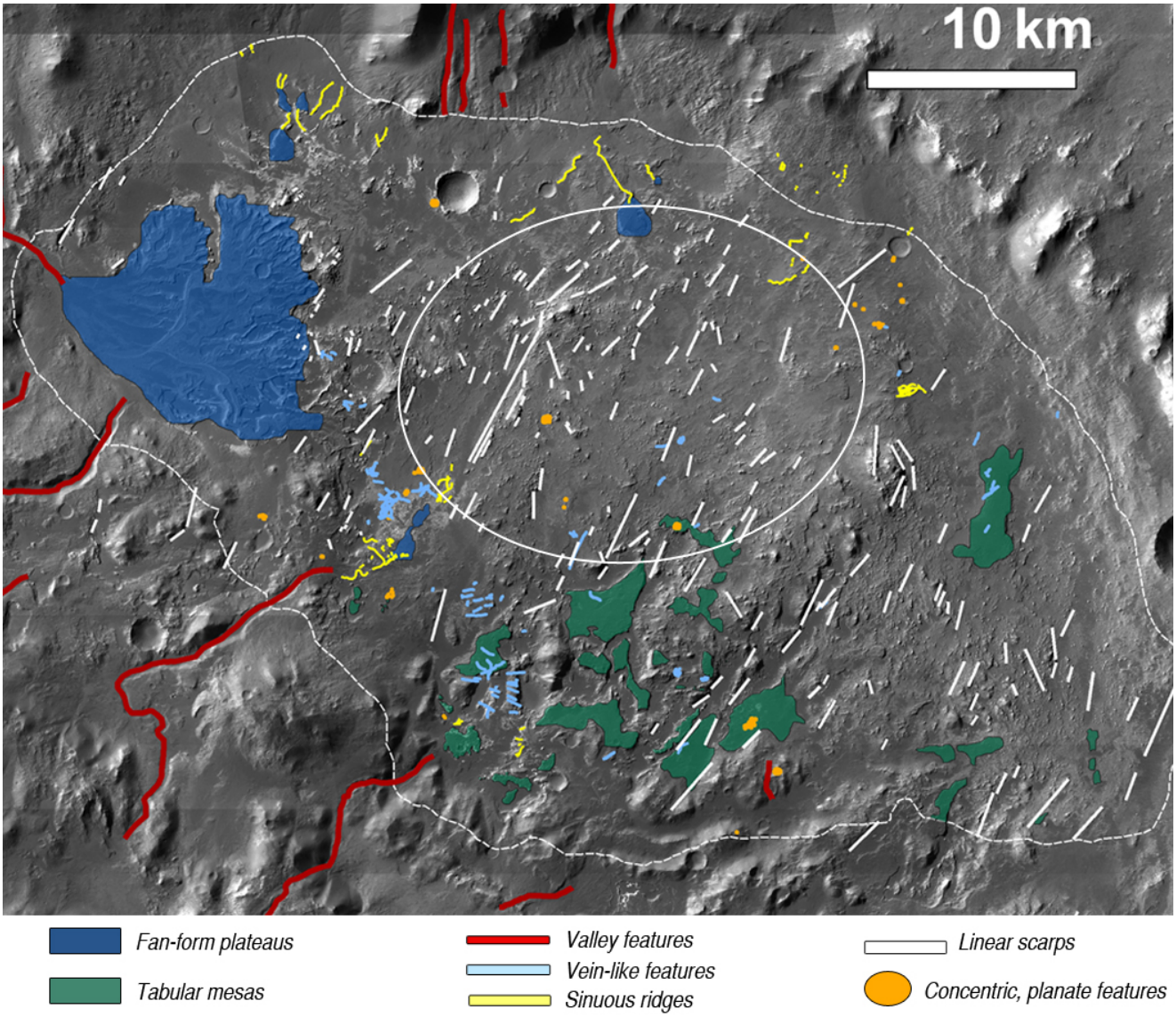

Figure 16. Map of inferred geomorphic units inside Eberswalde crater. The white line indicates the location of the proposed MSL landing ellipse. See text for detailed descriptions of units. (figure16.jpg)

Dark-toned bedforms unit

Observations. In a few isolated locations in the western portion of the crater, dark-toned (albedo 0.07-0.09), complex bedforms abut east-facing topographic obstacles (such as the brecciated ridge forming unit in Figure 15b). The dark-toned bedform unit does not preserve small impact craters and is the only unit that is not covered in part by the mantling unit.

Hypotheses and interpretations. The dark-toned bedforms appear to be the youngest deposits in Eberswalde crater, and the paucity of impact craters superposed on them suggests that the bedform material has been recently reworked. We interpret this unit as modern aeolian bedforms, similar to the El Dorado dunes observed by the Mars Exploration Rover Spirit in Gusev Crater (Sullivan et al. 2008).

Inferred geomorphic units

We have identified seven geomorphic units within Eberswalde crater, which we have mapped in Figure 16. The detailed descriptions of our observations, hypotheses, and interpretations of each unit are given below, and a summary of all units is provided in Table 2.

Observations. Several stratigraphic units within Eberswalde crater are cut by light-toned vein-like features < 5 m in width and ranging from 10 to 1000 m in length (Figure 17). In the brecciated unit, these features can be either linear with parallel orientations or randomly aligned with varying thicknesses (Figure 6b-c). Within other units, the vein-like features are typically narrower and can occur as isolated, linear (*e.g.*, Figure 17b) to arcuate (*e.g.*, Figure 17e) forms. Where these features meet, they consistently do so at right angles (*e.g.*, Figures 17d-e). Shadows cast by these features indicate that, in some cases, they are ridges with positive relief; in other examples, no relief can be inferred and a dark-toned line is observed along the center of the light-toned

Table 2. Summary of geomorphic units

Geomorphic Unit	Figures	Description	Elevations (m) †	Contact Relationships	Process Interpretation*	Comparison to Previous Studies
Vein-like features	17, 24	Narrow; linaer to arcuate ridges; meet at right angles; some networks	-1500 to -1280	Found in the brecciated and pitted units	Breccia injection dikes; cemented fracture fill	none
Valley features	18, 25	Linear to sinuous valleys; 200-800 m wide	> -1330	Incising the brecciated unit at the margins of the crater; partially filled by the mantling unit	Fluvial valleys	[1-8] Fluvial valleys
Sinuous ridges	14e, 19, 25	Sinous with raised relief; 10^1-10^3 m long; light-toned material at base; sometimes meandering or branching	-1490 to -990	Above the brecciated unit, the sub-polygonally fractured unit, and/or the pitted unit; covered by the mantling unit	Inverted, fluvial channels	[6-9] Inverted, fluvial channels
Fan-form plateaus	11a, 12b, 12c, 20b, 25	Fan-shaped, layered plateaus; preserve sinuous landforms; light-toned rock exposed in cliff faces	-1490 to -1250	Onlapping the brecciated unit and/or the pitted unit; covered by the mantling unit	Remnant deltas	[1-9] Remnant deltas; [10]Remnant alluvial fans
Tabular mesas	13g, 20c-d	Irregular-shaped mesas; pitted, scalloped surfaces; preserve small craters; light-toned material exposed in cliff faces	-1510 to -1205	Above the brecciated unit and/or the pitted unit; covered by the mantling unit	Fluvial deposits? Lacustrine sediments?	none
Concentric, planate features	21	Small (<500 m), concentric, quasi-circular to irregularly-shaped landforms; some fracturing; largely obscured by the mantling	-1495 to -1260	Above the brecciated unit and/or the pitted unit; covered by the mantling unit	Filled craters	none
Linear scarps	8, 22	NNE-SSW trending lineations; form cliff faces > 5 m high	> -1570	Found in the massive basal, orthogonally fractured, brecciated, pitted, sub-polygonally fractured, and light-toned layered units; in places overlain by the sub-polygonally fractured, light-toned layered, and mantling units	Dip-slip faults	[6] Faults; [9] Dip-slip faults

* See text for a description of alternate hypotheses

† Observations were restricted to below -1200 m

[1] Malin & Edget (2003); [2] Moore et al. (2003); [3] Bhattacharya et al. (2005); [4] Wood (2006); [5] Lewis & Aharaonson (2006); [6] Pondrelli et al. (2008); [7] Pondrelli et al. (2010); [8] Scheiber (2007); [9] Rice et al. (submitted); [10] Jerolmack et al. (2004)

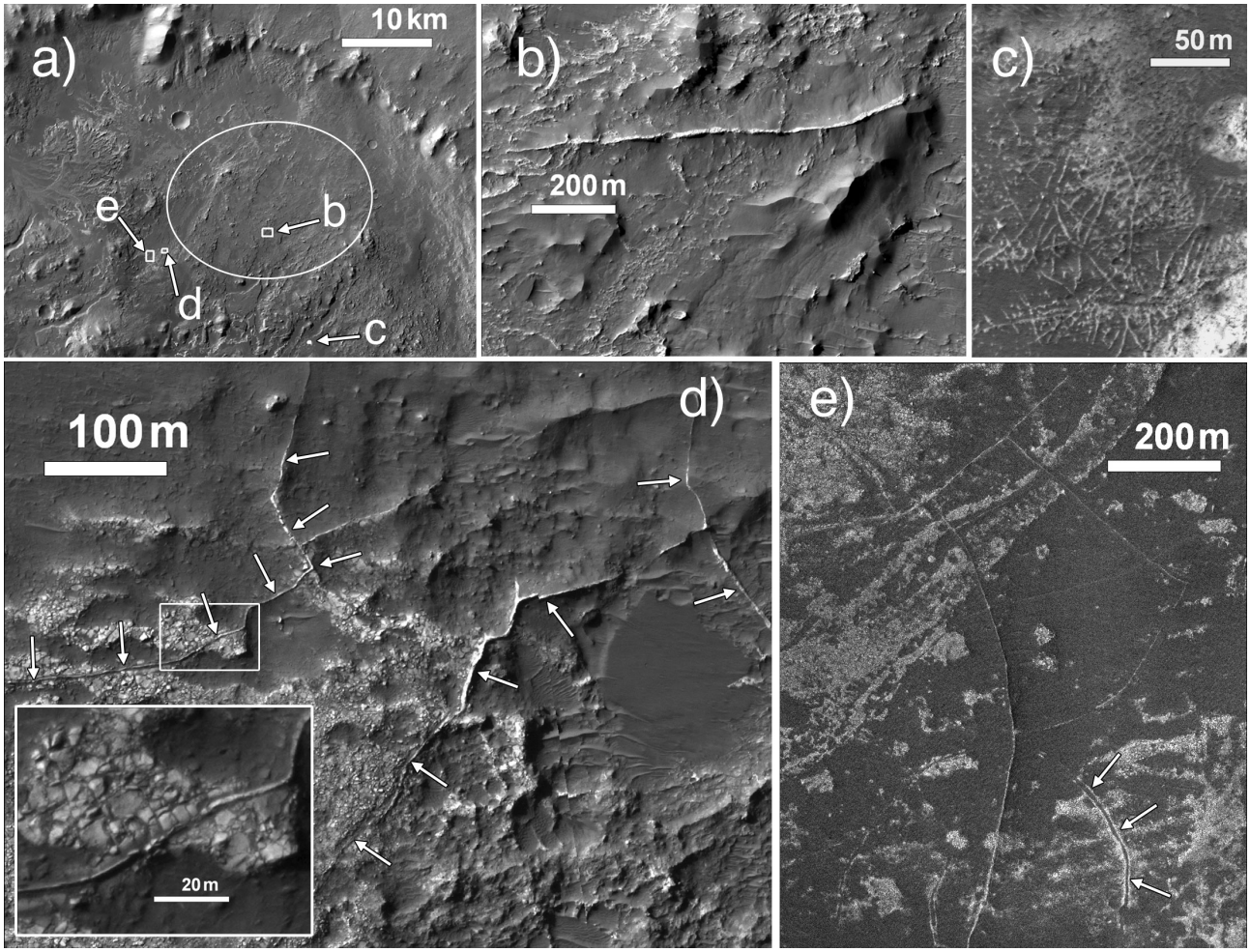

Figure 17. Examples of vein-like features: (a) CTX mosaic of Eberswalde crater indicating the location of 17b-e and the proposed MSL landing ellipse; (b) a ~1 km linear, isolated vein-like ridge near the center of the landing ellipse (from HiRISE observation ESP_012610_1560_RED); (c) complex pattern of vein-like features (from HiRISE observation PSP_017845_1560_RED); (d) arcuate, vein-like ridges; the inset shows where polygonally fractured material overlies a ridge (from HiRISE observation PSP_004356_1560_RED); (e) arcuate, vein-like features in southwest Eberswalde; the arrows indicate a double-ridged levee (from HiRISE observation PSP_004356_1560_RED). North is oriented at the top of the page in all images. (figure17.jpg)

features (Figure 17e). Within some outcrops of the pitted, discontinuous light-toned unit, the vein-like features occur as networks of polygonal patterns (Figure 17c). We have observed no large-scale patterns associated with the alignments of the vein-like features, with the exception of the linearly aligned features at the kilometer-scale within some occurrences of the brecciated unit.

Hypotheses and interpretations. We interpret the vein-like features as fracture-fills within the brecciated, ridge-forming and other stratigraphic units. The dark-toned line observed dividing some features (Figure 17e) could be the fracture itself, while the lighter-toned ridges consist of the erosion-resistant material filling or cementing a fracture. In some locations such as these, where the light-toned ridges occur in parallel pairs, they may also be the arched up antiform margins of megapolygons (or "teepees") (Kendall and Warren 1987). The origin of the fractures within multiple units may be regional stresses or residual stresses from the formation of Eberswalde crater. In the latter case, the fractures would be expected to be aligned radially from the center of the impact and parallel to the crater rim (*e.g.*, Melosh 1989); however, because we observe no large-scale pattern in the alignment of features, we cannot distinguish large-scale impact-induced stresses from smaller-scale regional (including possible impact-related) stresses.

The composition and origin of the fracture-filling material is unknown; however, on Earth, a variety of fracture filling minerals, derived from precipitation of fluids, can be found in basaltic settings. These include carbonate, clay, silica (opaline and quartz), zeolites, or sulfates, the occurrence of which are dependent on the host rock composition, source of the precipitating fluids, pH, water-rock ratio, and temperature (*e.g.*, Kendall and Warren 1987). Fracture-fills have been observed within martian meteorites (*e.g.* Rao et al. 2008), and have previously been identified elsewhere on Mars with *in-situ* (Knoll et al. 2008) and orbital (Okubo and McEwen 2007) observations. Alternately, the vein material may be an alteration of the host rock that is more resistant to erosion.

The vein-like features could also be dikes formed by igneous intrusions (which have been proposed for similar features in other martian craters by Head and Mustard 2006) or pressurized/fluidized sediment (*e.g.*, mud-sand dikes). The vein-like features within megabreccias associated with Holden crater have been interpreted as breccia injection dikes (Grant et al. 2008; Tornabene et al. 2009), and are morphologically similar to those observed with the brecciated ridge-forming unit in Eberswalde. Igneous dike swarms tend to be parallel, en echelon, or radially oriented (Neuendorf et al. 2005), which is consistent with some (but not all) of those observed within the brecciated unit (Figure 6b-c). Another possibility is that the veins represent fractures that captured loose/transported sediment and debris, potentially of differing composition, which was then buried and lithified and is now being exhumed and preserved in inverted relief.

Valley features

Observations. Several valley features are observed on the northern, western, and southern rims of Eberswalde crater. These features are 200-800 m wide, linear to sinuous valleys that originate on the plains surrounding Eberswalde and terminate within the crater. The valley-fill material is mapped as the mantling unit in Figure 3, which is fluted with grooves parallel to the valley walls (*e.g.*, Figure 18b). Near the basinward terminations of these features, the valley-fill material is eroded into linear ridges that resemble yardangs. Throughout the valleys, the dark valley-fill material is superposed by linear bedforms spaced ~10 m apart and aligned perpendicular to the valley walls (*e.g.*, Figure 18c).

Hypotheses and interpretations. Sinuous valleys similar to those along the walls of Eberswalde crater have been observed on Mars since the Mariner 9 mission, and have been interpreted to have been carved by the movement of liquid water (*e.g.*, Carr 1996). The linear grooves parallel to the valley walls are morphologically similar to the lineated valley fill observed near the northern dichotomy boundary (Squyres 1978) that has been interpreted as debris-covered glaciers (Morgan et al. 2009). However, we have observed no lobate debris aprons at the valley termini that would support the presence of glaciers. Instead, we interpret the grooved features present where the valleys meet the basin as yardangs (*e.g.*, McCauley et al. 1977) carved from the valley floor materials by wind erosion. These features may also be preserved evidence of fluvial erosion at the mouths of ancient channels.

Sinuous ridges

Observations. We have identified many sinuous features with raised relief (locations shown in Figure 16), with lengths ranging from 10 m to 3 km and widths ranging from 10-100 m. These ridges occur as thin forms (*e.g.*, Figure 19b,e), as wider, meander-like forms (*e.g.*, Figure 19d), or as networks of branching features (*e.g.*, Figure 10a, Figure 14e, Figure 19c). All sinuous ridges observed are covered by the mantling unit along the ridge and expose lighter-toned material to varying degrees along their edges.

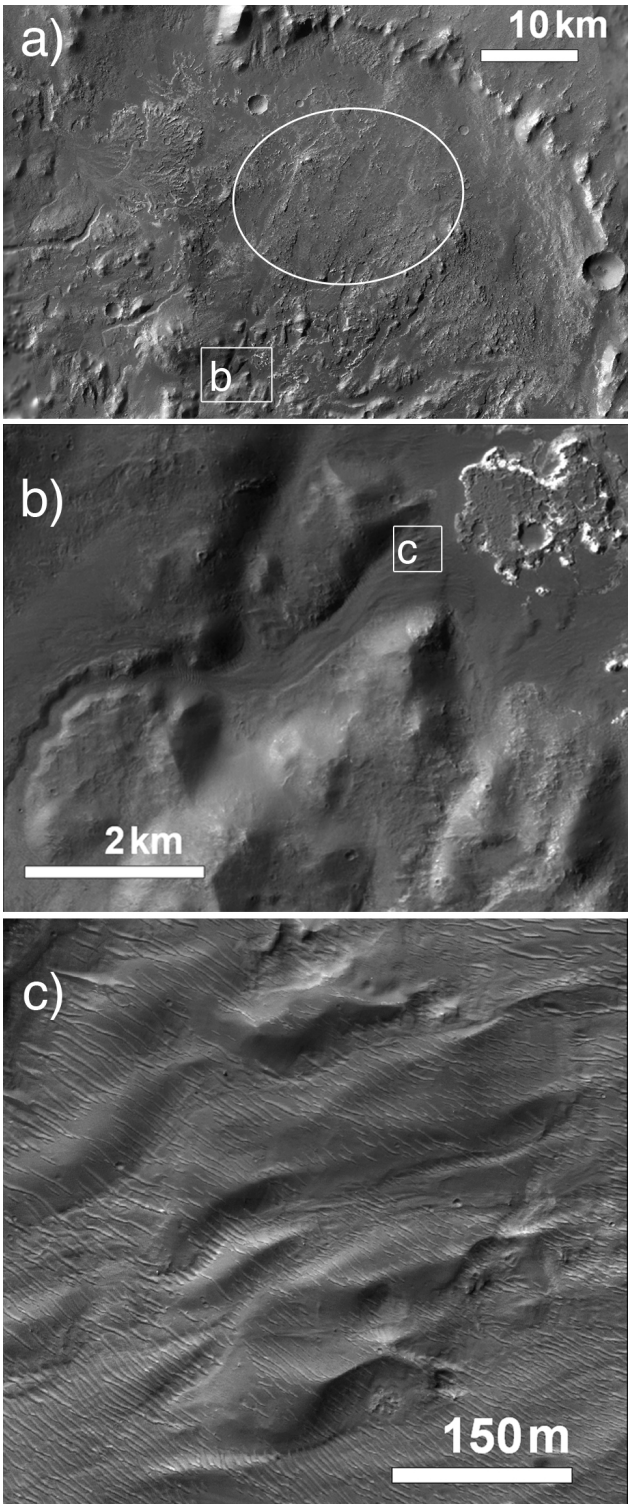

Figure 18. Example of a channel-like feature in southern Eberswalde: (a) CTX mosaic of Eberswalde crater indicating the location of 18b and the proposed MSL landing ellipse; (b) a channel-like feature cutting the south rim of Eberswalde crater, the white box shows the location of 18c (from HiRISE observation ESP_018056_1560_RED); (c) detail of yardangs and bedforms at the end of the valley. North is oriented at the top of the page in all images. (figure18.jpg)

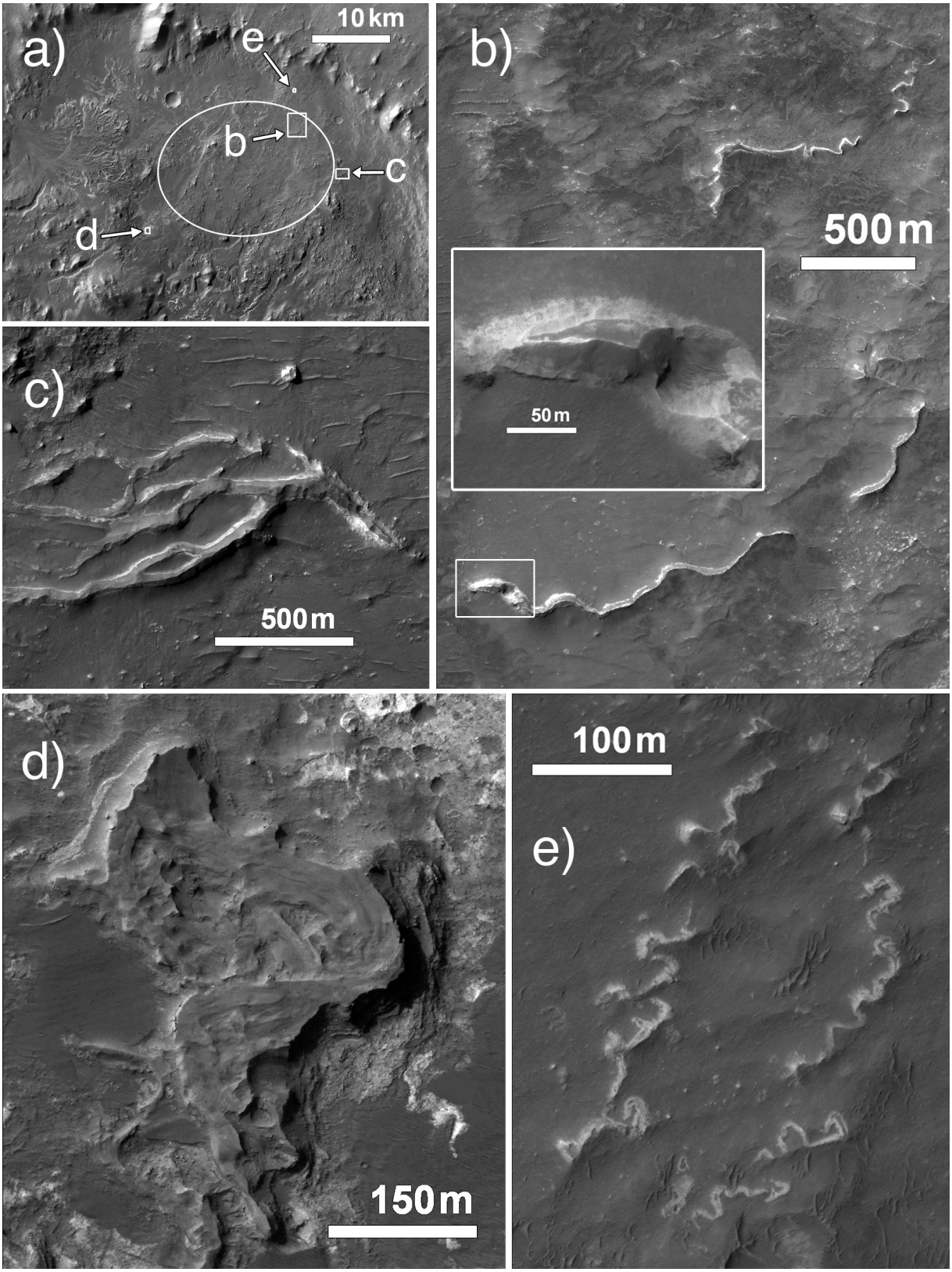

Figure 19. Examples of sinuous ridges in Eberswalde crater: (a) CTX mosaic of Eberswalde crater indicating the location of 19b-e and the proposed MSL landing ellipse; (b) sinuous ridges within the landing ellipse, with the inset showing light-toned material exposed beneath the ridge (from HiRISE observation PSP_016065_1560_RED); (c) branching, sinuous ridge structure in eastern Eberswalde (from HiRISE observation PSP_001600_1560_RED); (d) sinuous ridge in southwest Eberswalde with layers visible (from HiRISE observation ESP_018056_1560_RED); (e) highly sinuous ridges on the northern crater wall (from HiRISE observation PSP_001600_1560_RED). North is oriented at the top of the page in all images. (figure19.jpg)

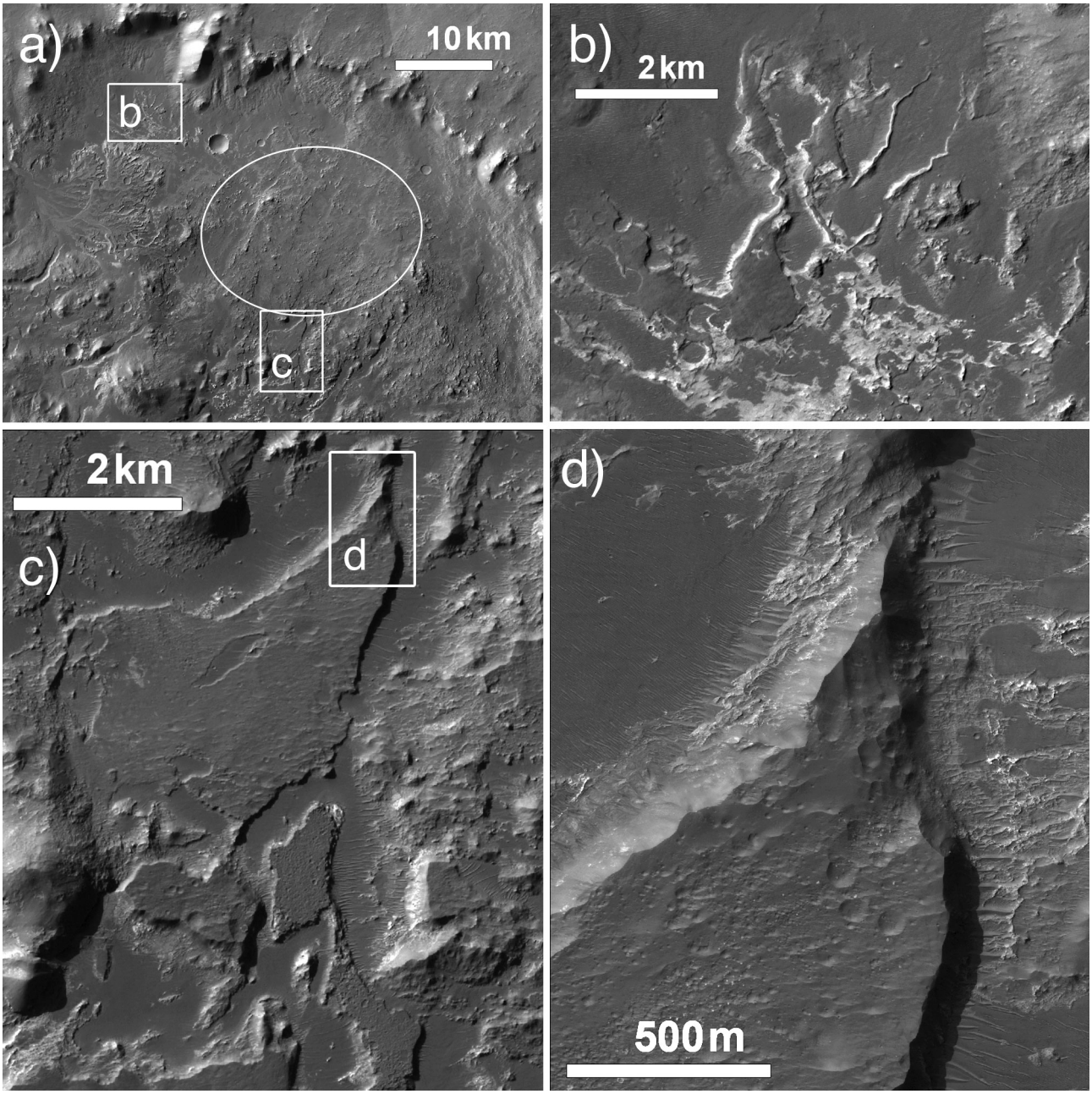

Figure 20. Examples of fan-like plateaus and tabular mesas in Eberswalde crater: (a) CTX mosaic of Eberswalde crater indicating the location of 20b-d and the proposed MSL landing ellipse; (b) fan-like mesas associated with sinuous ridges in northwest Eberswalde (from CTX observation P01_001336); (c) tabular mesas in southern Eberswalde (from HiRISE observation PSP_009274_1560_RED); (d) edge of a mesa showing the cratered and scalloped morphology and the discontinuous, light-toned unit exposed below (from HiRISE observation PSP_010474_1560_RED). North is oriented at the top of the page in all images. (figure20.jpg)

The sinuous features in different regions of Eberswalde crater have distinct morphologies. Those in the northern and eastern portions of the crater, for example, form sharp ridges covered by the mantling unit and revealing the massive light-toned unit at their bases (Figure 19b-c). Those in the south and western portions of the crater are wider plateaus covered by the mantling unit and exposing the layered light-toned unit (*e.g.*, Figure 19d) or the fractured light-toned unit (*e.g.*, Figure 15c) along cliff faces. The northern crater wall is covered with sinuous ridges distinct from those observed elsewhere in the Eberswalde basin in that they are extremely narrow, highly sinuous, and often occur as chains of elongated mesas (*e.g.*, Figure 19e).

Hypotheses and interpretations. Sinuous ridges similar to those observed in Eberswalde crater are common on Mars (Edgett 2005) and have been interpreted as inverted channels similar to those observed in Oman (Maizels 1990) and the Colorado Plateau (Williams et al. 2009). In arid environments on Earth, ancient fluvial channels become

inverted in relief when they are filled with a material that is more erosion resistant than the surrounding terrain, either by chemical cementation, "armoring" by course grains, or infilling by lava flows (Pain et al. 2007; Williams et al. 2009). The surrounding, less resistant material erodes before the channel-fill, and the channel remains as a raised ridge or a chain of mesas/hills.

An alternate hypothesis is that some ridges are an erosion-resistant fracture-fill material, similar to the vein-like features. The sinuosity of the ridges, however, is distinct from the vein-like features, which are linear to arcuate, and are typically much narrower. Furthermore, the sinuous ridges often branch and anastomose (*e.g.* Figures 10e, 19c), which is also more consistent with the morphology of fluvial channels.

We interpret the sinuous ridges as inverted fluvial channels composed of cemented and/or course-grained material. Because we observe no accumulations of boulders or talus at the base of these features, we suggest that the ridge-forming material weathers into sand-sized grains (< 300 μm; Sharp 1963) that are transported away by winds.

The sinuous ridges near the margins of the basin that are associated with valley features may be fluvial sediments that have been deposited either subaerially or subaqueously (within an Eberswalde basin lake), and may have been transported from the plains surrounding Eberswalde crater via the valleys. Some ridges, however, are not associated with valley features (such as those on the northern rim and those within the basin) and thus their sediment source regions are less easily inferred.

Fan-form plateaus

Observations. The most significant fan-form plateau in Eberswalde crater is the famous "delta" in the west (Figure 11) that has been extensively examined in previous studies (Malin and Edgett 2003; Moore et al. 2003; Bhattacharya et al. 2005; Jerolmack et al. 2004; Wood 2006; Lewis and Aharonson 2006; Pondrelli et al. 2008; 2011; Rice et al. 2011). This plateau of layered rock (with the layered, light-toned unit exposed along its edges) originates at a valley feature in the west of the crater and extends ~12 km into the basin (Figure 11a). The surface of this feature preserves sinuous ridges with measured sinuosities of 1.1 to 1.8 (Wood 2006). As described by Pondrelli et al. (2008), the forms of the preserved sinuous features range from rectilinear to meandering. They also appear to be grouped into multiple deposits, and have been mapped in previous studies as three (Bhattacharya et al. 2005) or five (Wood 2006; Pondrelli et al. 2008) separate lobes.

A smaller (~1.5 km wide), fan-shaped plateau of layered rocks in the north of the crater (Figure 12b) was noted by Schieber (2008). The layers are not traceable around the entire plateau, due to obscuration by the mantling unit, but are visible for ~100 m along its edge (Figure 12c). A ~300 m wide fan-shaped feature immediately northeast (Figure 12b) terminates at the end of a highly sinuous ridge. Due

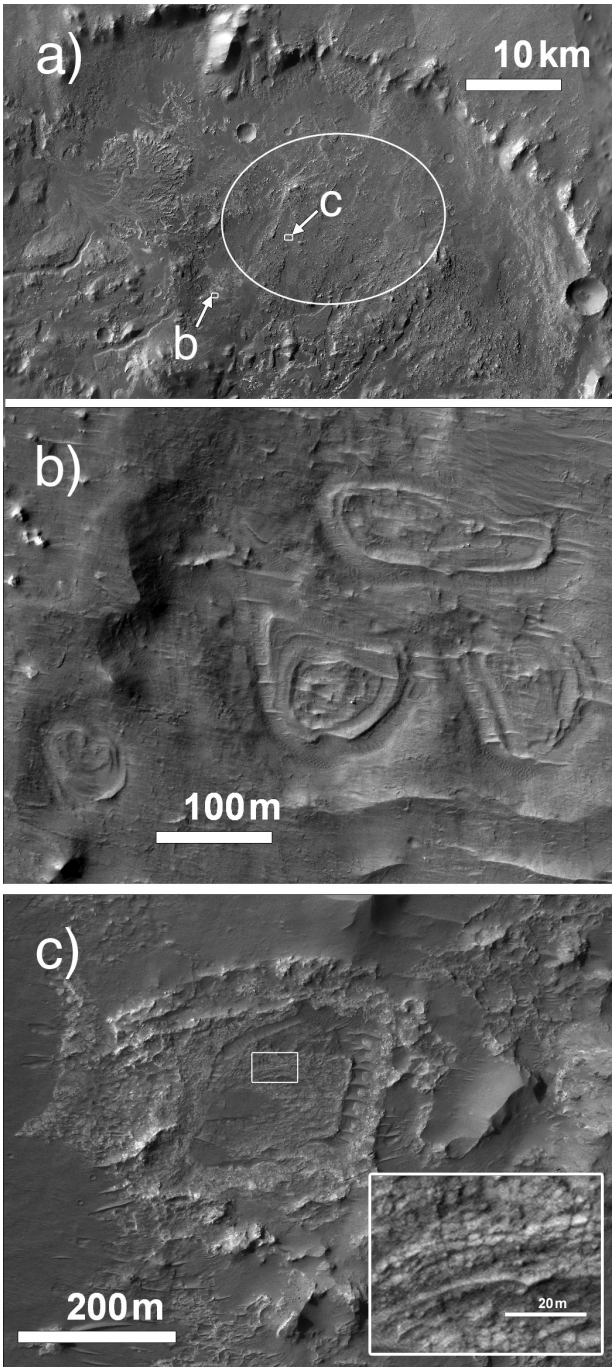

Figure 21. Examples of concentric, planate features in Eberswalde crater: (a) CTX mosaic of Eberswalde crater indicating the location of 21b-c and the proposed MSL landing ellipse; (b) features in southwest Eberswalde covered by the mantling unit (from HiRISE observation ESP_018056_1560_RED); (c) feature within the landing ellipse, with the inset showing fractured, light-toned material (from HiRISE observation PSP_007481_1560_RED). North is oriented at the top of the page in all images. (figure21.jpg)

north of the proposed Eberswalde delta, two fan-form plateaus are associated with a network of sinuous ridges (Figure 20b). These features were mapped as an extension of the putative Eberswalde delta by Pondrelli et al. (2008). An additional fan-form plateau is located in the southwest of

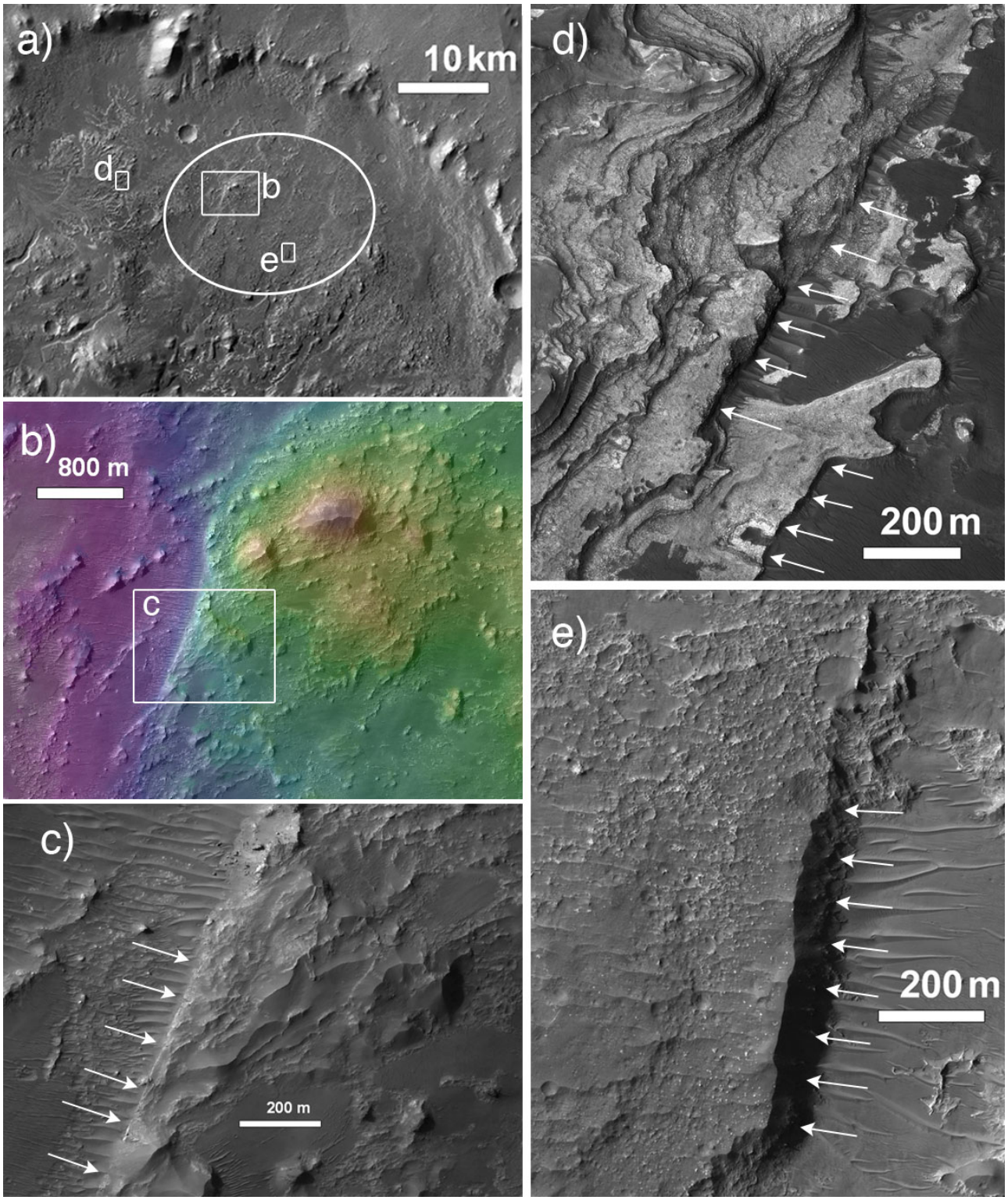

Figure 22. Examples of linear scarps in Eberswalde crater: (a) CTX mosaic of Eberswalde crater indicating the location of 22b,d,e and the proposed MSL landing ellipse; (b) HiRISE DTM (from PSP_008272_1560 and PSP_010474_1560, overlain on image PSP_010474_1560) showing topography of a prominent scarp in central Eberswalde (color scale: red = high = -1000 m; white = low = -1600 m); (c) HiRISE image (from PSP_010474_1560) of a linear scarp, location shown in (b); (d) linear scarps at the front of the "delta" (from HiRISE image PSP_04000_1560_RED); (e) linear scarp in the pitted unit (from HiRISE image ESP_019335_1560_RED). North is oriented at the top of the page in all images. (figure22.jpg)

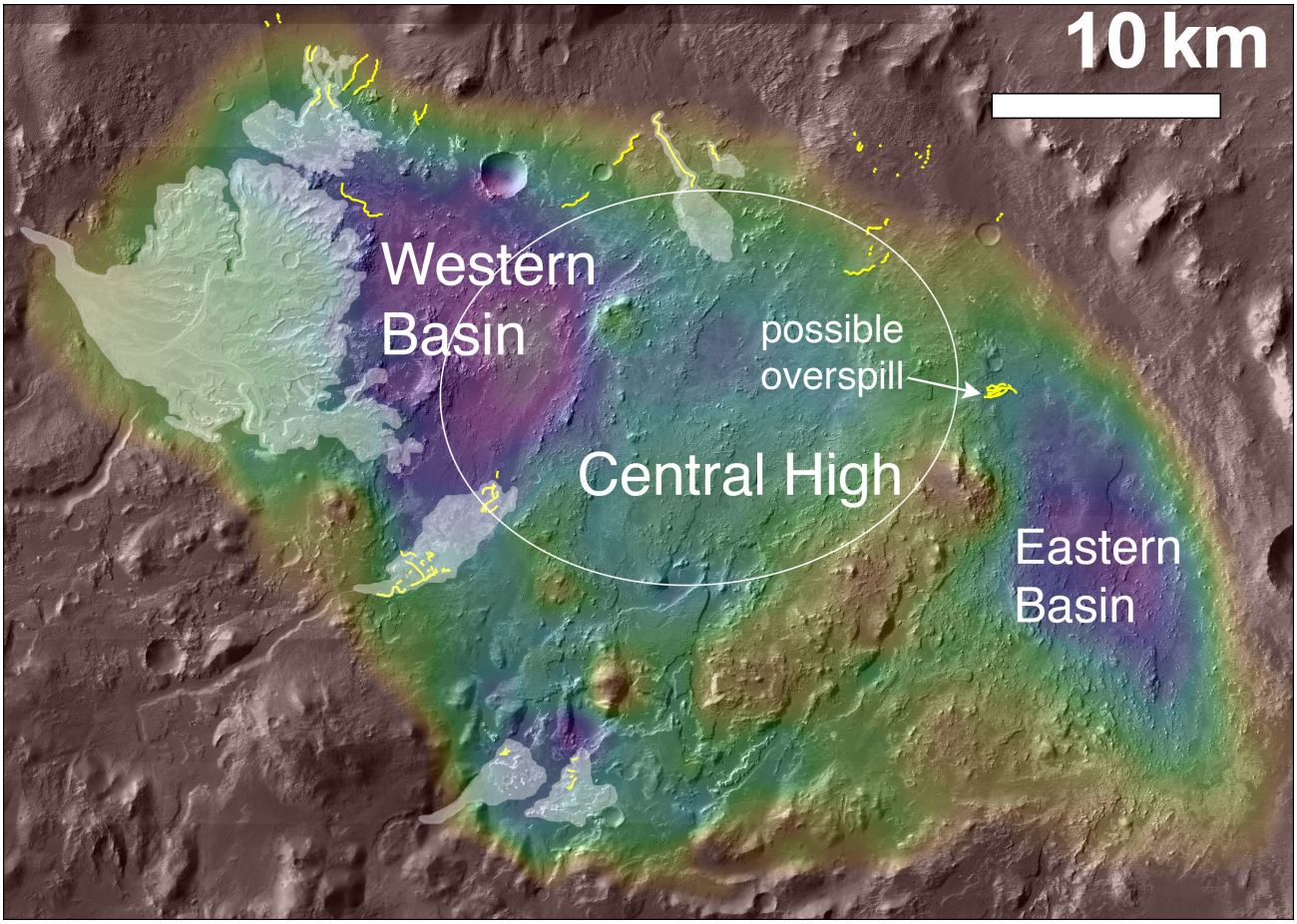

Figure 23. MOLA elevation map (color scale: red = high = −1000 m; purple = low = −1600 m) draped over a CTX mosaic, showing the first-order topography within Eberswalde crater: Western Basin, Central High, and Eastern Basin. White regions indicate the fluvio-deltaic systems identified by Rice et al. (2011); yellow lines indicate locations of features interpreted as inverted channels. (figure23.jpg)

the crater (Figure 13d). This feature preserves sinuous and digitate ridges that appear to have eroded into a stair-step pattern of layered rock (*e.g.*, Figure 13f). Further descriptions of these fans are provided by Rice et al. (2011).

Hypotheses and interpretations. Based on its morphology, association with a valley feature, lithology, and mineralogy, the largest fan-form plateau in the west of the crater has been widely interpreted as a lacustrine delta (Malin and Edgett 2003; Moore et al. 2003; Bhattacharya et al. 2005; Wood 2006; Lewis and Aharonson 2006; Pondrelli et al. 2008; Pondrelli et al. 2011). Schieber (2008) hypothesized that the fan-form plateau in northern Eberswalde crater was the erosional remnant of an additional delta, and Rice et al. (2011) interpreted this and the other fan-shaped features in Eberswalde as deltaic as well.

Jerolmack et al. (2004) proposed that the largest fan-shaped feature was an alluvial fan, and the other features in Eberswalde could be alluvial fans as well. However, the fan-shaped plateaus and layered deposits of the other features do not initiate at the break in slope associated with the wall of the crater, as might be expected for alluvial fan formation (*e.g.*, Williams et al. 2006). Instead, channel bifurcation to create a fan-shaped sediment body occurs basinward of the crater rim, implying that fluvially-transported sediments were deposited along a shoreline and into a standing body of water. The multiple, bifurcating inverted channels preserved on the fan-shaped features are consistent with this interpretation.

Tabular mesas

Observations. The southern rim of Eberswalde crater is partially covered with mesas that, like the fan-form plateaus, are obscured by the dark mantling unit but expose light-toned material at their bases and at cliff faces. Unlike the possible fans, however, these tabular mesas do not preserve sinuous ridges and do not exhibit any layering at the scale of HiRISE resolution (~25 cm/pix). The distribution of these features is shown in Figure 16. The surfaces of the mesas preserve many small craters and exhibit pitted, scalloped morphologies (*e.g.*, Figure 20c-d). Some of these mesas expose the layered light-toned unit beneath their mantled surfaces (*e.g.*, Figure 13), while others in the south of the crater appear to be comprised of the pitted unit (Figure 20d).

The tabular mesas have been eroded into irregular shapes (*e.g.*, Figure 20d) with no apparent preferred orientation.

Hypotheses and interpretations. Although the tabular mesas could be interpreted as remnants of fan-form plateaus, we infer that these features have a separate depositional history because of their distinct surface morphologies (pitted and scalloped), preservation of small craters, and lack of visible layering. The mesas comprised of the layered light-toned unit may be eroded lacustrine sediments. Those comprised of the pitted unit are more difficult to interpret, as the pitted unit covers much of the Eberswalde basin (Figure 4) and is only associated with the tabular mesas in the south of the crater. We hypothesize that the mesas of the pitted unit are the eroded remnants of formerly more continuous, crater-filling units. Locally, the tabular mesas occur at common elevations and thus may be remnants of a single, eroded surface; however, we find that within Eberswalde crater, these features span a range of elevations (-1510 to -1205 m; Table 2) and represent surfaces at multiple levels. The mesas likely remain because they are protected by a resistant capping unit.

It is possible that the tabular mesas are landforms carved by glacial movement, similar to the mesas interpreted to be associated with debris-covered glaciers in Deuteronilus Mensae (Dickson et al. 2008). Although there is no evidence for present glaciation in Eberswalde crater (such as lobate debris aprons), it may be that past glaciation had modified the southern rim of the crater and carved the irregular-shaped landforms. However, this hypothesis is speculative.

Concentric, planate features

Observations. In several locations within the Eberswalde basin, we have observed small (<500 m diameter), planate, quasi-circular to irregularly-shaped features with apparent layering. These features are mostly covered by the mantling unit and superposed by bedforms (*e.g.*, Figure 21b), but other features appear to be comprised of the sub-polygonally fractured unit (*e.g.*, Figure 21c).

Hypotheses and interpretations. We interpret the concentric, planate features as small, infilled impact craters, such as those observed elsewhere on Mars by Malin and Edgett (2000). Concentric crater fill has been interpreted as evidence for glaciations at high latitudes (*e.g.*, Squyres and Carr 1986), but at much larger scales than observed within Eberswalde crater (~100 m radii). Furthermore, there is no evidence for glacial flow into these features. More likely, we hypothesize that preexisting depressions (degraded impact craters) were once filled with sediment and entirely buried; as sediment was eroded and the craters were exhumed, the infilling layers were exposed such that they form concentric rings in plan view. Zimbelman et al. (1989) have interpreted similar features as aeolian crater fill materials.

Linear scarps

Observations. We have identified 233 linear scarps within Eberswalde crater (Rice et al. 2011), mapped in Figure 16. These features are characterized by cliff faces taller than ~5 m, and the lineations trend predominantly NNE-SSW (Figure 23); nearly two-thirds of these features trend within

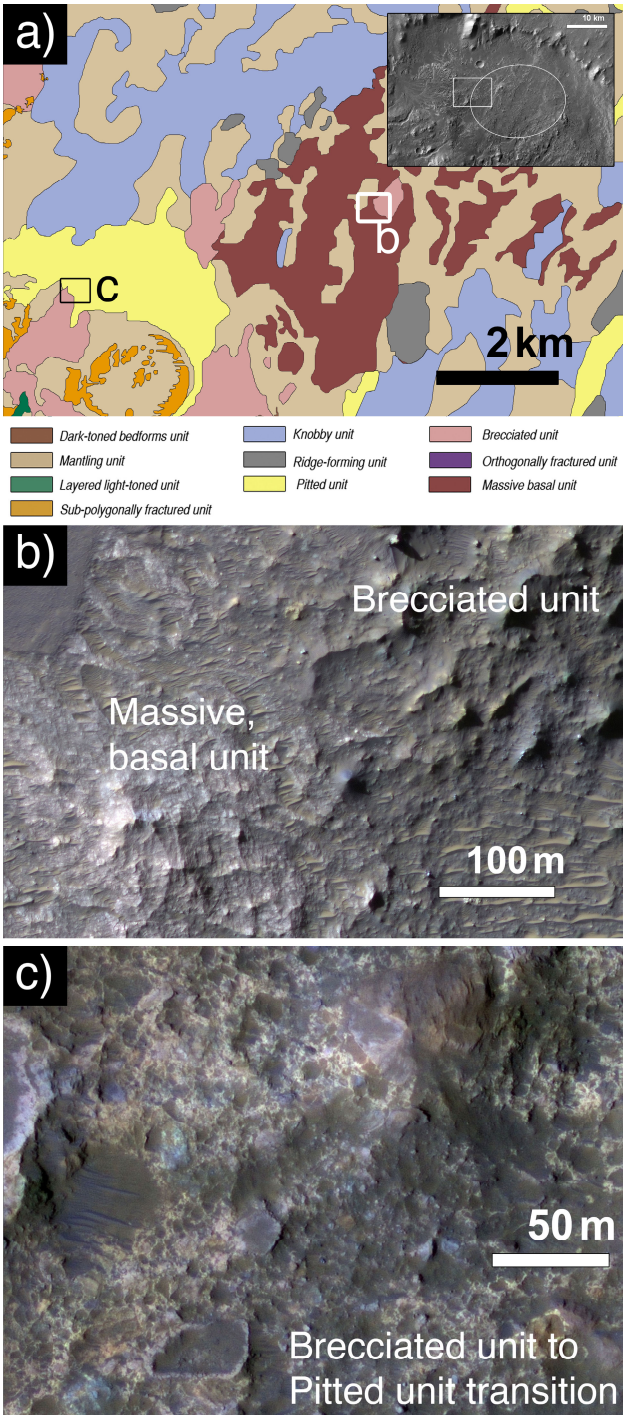

Figure 24. Relationship of brecciated unit to the massive, basal unit and the pitted unit. (a) Detail of stratigraphic unit map, location shown in the inset; (b) Contact between the brecciated and massive units (HiRISE PSP_004000_1560_COLOR); (c) Gradational contact between the brecciated and pitted units (HiRISE PSP_010052_1560_COLOR. (figure24.jpg)

15 to 45 degrees from north (Rice et al. 2011). All of these features are characterized by near-vertical scarps; we observe no lateral offsets associated with these lineaments. The linear scarps modify most crater floor materials, including the massive basal, orthogonally fractured, brecciated, pitted, and sub-polygonally fractured units. The light-toned layered unit

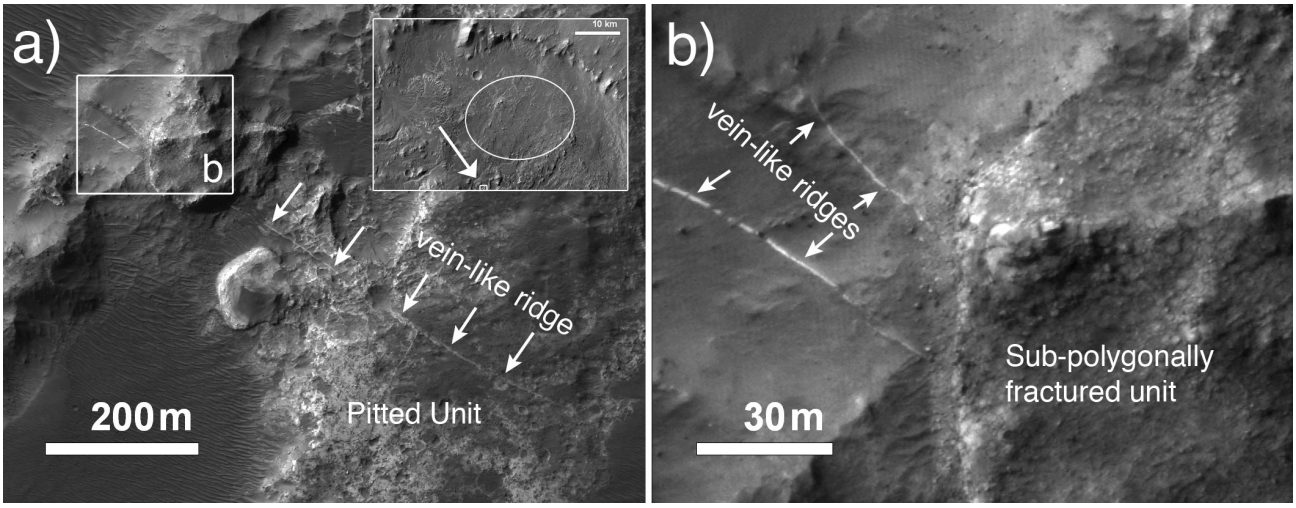

Figure 25. Example of contact relationships between the vein-like features and stratigraphic units. (a) Vein-like ridge cross-cutting the pitted unit but overlain by the sub-polygonally fractured unit (HiRISE ESP_018056_1560), location within Eberswalde crater shown in the inset; (b) Closer view of the sub-polygonally fractured unit overlying the vein-like features, location shown in (a). (figure25.jpg)

is cut by these scarps in some places as well (Figure 23), but in others this unit overlies the linear scarps (Rice et al. 2011).

Hypotheses and interpretations. Pondrelli et al. (2008) noted the presence of linear scarps at the front of the Eberswalde delta, which they interpreted as syn-sedimentary faults, and proposed a large fault system cutting the crater's center. We interpret the lineaments in Eberswalde crater to be dip-slip faults because we observe vertical offsets and no lateral offsets. The dominant NNE-SSW orientation of the faults is inconsistent with the stresses expected from the impact event that formed Eberswalde crater (which should be radial and parallel to the crater walls) (Melosh 1989). Rather, the faults follow this NNE-SSW trend across the width of the crater floor and across its northern rim, onto the highland plains north of the crater, as well as south onto the divide between Holden and Eberswalde craters. We therefore infer that larger, regional post-impact stresses must be responsible for the observed faulting, such as those expected from the formation of Tharsis, for example (Rice et al. 2011).

Unit associations, successions and geometries

The spatial distributions of stratigraphic units (Figure 3) and geomorphic features (Figure 16), their relationships to the present basin topography (Figure 23), and their contact relationships can aid our interpretations of the depositional history within Eberswalde crater. The elevation restrictions of each unit are provided in Tables 1 and 2. Below we describe the unit associations, successions and geometries, and use these observations to infer a stratigraphic sequence.

Observations

The large-scale topography in Eberswalde (Figure 23) divides the crater into three prominent regions: a Western Basin, a Central High, and an Eastern Basin (Rice et al. 2011). These regions are bounded by the linear scarps that trend NNE across the full extent of the crater. Topographically, the massive, basal unit is lower than any other stratigraphic unit; the exposed outcrops are restricted to below the -1495 m contour line. While this unit is variably covered by the mantling material, making contacts with other units difficult to infer, there are some locations where it clearly underlies the brecciated unit (Figure 24b) or the knobby unit.

The brecciated unit crops out at all but the very lowest elevations within the crater (> 1570 m). While this unit clearly superposes the massive, basal unit (Figure 24b), its relationship to the pitted unit is less clear. We have not observed contact relationships between the brecciated and pitted units; rather, one unit always appears to grade continuously into the other. Many outcrops that we have mapped as the brecciated unit in Figure 3 contain pits, and, conversely, many outcrops mapped as the pitted unit contain occasional clasts entrained within pits. Figure 24c shows an example of a transitional region between the brecciated and pitted units, where heterogeneous clasts and pits in the light-toned matrix material are found in close proximity. In this example, the outcrop to the north is predominantly pitted, and the outcrop to the south is predominantly brecciated (as shown in the unit map in Figure 24a). The vein-like features clearly cut the pitted and brecciated units, but no other crater floor material. Figure 25 shows an example of vein-like ridges within the pitted unit, with the sub-polygonally fractured unit overlying them. The inset in Figure 17d provides a further example of sub-polygons overlying a vein-like ridge.

The stratigraphic context of the knobby unit is difficult to infer, as contacts with other units are obscured by the mantling unit. The knobs are also not restricted by elevation; they occur at all elevations within the mapped region of the crater (except for the lowest 5 m where the massive, basal unit crops out).

The layered light-toned and sub-polygonally fractured units are restricted to elevations below -1300 and -1320 m, respectively. These two units both appear to unconformably overlay the brecciated and pitted units. At the front of the fan-form plateau in the western portion of the crater (the Eberswalde "delta"), for example, the light-toned layers onlap against the brecciated unit (Figure 26). At this location, and at the other fan-form plateaus associated with valley features at the margins of the crater, we observe a repeated package of three stratigraphic units: (1) the layered light-toned unit conformably overlying (2) the sub-polygonally fractured unit unconformably overlying (3) the pitted unit.

At each of the six systems of outcrops associated with valleys that Rice et al. (2011) interpreted as fluvio-deltaic systems (mapped in Figure 23), these three units are observed in succession. Examples from the northern, southwestern and southern systems are shown in Figure 27.

The sinuous ridges in Eberswalde crater, which we interpret as inverted channels, are restricted to elevations above -1490 m. The distribution of these features with respect to the crater topography is provided in Figure 23; with one notable exception, all sinuous ridges are confined to the margins of the crater and/or are associated with a drainage valley and a proposed fluvio-deltaic system. The exception (Figure 19c) occurs along the boundary of the Central High and the Eastern Basin (location shown in Figure 23). The mantling unit is the only unit observed in contact with every other crater floor unit. We observe that the mantling material consistently overlies every unit except for the dark-toned bedforms unit. No stratigraphic unit appears to overlay the mantling unit, with the possible exception of the layered light-toned unit (it is possible that the lower-albedo layers observed within this unit are interbedded mantling deposits).

Hypotheses and interpretations

Based on these observations, we infer the following stratigraphic sequence for the units in Eberswalde crater (illustrated in Figure 28): (1) the dark-toned bedforms unit overlies (2) the mantling unit, which may be interbedded with (3) the light-toned layered unit. This unit conformably overlies (4) the sub-polygonally fractured unit, but the relationship between (3-4) and (5) the ridge-forming unit and (6) the knobby unit remains unclear. However, (3-6) all uncomformably overlay (7) the pitted unit, which grades continuously into (8) the brecciated unit, which may have been emplaced contemporaneously with (9) the orthogonally fractured unit. The deepest unit is (10) the massive, basal unit, which unconformably underlies (7-8).

Impact crater statistics and chronology of Eberswalde crater floor materials

Observations

Our crater counts within Eberswalde crater include all craters with diameters (D) > 100 m, and are plotted in Figure 29a. The total area of the crater floor is 1188 km^2 and includes 571 impact craters. For craters with D > 700 m (only 7), the cumulative frequency curve roughly follows the 3.5 Ga isochron.

A reduction in slope of the cumulative frequency histogram for craters with D = 200 m to 700 m is indicative of a process of crater resurfacing. At D < 200 m, the data closely follow an established isochron (Hartmann and Neukum, 2001; Ivanov 2001). A resurfacing correction (Michael and Neukum 2010) was therefore applied to the data at D < 200 m and indicates a crater retention age of 343 Ma ± 15. To reveal variation in impact crater density across Eberswalde crater, and to therefore identify lateral heterogeneity in material properties and crater retention ages, we generated a

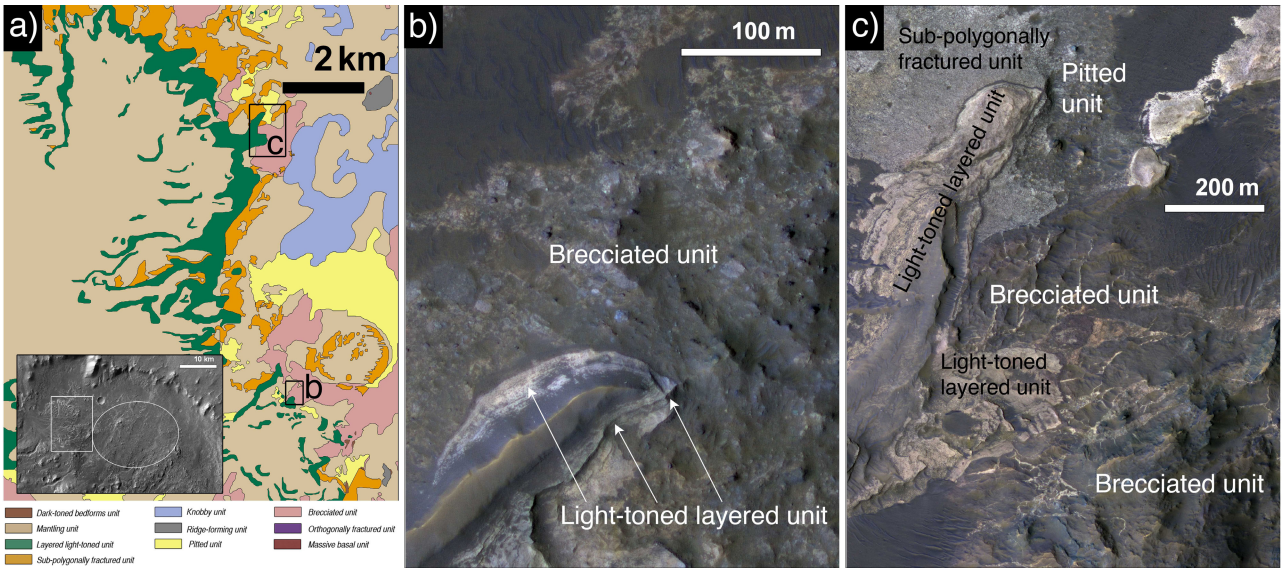

Figure 26. Examples of the light-toned layered unit in contact with other units at the front of the Eberswalde "delta". (a) Detail of stratigraphic unit map, location shown in the inset; (b) Light-toned layers unconformably overlying the brecciated unit; (c) The layered light-toned and sub-polygonally fractured units directly overlying the brecciated and pitted units at the delta front (HiRISE PSP_004000_1560_COLOR). (figure26.jpg)

crater density map (Figure 29b) by assigning the center of each crater to a point shapefile in ArcGIS. The density map indicates that the center of Eberswalde crater, in the region where we map the most extensive aeolian mantle, has the lowest impact crater density. The crater density throughout the majority of the crater floor appears fairly uniform, aside from pockets of high density in the southeast portion of the crater where we have observed well-indurated tabular mesas.

Hypotheses and interpretations

The small area and number of craters counted in this analysis limits our ability to obtain absolute model ages for specific

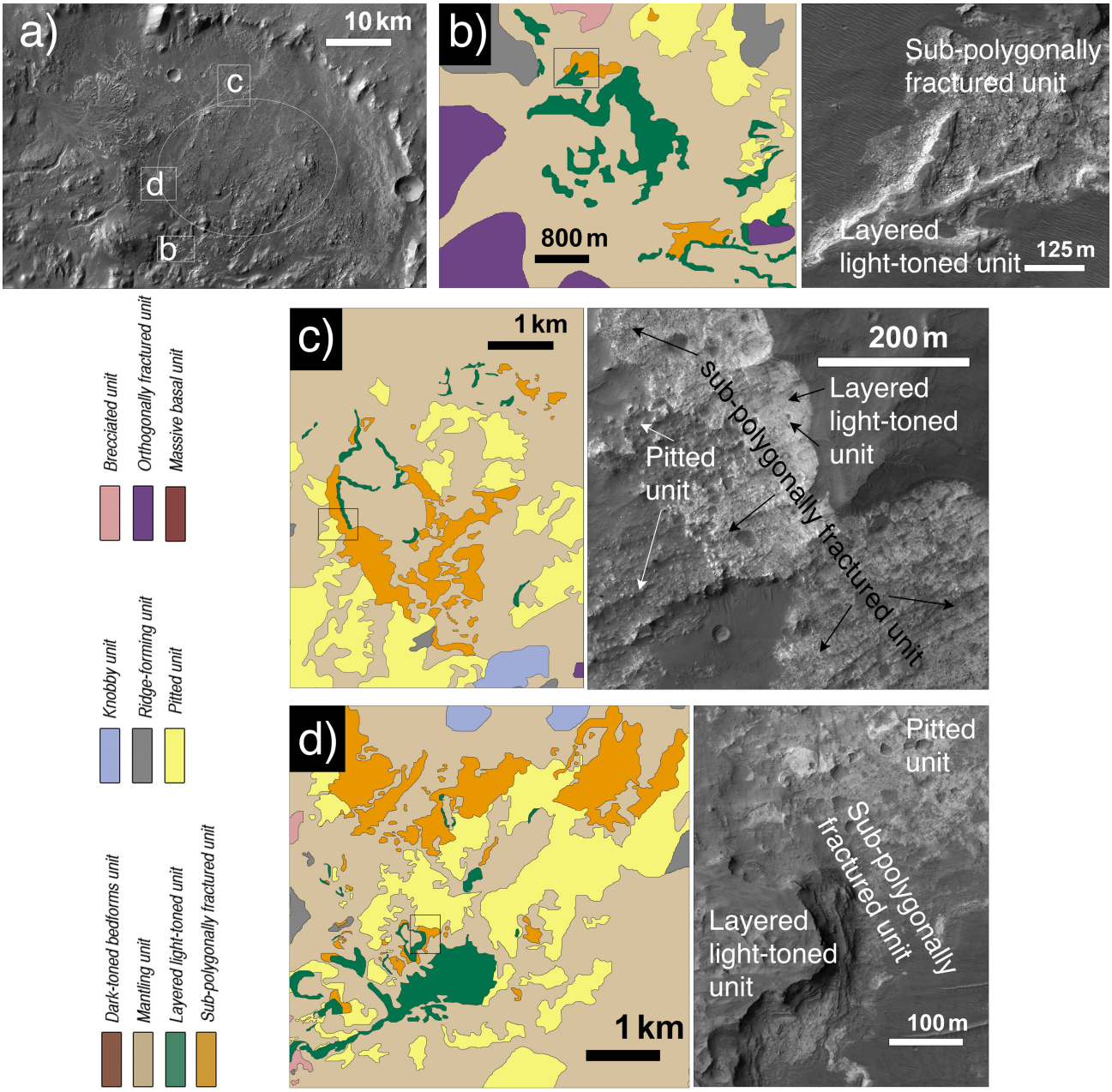

Figure 27. Examples of the three-unit pattern observed in association with channels that cut the Eberswalde crater walls: (1) the layered light-toned unit (mapped in green) conformably overlying (2) the sub-polygonally fractured unit (mapped in orange) unconformably overlying (3) the pitted unit (mapped in yellow). (a) CTX mosaic of Eberswalde crater indicating the location of 27b-d and the proposed MSL landing ellipse; (b) Detail of stratigraphic unit map in the south of the crater (left) where light-toned layers are in contact with the sub-polygonally fractured unit (right; HiRISE ESP_018056_1560_RED) and topographically above the pitted unit; (c) Detail of stratigraphic unit map at fan-form plateau interpreted as a remnant delta in the north of the crater (left) where light-toned layers are in contact with the sub-polygonally fractured unit, which overlies the pitted unit (right; HiRISE PSP_005556_1560_RED); (d) Detail of stratigraphic unit map at fan-form plateau interpreted as a remnant delta in southwest Eberswalde (left) where the light-toned layers exposed at the edge of a sinuous ridge are in contact with the sub-polygonally fractured unit, which overlies the pitted unit (right; HiRISE ESP_018056_1560_RED). (figure27.jpg)

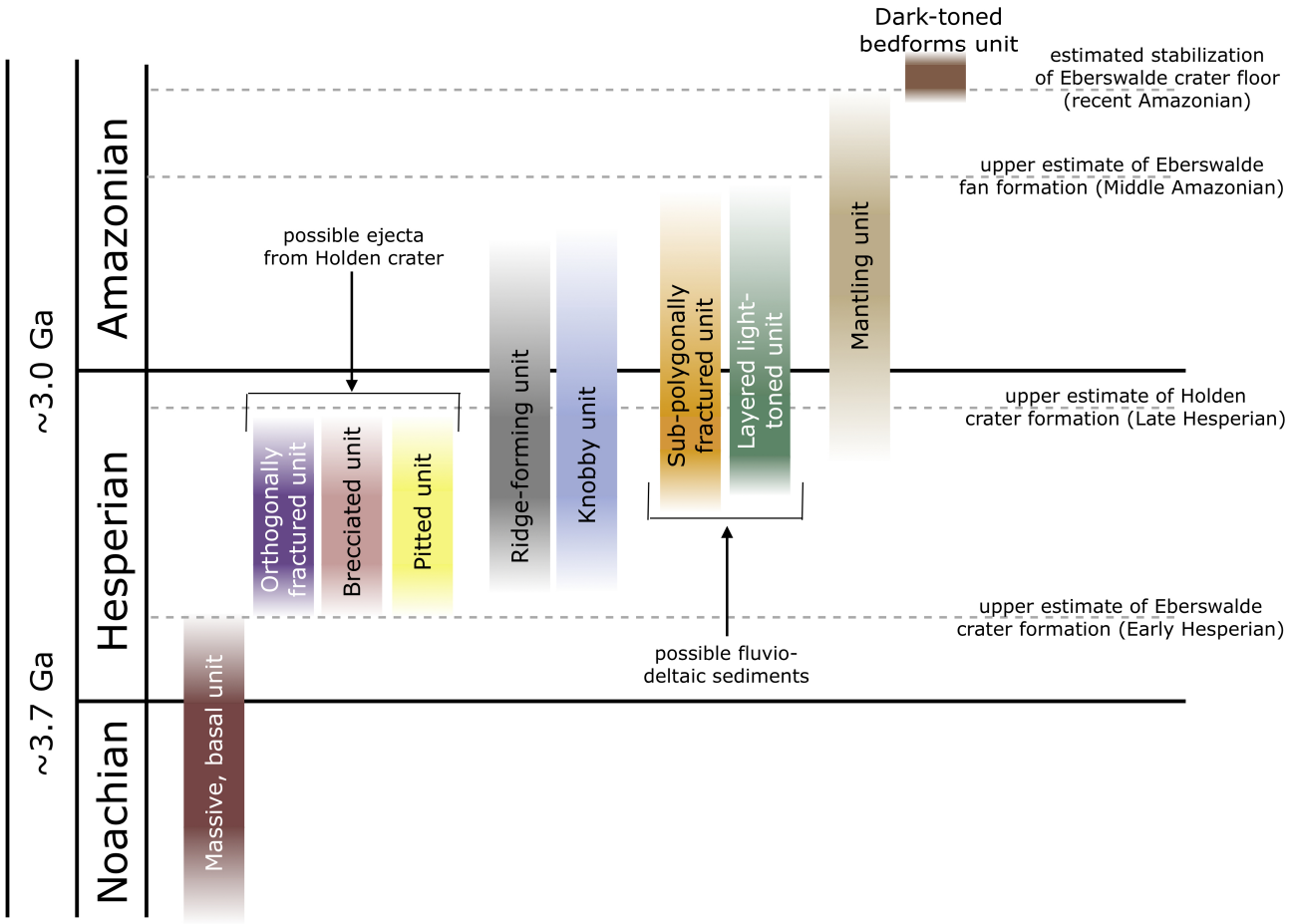

Figure 28. Inferred chronostratigraphy of the Eberswalde crater units mapped in Figure 3. The size of each bar represents the uncertainty in the formation age of each unit (we interpret deposition to have occurred within the indicated time ranges, but deposition may not have been continuous over the entire period). Estimates of the Noachian, Hesperian and Amazonian periods as well as the approximate model ages that define the boundaries between them are shown in the left columns. Dashed lines indicate age estimates for major events in Eberswalde's geologic history: the crater's formation (upper estimate of Early Hesperian, as shown by this work); the formation of Holden crater (upper estimate of Late Hesperian; Irwin and Grant 2011); upper limit on the formation of the Eberswalde fan (Middle Amazonian; Grant and Wilson 2011); and the stabilization of the Eberswalde crater floor (recent Amazonian, as shown by this work). Interpretations of unit successions and depositional age estimates are discussed further in the text. (figure28.jpg)

units (e.g., the fluvial-deltaic units). We therefore obtained a crater model age (Figure 29a) for the entire floor of Eberswalde crater including all craters that have impacted into the geologic units described in this analysis. Crater model ages obtained from a bulk analysis may be deceiving if the crater statistics are included from several spatially distinct geologic formations that have broad differences in formation ages and/or crater retention characteristics. If both old basement rock and younger infilling units are present, for example, there may be an overall shift in the cumulative frequency histogram, providing an age estimate that is not truly representative of either material. However, crater statistics that are separated for individual geologic units that cover small areas (on the order of 10 km^2 to 100 km^2 at CTX resolution) by probability of surface crater density may exclude the large crater population (only 12 craters within Eberswalde with D > 500 m and only 1 crater with D > 500 m on the main fan). Small area crater counts therefore provide a model age that may only include the population of small-diameter impact craters that is most susceptible to processes of resurfacing, thus providing erroneously young ages (Neukum et al. 2010). Here, we use both the model age estimates and the shape of the cumulative frequency curve for Eberswalde crater to provide general information about the overall geologic history of the crater and its interior deposits.

The kink in the slope of the cumulative frequency histogram for craters with D < 700 m (Figure 29a) is consistent with small crater resurfacing, most likely the result of preferential burial (e.g., by airfall deposits) and/or preferential erosion of smaller craters. Both processes have likely operated within different regions of the Eberswalde crater floor since the basin formed, as we observe both degraded rims on craters

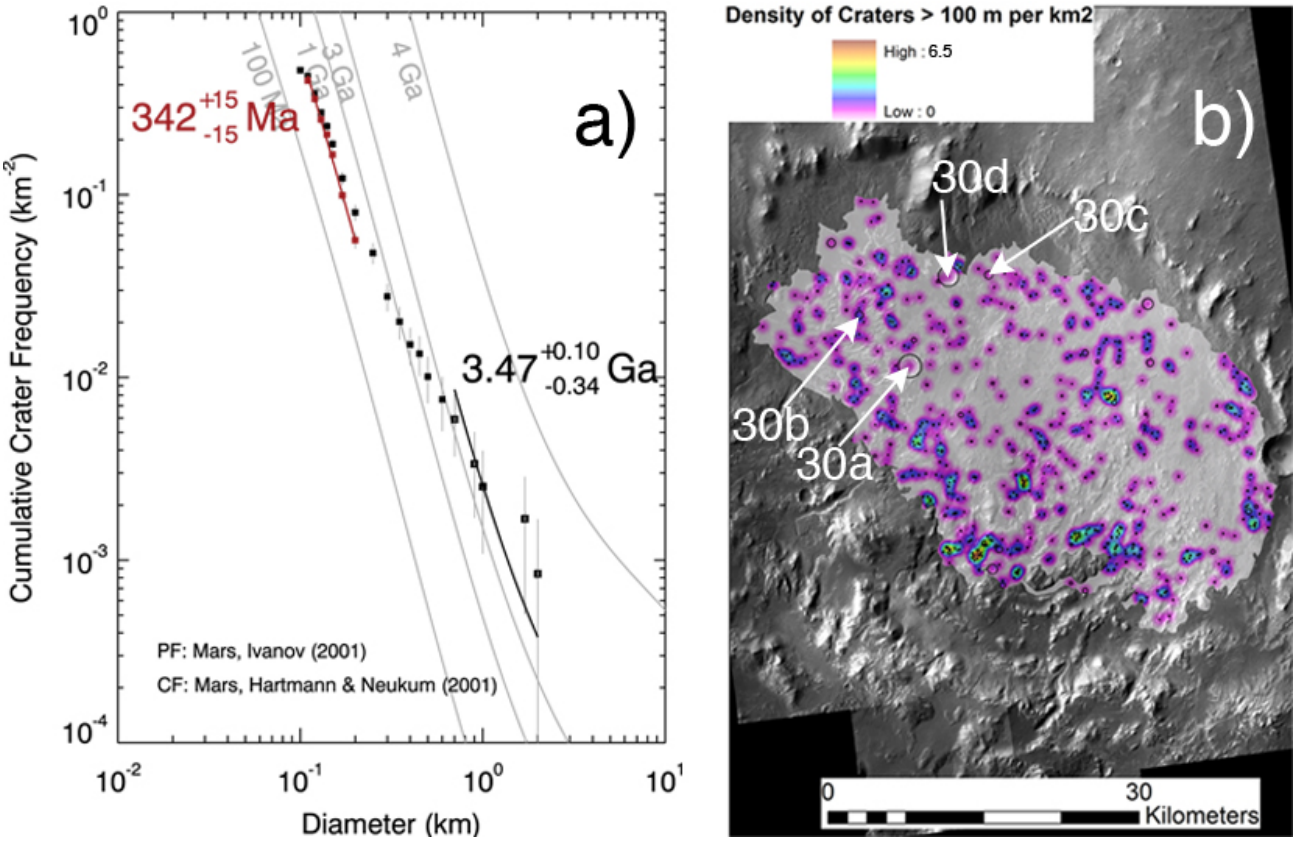

Figure 29. (a) Crater size-frequency distribution for the Eberswalde crater floor materials. CF is chronology function (Hartmann and Neukum, 2001), PF is a production function (Ivanov, 2001). (b) Crater density map of the 1188 km^2 region within Eberswalde crater discussed in this study, overlain on a CTX basemap (north is up). The largest craters are indicated by black outlines, and arrows indicate the locations of Figure 30a-d. (figure29.jpg)

across the basin and a mantling unit that obscures the smallest craters in the center and western regions of Eberswalde crater (Figure 29b). The gradual, but consistent decline in slope of the histogram between D = 200 m and 700 m is more typical of a steady state, long-term resurfacing process where larger craters are better preserved relative to smaller craters (e.g., dust burial or wind erosion), rather than an instantaneous resurfacing (such as a volcanic event) or an exhumation process upon which a new, younger population is established (Neukum et al. 2010). However, a fairly good fit is re-established for D < 200 m (including 480 craters), suggesting that there has been limited crater degradation in the recent Amazonian.

There are only seven craters with D > 700 m within the Eberswalde basin. From these data, we obtained an Early Hesperian crater retention age (Hartmann, 2005 age system) of ~3.5 Ga (+0.1/-0.3 Ga). Several of these craters have highly degraded rims that indicate some process of crater destruction that was also likely responsible for complete resurfacing of the smaller, D < 200 m crater population (Figure 30). Due to the poor preservation of their crater rims and ejecta blankets, the geologic context of this crater population relative to the stratigraphic units is difficult to determine. The possible fluvio-lacustrine materials both bury and are impacted by members of this population (Figure 30a-b). In the center of the Eberswalde basin, several of the largest craters have elevated rims that appear to exhume lower stratigraphic units (e.g., the orthogonally fractured, brecciated and pitted units), possibly including the basement materials (the massive, basal unit) (Figure 30a, c).

We therefore hypothesize that this D > 700 m population could either represent: (1) impacts that include those most ancient craters that formed entirely within the primary bedrock floor material of Eberswalde crater; or (2) impacts that occurred entirely on top of crater-fill materials (e.g., Holden ejecta). For case (1), the Early Hesperian model age represents an estimate for the formation age of Eberswalde crater. This age is chronologically consistent with previous age estimates for the younger Holden crater (Early-Late Hesperian) (Irwin and Grant 2011). In the case of (2), infill of Eberswalde crater by Holden ejecta or other secondary materials would have been of sufficient thickness to obscure all the basement bedrock craters of Eberswalde crater (100 m – 1.6 km of ejecta is expected to cover the entire Eberswalde floor, based on expressions for the radial decay of ejecta thickness by Garvin and Frawley 1998). In that model, the 3.5 Ga model age would not represent the time of Eberswalde crater formation, but the time of resurfacing by some secondary process (e.g., by Holden impact ejecta).

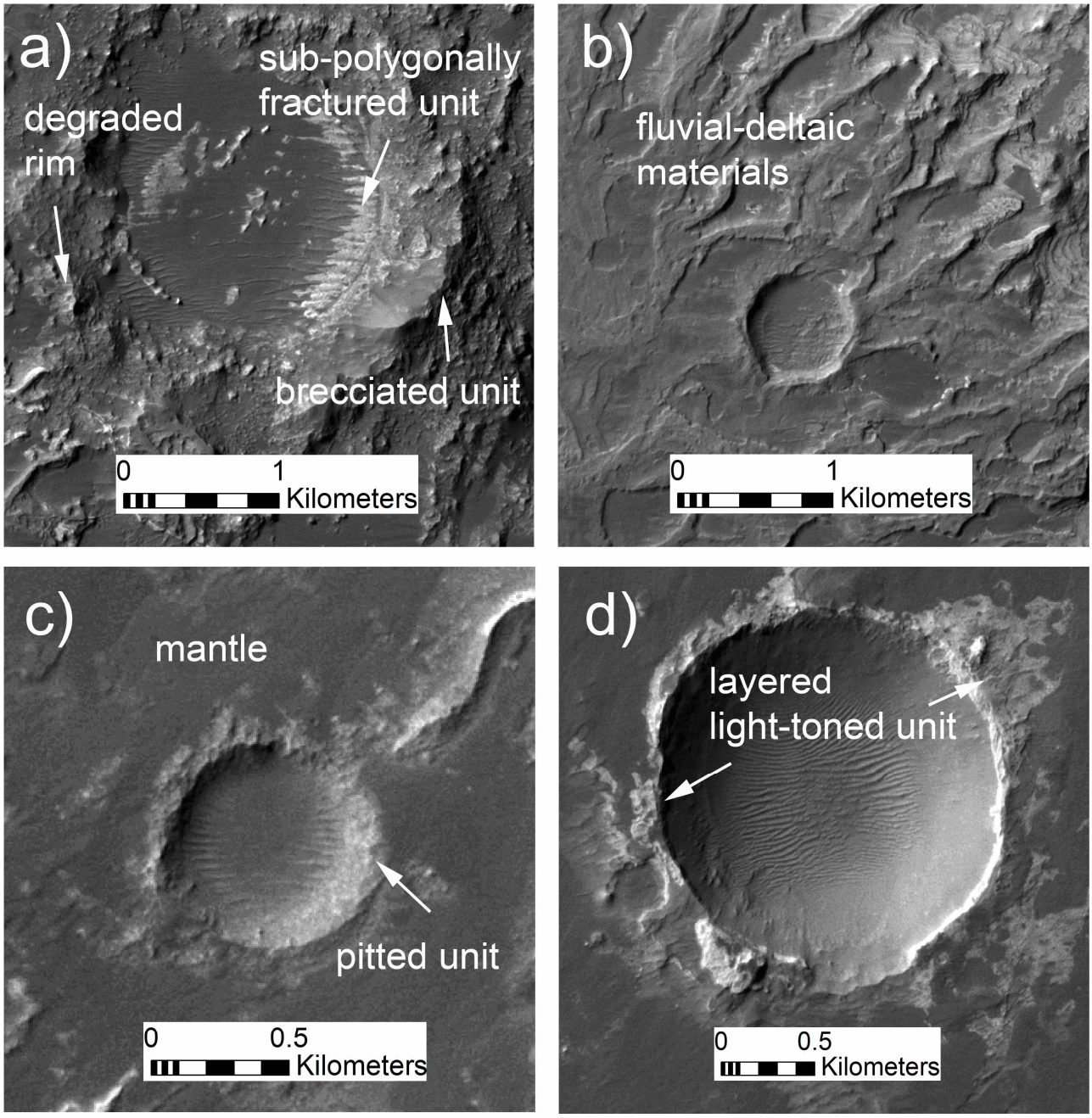

Figure 30: CTX image montage of large (D > 700 m) impact craters on the floor of Eberswalde crater: (a) 2-km-diameter impact crater that sits within Eberswalde crater floor materials. Light-toned units that are part of the fluvial-deltaic sequences of the putative delta rest on the floor of the crater. The rim is highly degraded and the crater contains significant aeolian infill; (b) 700-m-diameter impact crater that rests on top of the putative delta. This crater exhibits significant rim degradation; (c) 700-m-diameter crater that rests on the floor materials of Eberswalde crater. Low-albedo mantling material obscures the crater rim and ejecta blanket; (d) 1.8-km-diameter crater on the floor of Eberswalde crater. Isolated remnants of layered light toned materials rest on top of the crater rim. (figure30.jpg)

Discussion

Following the formation of Eberswalde crater, the first major event inferred by our observations is the infilling of some or all of the crater by ejecta from the Holden crater impact. We favor the interpretation that the orthogonally fractured unit, the brecciated unit, and the pitted unit are various expressions of megabreccia related to the Holden event. It is possible that the deposits covering the Eberswalde crater floor could have derived from other nearby impacts, but the proximity of Holden crater and the extensive modification of Eberswalde's southern rim suggests that Holden had an important role in the geologic history of Eberswalde crater.

Long periods in Eberswalde crater's history remain unaccounted for, such as the time before the formation of Holden crater. It is possible, for example, that the Holden

ejecta deposits are obscuring a record of Noachian fluvio-lacustrine sedimentation in Eberswalde; the most deeply exhumed portion of the crater reveals only the massive, basal unit beneath the inferred megabreccia deposits. What underlies these putative megabreccias in the central and eastern portions of the crater, however, remains unknown.

Because we observe the vein-like features in the inferred megabreccia deposits, but not in the massive, basal unit, we interpret that some process created the vein-like features after – or perhaps concurrent with – the formation of Holden crater (however, this process would not have effected the underlying bedrock). If these features are indeed hydrothermal, they could have important implications for the habitability potential of Eberswalde crater before the deposition of the fluvio-lacustrine sediments (the sub-polygonally fractured and layered light-toned units); Summons et al. (2011) list hydrothermal systems as among the best known environments for supporting the synthesis, concentration and preservation of organic matter.

The linear scarps also occur predominantly in the brecciated, pitted and orthogonally-fractured units. The relationship of these candidate faults to the crater floor materials suggests that regional faulting occurred after the formation of Holden crater. The largest of these features defines the first-order topography within Eberswalde crater (Figure 23). The fluvio-deltaic systems conform to this topography (Rice et al. 2011), except for the western delta, which has linear scarps along its front (Figure 22); this feature may have formed contemporaneously with the faulting, implying multiple eras of deltaic deposition and/or faulting.

The relationship of the large-scale topography to the distribution of units in Eberswalde crater has implications for the presence of an ancient lake. For example, if the ridge-forming unit is interpreted as lacustrine sediments (rather than as other units obscured by airfall), an Eberswalde lake would have to have risen above the tallest ridges on the Central High (-1220 m). This height exceeds the lake level estimate of -1400 m by Lewis and Aharonson (2008), and would imply that it was higher than the topographic divide separating the Central High from the Eastern Basin. Therefore, the lake in this scenario would have filled the Eastern Basin to the -1220 m contour as well. The presence of the knobby unit in this portion of the crater – which may be the remnant of a formerly extensive sub-polygonally fractured or ridge-forming unit – is consistent with this hypothesis. The various elevations of the different features, however, suggest that the lake-level history may have been complex.

The sinuous ridges interpreted as inverted channels may be sublacustrine or may have formed subareally after the lake level dropped. The prominent feature on the drainage divide (Figure 19c) may indicate a "spillover" from a western lake into the Eastern Basin. If this feature is indeed an overspill, it could have provided a possible means of stabilizing the water level of the western lake.

We have not observed any direct evidence for layered material with a similar stratigraphy and crater density to the Eberswalde delta along the margins of the Central High or along the eastern wall of the crater. This may indicate that (1) the layered materials were present here but have since been stripped away and/or degraded to become the knobby unit; (2) the layered materials are still present, but are buried beneath the mantling unit; or (3) the layered materials were never deposited toward the center of the crater or in the Eastern Basin. The relationships between the candidate fluvio-deltaic systems at the margins of the crater and the knobby and ridge-forming units in the central portion of the crater are unclear. These may be sediments that formed in the lake at the same era of fluvio-deltaic deposition, or perhaps much later. The preservation of impact craters on the ridge-forming and knobby units is poor, and we are unable to constrain relative ages for these materials. Toward the center of the crater, for example, the impact crater density (Figure 29b) is very low.

Extensive removal of crater floor materials has occurred within Eberswalde crater, as evidenced by the prevalence of the knobby unit (which we interpret as remnants of a continuous floor-covering unit) and the inverted channels. The kink in the fit on the crater-frequency plot (Figure 29a) supports this interpretation of the geomorphology. Perhaps the most extreme example of exhumation is in the Western Basin, where the massive, basal unit is visible beneath the brecciated unit. We see no reason why there would have been "holes" left here during the deposition of the brecciated and pitted units that cover most of the rest of the crater floor, especially given our favored interpretation of them as Holden crater ejecta. More likely, this portion of the crater has been subjected to the most severe removal.

In this western region, we also see extensive cover by the mantling unit, which likely obscures the older crater population; however, the mantle also appears to be degrading in places (*e.g.*, Figure 15b). Importantly, a fairly good fit on the crater-frequency plot (Figure 29a) is re-established for $D < 200$ m, suggesting that there has been limited crater degradation in the Amazonian, which may explain why the bedforms associated with the mantling unit appear to be stable, showing evidence for intact impact craters.

Evidence for geologic processes occurring in the late-Amazonian to the present is limited to the presence of dark-toned bedforms. These may still be active, as we have observed no small impacts or significant dust cover. The disintegration of the sub-polygonally fractured, layered light-toned, knobby and ridge-forming units (which appear to be actively shedding boulders) and the mantling unit (which appears to be indurated and developing cliffs) likely has continued into the present day as well.

Conclusions

Observations of the stratigraphy, geomorphology, topography and crater densities within Eberswalde crater allow us to infer the following sequence of major events:

1) From regional geologic relationships, Eberswalde crater

forms in the Late-Noachian to Early Hesperian with impact crater statistics indicating a possible Early Hesperian formation age (perhaps around 3.5 Ga);

2) Holden crater forms in the Early Hesperian to Late Hesperian, and the associated ejecta blanket covers much or all of the floor of Eberswalde crater and heavily modifies the southern rim. The orthogonally fractured and brecciated units, which are interpreted as allochthonous and/or parautochthonous megabreccias, are deposited during this event;

3) Extensive faulting from regional stresses creates the Western Basin, Eastern Basin and Central High within the crater. Fracturing and cementation (and/or impact-induced hydrothermal activity) occurs within the brecciated unit, forming the vein-like features (timing of this relative to faulting is unconstrained);

4) Valley features are carved in the crater walls as water flows into the crater, creating an Eberswalde lake. Delta formation occurs within the lake, depositing the sub-pologyonally fractured unit (possible lacustrine bottomset beds) and the layered light-toned unit (deltaic sediments) along the margins of the crater. Faulting may have continued during the formation of the main Eberswalde delta, but the smaller fluvio-deltaic systems in the north and south of the crater conform to the fault-controlled topography. The ridge-forming unit forms, possibly as lacustrine deposits;

5) After the lacustrine era, extensive exhumation and degradation of the crater floor materials occurs, perhaps simultaneously with the deposition of the airfall mantling unit. The brecciated unit degrades into a pitted expression (the pitted unit), the sedimentary crater-fill material (the layered light-toned, sub-polygonally fractured, and/or ridge-forming units) degrades into isolated hillocks (the knobby unit), and fluvial channels are exhumed with inverted relief. The deepest exhumation occurs in the Western Basin, exposing the Eberswalde basement rock (the massive, basal unit) beneath the brecciated unit. The mantling unit becomes indurated and degrades as well;

6) Very little geologic activity occurs in the Amazonian, aside from the formation and movement of dark-toned aeolian bedforms and some degredation/exhumation of other crater floor units that likely continues in present-day Eberswalde crater.

Appendix

The data products used in this study listed in Table A1 (MOC images), Table A2 (CTX images), Table A3 (images used in CTX DEMs), Table A4 (HiRISE images), and Table A5 (HiRISE stereo pairs and images used to produce DEMs).

Table A1. MOC images of Eberswalde Crater

Product ID		
E14-01039	R09-01067	S11-01980
E17-01342	R10-02155	S12-01927
E18-00401	R11-02067	S13-02008
E20-001420	R13-02140	S14-01406
E21-00076	R14-00769	S14-02900
E21-01153	R19-02022	S15-02083
E22-01159	R20-00176	S16-01405
E23-00003	R22-00520	S18-01890
M15-00319	R23-00038	S18-02542
M18-00020	R23-01163	S19-01794
R06-00324	S01-00795	S19-01974
R06-00726	S01-00196	S20-00003
R06-01110	S03-01417	S20-00505
R07-00821	S04-01110	S20-00616
R07-01352	S05-00866	S20-01501
R07-01859	S07-02812	S21-01273
R08-01104	S09-01261	S22-01189

Table A2. CTX images of Eberswalde Crater

Product ID
P01_001336_1560_XI_24S033W*
P01_001534_1559_XI_24S033W
P01_001600_1561_XI_23S033W*
P03_002233_1558_XI_24S033W
P06_003222_1561_XI_23S033W
P13_005978_1543_XI_25S032W
P16_007125_1530_XN_27S033W
P16_007270_1546_XI_25S033W
P17_007481_1544_XI_25S033W
P18_008127_1548_XI_25S034W
P19_008272_1545_XI_25S033W
P21_009274_1558_XN_24S033W*
B01_010052_1559_XI_24S033W
B01_010197_1545_XI_25S032W
B02_010263_1557_XI_24S034W
B02_010408_1548_XI_25S033W
B02_010474_1558_XI_24S033W
B02_010553_1558_XI_24S033W
B02_010619_1561_XI_23S033W
B03_010764_1560_XI_24S033W
B03_010830_1560_XI_24S033W
B04_011265_1558_XI_24S033W
B04_011331_1558_XI_24S033W
B07_012465_1559_XN_24S033W
B10_013533_1560_XN_24S033W
B16_016065_1558_XN_24S033W
B17_016210_1558_XN_24S033W

* indicates images included in the mosaic used for this study

Table A3. List of images used in CTX DTMs

CTX stereo pair product IDs	
P17_007481_1544_XI_25S033W_080301	P19_008272_1545_XI_25S033W_080502
P01_001336_1560_XI_24S033W_061108	P01_001534_1559_XI_24S033W_061123
P01_001600_1561_XI_23S033W_061129	P06_003222_1561_XI_23S033W_070404

Table A4. HiRISE images of Eberswalde Crater

Product ID	
PSP_001336_1560	ESP_016210_1560
PSP_001534_1560	ESP_016777_1560
PSP_001600_1560	ESP_017845_1560
PSP_002233_1560	ESP_018056_1560
PSP_004000_1560	ESP_018267_1560
PSP_004356_1560	ESP_018412_1560
PSP_005556_1560	ESP_018557_1560
PSP_007270_1560	ESP_019111_1560
PSP_007481_1560	ESP_019190_1560
PSP_008272_1560	ESP_019335_1560
PSP_010052_1560	ESP_019757_1560
PSP_010474_1560	ESP_020034_1560
PSP_010553_1560	ESP_020324_1555
PSP_010764_1560	ESP_020390_1555
ESP_011265_1560	ESP_020891_1560
ESP_011331_1560	ESP_021669_1560
ESP_012465_1560*	ESP_022025_1560
ESP_012610_1560	ESP_022236_1560
ESP_013533_1560	ESP_022447_1560
ESP_016065_1560	

* cloud-covered image; not included in the coverage map shown in Figure 2

Table A5. List of HiRISE stereo pairs

HiRISE stereo pair product IDs	
PSP_001336_1560	PSP_001534_1560
PSP_004356_1560	PSP_012610_1560
PSP_010052_1560	PSP_010553_1560*
PSP_008272_1560	PSP_010474_1560*
ESP_011265_1560	ESP_011331_1560*
ESP_016065_1560	ESP_016210_1560*
ESP_016777_1560	ESP_018412_1560
ESP_018056_1560	ESP_018557_1560
ESP_019190_1560	ESP_019335_1560*
ESP_019757_1560	ESP_020034_1560*
ESP_020324_1560	ESP_020390_1560*

* indicates pairs used to derive DTMs

Directory of supporting data

root directory
- manuscript.pdf this file
- Fig. 1 figure1.jpg
- Fig. 2 figure2.jpg
- Fig. 3 figure3.jpg
- Fig. 4 figure4.jpg
- Fig. 5 figure5.jpg
- Fig. 6 figure6.jpg
- Fig. 7 figure7.jpg
- Fig. 8 figure8.jpg
- Fig. 9 figure9.jpg
- Fig. 10 figure10.jpg
- Fig. 11 figure11.jpg
- Fig. 12 figure12.jpg
- Fig. 13 figure13.jpg
- Fig. 14 figure14.jpg
- Fig. 15 figure15.jpg
- Fig. 16 figure16.jpg
- Fig. 17 figure17.jpg
- Fig. 18 figure18.jpg
- Fig. 19 figure19.jpg
- Fig. 20 figure20.jpg
- Fig. 21 figure21.jpg
- Fig. 22 figure22.jpg
- Fig. 23 figure23.jpg
- Fig. 24 figure24.jpg
- Fig. 25 figure25.jpg
- Fig. 26 figure26.jpg
- Fig. 27 figure27.jpg
- Fig. 28 figure28.jpg
- Fig. 29 figure29.jpg
- Fig. 30 figure30.jpg

Acknowledgements

We thank the MRO engineering and science teams for providing the spectacular imaging and topographic datasets that made this study possible. We also thank Becky Williams, Alan Howard and Jeffrey Plescia for insightful comments that improved the quality of this work. MSR was funded by a NSF Graduate Research Fellowship. SG and NHW were funded by the UK STFC (grant ST/F003099/1).

References

Anderson, R. B. and Bell, J. F. III (2010) "Geologic mapping and characterization of Gale Crater and implications for its potential as a Mars Science Laboratory landing site" Mars 5, 76-128. doi:10.1555/mars.2010.0004

Bell, J. F. et al. (2008) "Surface albedo observations at Gusev Crater and Meridiani Planum, Mars" Journal of Geophysical Research 113, E06S18 doi:10.1029/2007JE002976

Bhattacharya, J. P. et al. (2005) "Dynamic river channels suggest a long-lived Noachian crater lake on Mars" Geophysical Research Letters 32, L10201 doi:10.1029/2005GL022747

Boyce, J. M. et al. (2011) "Pitted deposits in fresh Martian impact craters" Lunar and Planetary Science XXXXII, p. 2701.

Bridges, N. T. et al. (2010) "Aeolian bedforms, yardangs, and indurated surfaces in the Tharsis Montes as seen by the HiRISE Camera: Evidence for dust aggregates" Icarus 205, 165-182. doi:10.1016/j.icarus.2009.05.017

Broxton, M. J. and Edwards, L. J. (2008) "The Ames Stereo

Pipeline: Automated 3D Surface Reconstruction from Orbital Imagery" Lunar and Planetary Science XXXIX, p. 2419.

Carr, M. H. (1996) "Water on Mars" New York: Oxford University Press

Christensen, P. R. (1986) "Regional dust deposits on Mars - Physical properties, age, and history" Journal of Geophysical Research 91, 3533-3545. doi:10.1029/JB091iB03p03533

Christensen, P. R., N. S. Gorelick, G. L. Mehall and K. C. Murray (2006) THEMIS data collection. Planetary System node, Arizona State University.

Delamere, W. A. et al. (2010) "Color imaging of Mars by the High Resolution Imaging Science Experiment (HiRISE)" Icarus 205, 38-52. doi:10.1016/j.icarus.2009.03.012

Di Achille, G. et al. (2007) "Evidence for late Hesperian lacustrine activity in Shalbatana Vallis, Mars" Journal of Geophysical Research 112, E07007 doi:10.1029/2006JE002858

Dickson, J. L. et al. (2008) "Late Amazonian glaciation at the dichotomy boundary on Mars: Evidence for glacial thickness maxima and multiple glacial phases" Geology, vol. 36, Issue 5, p.411-414 doi:10.1130/G24382A.1

Edwards, L. and Broxton, M. (2006), "Automated 3D Surface Reconstruction from Orbital Imagery", AIAA, Space 2006, San Jose California, Sep. 19-21

Edgett, K. S. (2005) "The sedimentary rocks of Sinus Meridiani: Five key observations from data acquired by the Mars Global Surveyor and Mars Odyssey orbiters" Mars, Vol. 1, p. 5-58. doi:10.1555/mars.2005.0002

Eliason, E. M. et al. (2001) "ISIS Image Processing Capabilities for MGS/MOC Imaging Data" Lunar and Planetary Science XXXII, p. 2081

French, B. M. (1998) "Traces of Catastrophe: A Handbook of Shock-Metamorphic Effects in Terrestrial Meteorite Impact Structures" Technical Report, LPI-Contrib-954

Garvin, J. B. and Frawley, J. J. (1998) "Geometric properties of Martian impact craters: Preliminary results from the Mars Orbiter Laser Altimeter" Geophysical Research Letters 25, 4405-4408 doi:10.1029/1998GL900177

Gillespie, et al. (1986) "Color enhancement of highly correlated images. I. Decorrelation and HSI contrast stretches" Remote Sensing of Environment, v. 20, Issue 1, p. 209-235

Grant, J. A. and Parker, T. J. (2002) "Drainage evolution in the Margaritifer Sinus region, Mars" Journal of Geophysical Research 107, 5066 doi:10.1029/2001JE001678

Grant, J. A. and Wilson, S. A. (2011) "Late Alluvial Fan Formation in Southern Margaritifer Terra, Mars" Geophysical Research Letters, 38, L08201 doi:10.1029/2011GL046844

Grant, J. A. et al. (2008) "HiRISE imaging of impact megabreccia and sub-meter aqueous strata in Holden crater, Mars" Geology, vol. 36, Issue 3, 195-198 doi:10.1130/G24340A.1

Grant, J. A. et al. (2011) "The science process for selecting the landing site for the 2011 Mars Science Laboratory" Planetary and Space Science, v. 59, Issue 11, 1114-1127 doi:10.1016/j.pss.2010.06.016

Gregg, T. K. P. et al. (2007) "Ice-rich terrain in Gusev Crater, Mars?" Icarus 192, 348-360. doi:10.1016/j.icarus.2007.08.010

Grotzinger, J. (2009) "Beyond water on Mars" Nature Geoscience, Volume 2, Issue 4, pp. 231-233 (2009). doi:10.1038/ngeo480

Hamilton, V. E. et al. (2007) "THEMIS Decorrelation Stretched Infrared Mosaics of Candidate 2009 Mars Science Laboratory Landing Sites: Evidence for Significant Spectral Diversity" Lunar and Planetary Science XXXVIII, p. 1725.

Harrison, T. N. et al. (2010) "Impact-induced overland fluid flow and channelized erosion at Lyot Crater, Mars" Geophysical Research Letters 37, L21201 doi:10.1029/2010GL045074

Hartmann, W. K. and Neukum, G. (2001) "Cratering Chronology and the Evolution of Mars" Space Science Reviews, v. 96, Issue 1/4, p. 165-194 (2001).

Hartmann, W. K. (2005) "Martian cratering 8: Isochron refinement and the chronology of Mars" Icarus 174, 294-320. doi:10.1016/j.icarus.2004.11.023

Howard, A. D. et al. (2007) "Boulder Transport Across the Eberswalde Delta" Lunar and Planetary Science XXXVIII, p. 1168.

Head, J. W. and Mustard, J. F. (2006) "Breccia dikes and crater-related faults in impact craters on Mars: Erosion and exposure on the floor of a crater 75 km in diameter at the dichotomy boundary" Meteoritics and Planetary Science, vol. 41, Issue 10, p.1675-1690 doi:10.1111/j.1945-5100.2006.tb00444.x

Irwin, R. P. III (2011) "Timing, duration and hydrology of the Eberswalde crater paleolake, Mars" Lunar and Planetary Science XXXXII, p. 2748

Irwin, R. P. III, and Grant, J. A. (2011) "Geologic map of MTM −15027, −20027, −25027 and −25032 quadrangles, Margaritifer Terra region of Mars, scale 1:500,000" U.S. Geol. Surv. Sci. Invest. Map, in press

Ivanov, B. A. (2001) "Mars/Moon Cratering Rate Ratio Estimates" Space Science Reviews, v. 96, Issue 1/4, p. 87-104.

Ivanov, B. A. and Pierazzo, E. (2011) "Impact cratering in H2O-bearing targets on Mars: Thermal field under craters as starting conditions for hydrothermal activity" Meteoritics & Planetary Science, Volume 46, Issue 4, pp. 601-619. doi:10.1111/j.1945-5100.2011.01177.x

Jerolmack, D. J. et al. (2004) "A minimum time for the formation of Holden Northeast fan, Mars" Geophysical Research Letters 31, L21701 doi:10.1029/2004GL021326

Kendall, C. G. S. C. and Warren, J. (1987) "A review of the origin and setting of tepees and their associated fabrics" Sedimentology 34, p. 1007–1027 doi:10.1029/2007JE003000

Kite, E. S. et al. (2011) "Localized precipitation and runoff on Mars" Journal of Geophysical Research 116, E07002 doi:10.1029/2010JE003783

Kirk, R. L. et al. (2008) "Ultrahigh resolution topographic mapping of Mars with MRO HiRISE stereo images: Meter-scale slopes of candidate Phoenix landing sites" Journal of Geophysical Research 113, E00A24. doi:10.1029/2007JE003000

Knauth, L. P. et al. (2005) "Impact origin of sediments at the Opportunity landing site on Mars" Nature 438, 1123-1128. doi:10.1038/nature04383

Knoll, A. H. et al. (2008) "Veneers, rinds, and fracture fills: Relatively late alteration of sedimentary rocks at Meridiani Planum, Mars" Journal of Geophysical Research 113, E06S16 doi:10.1029/2007JE002949

Kraal, E. R. et al. (2008) "Martian stepped-delta formation by rapid water release" Nature 451, 973-976. doi:10.1038/nature06615

Kraal, E. R. and Postma, G. (2008) "The Challenge of Explaining Meander Bends in the Eberswalde Delta" Lunar and Planetary Science XXXIX, p. 1897.

Lewis, K. W. and Aharonson, O. (2006) "Stratigraphic analysis of the distributary fan in Eberswalde crater using stereo imagery" Journal of Geophysical Research 111, E06001 doi:10.1029/2005JE002558

Maizels, J. (1990) "Raised channel systems as indicators of palaeohydrologic change: a case study from Oman" Palaeogeography, Palaeoclimatology, Palaeoecology 76, 3-4, p. 241–277.

Malin, M. C. et al. (2007) "Context Camera Investigation on board the Mars Reconnaissance Orbiter" Journal of Geophysical Research 112, E05S04 doi:10.1029/2006JE002808

Malin, M. C. and Edgett, K. S. (2001) "Mars Global Surveyor Mars Orbiter Camera: Interplanetary cruise through primary mission" Journal of Geophysical Research 106, 23429-23570. doi:10.1029/2000JE001455

Malin, M. C. and Edgett, K. S. (2003) "Evidence for Persistent Flow and Aqueous Sedimentation on Early Mars" Science 302, 1931-1934. doi:10.1126/science.1090544

Malin, M. C. and Edgett, K. S. (2000) "Sedimentary Rocks of Early Mars" Science 290, 1927-1937. doi:10.1126/science.290.5498.1927

Malin, M. et al. (2010) "An overview of the 1985–2006 Mars Orbiter Camera science investigation" Mars 5, 1-60. doi:10.1555/mars.2010.0001

Mangold, N. (2011) "Post-early Mars fluvial landforms on mid-latitude impact ejecta" Lunar and Planetary Science XXXXII, p. 1370

McEwen, A. S. et al. (2007) "Mars Reconnaissance Orbiter's High Resolution Imaging Science Experiment (HiRISE)" Journal of Geophysical Research 112, E05S02 doi:10.1029/2005JE002605

McEwen, A. S. et al. (2007) "A Closer Look at Water-Related Geologic Activity on Mars" Science 317, 1706. doi:10.1126/science.1143987

McEwen, A. S. et al. (2010) "The High Resolution Imaging Science Experiment (HiRISE) during MRO's Primary Science Phase (PSP)" Icarus 205, 2-37. doi:10.1016/j.icarus.2009.04.023

McCauley, J. F. et al. 1977. Yardangs. In: Doehring, D.O. (Ed.), Geomorphology in Arid Regions. Allen and Unwin, Boston, p. 33–269.

McKeown, N. K. and M.S. Rice (2011) "Detailed mineralogy of Eberswalde crater" Lunar and Planetary Science XXXXII, p. 2450

Melosh, H. J. (1989) Impact Cratering: A Geologic Process, Cambridge University Press.

Michael, G. and Neukum, G. (2008) "Surface Dating: Software Tool for Analysing Crater Size-Frequency Distributions Including Those Showing Partial Resurfacing Events" Lunar and Planetary Science XXXIX, p. 1780.

Michael, G. G. and Neukum, G. (2010) "Planetary surface dating from crater size-frequency distribution measurements: Partial resurfacing events and statistical age uncertainty" Earth and Planetary Science Letters 294, 223-229. doi:10.1016/j.epsl.2009.12.041

Milliken, R. E. and Bish, D. L. (2010) "Sources and sinks of clay minerals on Mars" Philosophical Magazine, vol. 90, issue 17, pp. 2293-2308 doi:10.1080/14786430903575132

Montgomery, D. R. et al. (2011) "Wind-carved transverse erosional ridges on Mars" Lunar and Planetary Science XXXXII, p. 2488

Moore, J. M. et al. (2003) "Martian Layered Fluvial Deposits: Implications for Noachian Climate Scenarios" Geophysical Research Letters 30, 2292 doi:10.1029/2003GL019002

Morgan, G. A. et al. (2009) "Lineated valley fill (LVF) and lobate debris aprons (LDA) in the Deuteronilus Mensae northern dichotomy boundary region, Mars: Constraints on the extent, age and episodicity of Amazonian glacial events" Icarus 202, 22-38. doi:10.1016/j.icarus.2009.02.017

Murchie, S. et al. (2007) "Compact Reconnaissance Imaging Spectrometer for Mars (CRISM) on Mars Reconnaissance Orbiter (MRO)" Journal of Geophysical Research 112, E05S03 doi:10.1029/2006JE002682

Neukum, G. et al. (2010) "The geologic evolution of Mars: Episodicity of resurfacing events and ages from cratering analysis of image data and correlation with radiometric ages of Martian meteorites" Earth and Planetary Science Letters 294, 204-222. doi:10.1029/2006JE002682

Neuendorf, K.K.E.; Mehl, J.P., Jr.; Jackson, J.A. (Eds.) (2005) Glossary of Geology, 5th Edition, American Geological Institute, Alexandria, Virginia

Okubo, C. H. and McEwen, A. S. (2007) "Fracture-Controlled Paleo-Fluid Flow in Candor Chasma, Mars" Science 315, 983. doi:10.1126/science.1136855

Pain, C. F. et al. (2007) "Inversion of relief on Mars" Icarus 190, 478-491. doi:10.1016/j.icarus.2007.03.017

Pondrelli, M. et al. (2008) "Evolution and depositional environments of the Eberswalde fan delta, Mars" Icarus 197, 429-451. doi:10.1016/j.icarus.2008.05.018

Pondrelli, M. et al. (2011) "Geological, Geomorphological, Facies and Allostratigraphic Maps of the Eberswalde Fan Delta" Planetary and Space Science, v. 59, Issue 11, 1166-1178. doi:10.1016/j.pss.2010.10.009

Rao, M. N. et al. (2008) "The nature of Martian fluids based on mobile element studies in salt-assemblages from Martian meteorites" Journal of Geophysical Research 113. doi:10.1029/2007JE002958

Rice, M. S. et al. (2011) "Influence of fault-controlled topography on fluvio-deltaic sedimentary systems in Eberswalde crater, Mars" Geophysical Research Letters, 38, L16203. doi:10:1029/2011GL048149

Rogers, A. D. and Bandfield, J. L. (2009) "Mineralogical characterization of Mars Science Laboratory candidate landing sites from THEMIS and TES data" Icarus 203, 437-453. doi:10.1016/j.icarus.2009.04.020

Ruff, S. W. and Christensen, P. R. (2002) "Bright and dark regions on Mars: Particle size and mineralogical characteristics based on Thermal Emission Spectrometer data" Journal of Geophysical Research, 107, E12, 5127 doi:10.1029/2001JE001580

Schieber, J. (2007) "Reinterpretation of the Martian Eberswalde Delta in the Light of New HiRISE Images" Lunar and Planetary Science XXXVIII, p. 1982.

Scott, D.H. and Tanaka, K.L. (1986) "Geologic map of the western equatorial region of Mars" U.S. Geol. Surv. Misc. Invest. Ser., Map I-1802-A.

Sharp, R. P. (1963) "Wind ripples" Journal of Geology, vol. 71, no. 5, p. 617-36.

Shoemaker, E. M. and Hackman, R. J. (1962) "Stratigraphic Basis for a Lunar Time Scale" IN: THE MOON, (KOPAL,Z., AND MIKHAILOV,Z.K., EDITORS) IAU SYMPOSIUM 14, ACADEMIC, P. 289-300.

Simpson, J. I. et al. (2008) "3D crater database production on Mars by automated crater detection and data fusion" in The International Congress of the Photogrammetry, Remote Sensing and Spatial Information Sciences, edited, pp. 1049-1054, Beijing.

Smith, D. E. et al. (2001) "Mars Orbiter Laser Altimeter:

Experiment summary after the first year of global mapping of Mars" Journal of Geophysical Research 106, 23689-23722 doi:10.1029/2000JE001364

Squyres, S. W. (1978) "Martian fretted terrain - Flow of erosional debris" Icarus 34, 600-613. doi:10.1016/0019-1035(78)90048-9

Squyres, S. W. and Carr, M. H. (1986) "Geomorphic evidence for the distribution of ground ice on Mars" Science (ISSN 0036-8075), vol. 231, p. 249-252. doi:10.1126/science.231.4735.249

Sullivan, R. et al. (2008) "Wind-driven particle mobility on Mars: Insights from Mars Exploration Rover observations at 'El Dorado' and surroundings at Gusev Crater" Journal of Geophysical Research 113, E06S07 doi:10.1029/2008JE003101

Summons, R. E. et al. (2011) "Preservation of Martian Organic and Environmental Records: Final Report of the Mars Biosignature Working Group" Astrobiology 11, 2, doi:10.1089/ast.2010.0506

Tornabene, L. L. et al. (2007) "Evidence for the Role of Volatiles on Martian Impact Craters as Revealed by HiRISE" Lunar and Planetary Science XXXVIII, p. 2215.

Tornabene, L. L. et al. (2009) "Parautochthonous Megabreccias and Possible Evidence of Impact-induced Hydrothermal Alteration in Holden crater, Mars" Lunar and Planetary Science XL, p. 1766

Wang, C. et al. (2005) "Floods on Mars released from groundwater by impact" Icarus 175, 551-555. doi:10.1016/j.icarus.2004.12.003

Warner, N. et al. (2010) "Late Noachian to Hesperian climate change on Mars: Evidence of episodic warming from transient crater lakes near Ares Vallis" Journal of Geophysical Research 115, E06013 doi:10.1029/2009JE003522

Weitz, C. M. et al. (2006) "Formation of a terraced fan deposit in Coprates Catena, Mars" Icarus 184, 436-451. doi:10.1016/j.icarus.2006.05.024

Wilhelms, D. E. (1990) "Geologic Mapping" Planetary Mapping Edited by Ronald Greeley, and Raymond M. Batson. Cambridge, GB: Cambridge University Press, 1990., p.208

Wilhelms, D. E. (1974) "Interagency report: astrogeology 55, geologic mapping of the second planet. Part 1: Rationale and general methods of lunar geologic mapping. Part 2: Technicalities of map conventions, format, production mechanics, and reviewing. Part 3: History of the US Geological Survey lunar geologic mapping program" In NASA. Ames Res. Center A Primer in Lunar Geology p 199-238 (SEE N75-13730 04-91)

Williams, R. M. E. and Malin, M. C. (2008) "Sub-kilometer fans in Mojave Crater, Mars" Icarus 198, 365-383. doi:10.1016/j.icarus.2008.07.013

Williams, R. M. E. et al. (2006) "Aspects of alluvial fan shape indicative of formation process: A case study in southwestern California with application to Mojave Crater fans on Mars" Geophysical Research Letters 33, L10201 doi:10.1029/2005GL025618

Williams, R. M. E. et al. (2009) "Evaluation of paleohydrologic models for terrestrial inverted channels: Implications for application to martian sinuous ridges" Geomorphology 107, 3-4, p. 300–315. doi:10.1016/j.geomorph.2008.12.015

Wood, L. (2006) "Quantitative geomorphology of the Mars Eberswalde delta" Geological Society of America Bulletin 118, 5-6, 557 doi:10.1130/B25822.1

Zimbelman, J. R. et al. (1989) "Concentric crater fill on Mars - an aeolian alternative to ice-rich mass wasting" Lunar and Planetary Science , p. 397.

Zuber, M. T. et al. (1992) "The Mars Observer laser altimeter investigation" Journal of Geophysical Research 97, 7781-7797 doi:10.1029/92JE00341